3.00
+8

# Deformation of the Josephine Peridotite, California and Oregon

U.S. GEOLOGICAL SURVEY PROFESSIONAL PAPER 1378

# Deformation of the Josephine Peridotite, California and Oregon

*By* JAMES G. EVANS

U.S. GEOLOGICAL SURVEY PROFESSIONAL PAPER 1378


UNITED STATES GOVERNMENT PRINTING OFFICE, WASHINGTON : 1987

**DEPARTMENT OF THE INTERIOR**

**DONALD PAUL HODEL, *Secretary***

**U.S. GEOLOGICAL SURVEY**

**Dallas L. Peck, *Director***

**Library of Congress Cataloging in Publication Data**

Evans, James George, 1938–
Deformation of the Josephine Peridotite, California and Oregon.

(U.S. Geological Survey Professional Paper 1378)
Bibliography: p. 44–45
Supt. of Docs. No.: I 19.16:1378
1. Rock deformation—Klamath Mountains (Calif. and Oreg.). 2. Geology, stratigraphic—Mesozoic. 3. Peridotite—Klamath Mountains (Calif. and Oreg.). 4. Geology—Klamath Mountains (Calif. and Oreg.). I. Title. II. Series: United States. Geological Survey. Professional Paper 1378.
QE604.E88 1986 551.8'09794'21 87-600231

**For sale by the Books and Open-File Reports Section,
U.S. Geological Survey, Federal Center, Box 25425, Denver, CO 80225**

# CONTENTS



# ILLUSTRATIONS

## TABLE

# DEFORMATION OF THE JOSEPHINE PERIDOTITE, CALIFORNIA AND OREGON

By JAMES G. EVANS

ABSTRACT

The Josephine Peridotite, lying along the west edge of the Klamath Mountains, constitutes the lower part of an ophiolite sequence called the Josephine ophiolite. The peridotite is overlain by the upper parts of the ophiolite and by metasedimentary rocks, and lies in fault contact with the Upper Jurassic and Lower Cretaceous Franciscan Complex in northern California and the contemporaneous Dothan Formation in southern Oregon. The ophiolite in California, including the basal Josephine Peridotite, appears to be 2 km thick above a flat thrust. The Josephine peridotite consists of three zones: peridotite below a chromite-bearing zone, a chromite-bearing zone approximately 300 m thick, and peridotite above the chromite-bearing zone. These three units are folded and faulted on the macroscopic scale.

The presence of poikilitic enstatite in harzburgite suggests a magmatic stage sometime, most likely early, in the formation of the rocks. Enstatite and dunite layering may have formed as a result of cumulus processes and (or) metamorphic differentiation. Some of the dunite layers may be of intrusive origin. At least local metasomatic alteration of harzburgite to dunite cannot be ruled out.

Intense early plastic deformation resulted in the formation of isoclinal folds, chiefly with northwestward trends. Elongation along axial planes resulted in pulling apart of layers, disruption of fold hinges, separation of hinges from limbs, rotation of early layering into parallelism with axial planes, and nearly complete obliteration of preexisting primary and deformational textures and structures. Some elongation occurred parallel to fold axes as the axes were rotated toward the principal direction of elongation, trending generally north-northwest. An enstatite foliation in harzburgite developed parallel to the axial planes. Subsequently, the isoclinal folds were refolded in a more open style around northwest-trending axes. Fabric data suggest that this later folding was by flexural slip.

Younger northeast- and east-west-trending folds are open in style, with axial planes at large angles to earlier layering and foliation. Wide variation in the orientations of the axial planes of northeast-trending folds probably reflects the degree of heterogeneity of the deformation but also suggests rotation or refolding of these folds about northeast-trending axes. Chromite foliations formed locally, chiefly in chromitiferous dunite, parallel to the axial planes of northeast- and east-west-trending folds. Olivine grains were flattened in the plane of the foliation. During these episodes of folding, the chromite zones in dunite behaved more plastically than the dunite in harzburgite, as indicated by isoclinal chromite folds subparallel to open dunite folds. Fabric data suggest that the east-west-trending folds postdate the northeast-trending folds and formed chiefly by flexural slip.

The steep open folds may include one or more groups of folds: some may be conjugate ($B \perp B'$) to more dominant northeast-trending folds, and some may constitute one or more distinct groups of folds unrelated to the other fold groups and locally well developed in the peridotite.

Several stages of dunite emplacement occurred. Some dunite may have been emplaced in harzburgite before the early plastic deformation and now consists of irregular intricately folded dunite bodies. Other dunite dikes cut early layering and foliation in harzburgite, have apophyses parallel to the earlier planar structures, and must postdate the early plastic deformation. Some dunite dikes cut early layering and foliation, contain northeast- and east-west-trending but no northwest-trending folds, and are subparallel to axial planes of northeast-trending folds. These dikes, which probably predate some northeast-trending folds, may have been affected by a subsequent episode during which northeast-trending folds were formed, at least locally, within the dikes. The east-west-trending minor folds in these dikes seem unrelated to dike emplacement and probably postdate the northeast-trending folds.

Orthopyroxenite dikes cut early layering and foliation of the harzburgite and the dunite dikes. Local warping and faulting of the orthopyroxenite indicate low-intensity ductile and brittle deformation late in the development of the peridotite.

Broad folding of the ophiolite and metasedimentary rocks into a syncline plunging at a low angle south-southeast did not result in minor structures in the peridotite.

Olivine fabrics were probably developed principally by syntectonic recrystallization. Z is generally subparallel to a conspicuous mesoscopic linear structure, and X is perpendicular to a conspicuous planar element; the total fabric is orthorhombic or suborthorhombic. This type of fabric was found to be related to northwest-, northeast-, and east-west-trending folds. Triclinic fabrics of some rocks may be superposed orthorhombic fabrics of this type. In one chromitiferous dunite, a subfabric of possibly primary cumulate origin was found, with a Y maximum subparallel to chromite rods. This observation is consistent with interpretations of olivine and chromite net textures as being of possible primary origin.

Diopside fabric of a wehrlite sample is suborthorhombic, with Y subperpendicular to possible primary layering and X- and Z-girdles subparallel to the layering. This rock is probably part of the cumulate ultramafic rock unit overlying the harzburgite tectonite.

Ages of the deformations undergone by the Josephine Peridotite are based on the assumption that the chromite-bearing dunite was emplaced penecontemporaneously with the formation of the overlying Late Jurassic parts of the Josephine ophiolite. The northwest-trending and, possibly, some northeast-trending folds are pre-Late Jurassic; other northeast- and east- west-trending steep folds and the late low-intensity deformation are Late Jurassic. The broad folding of the ophiolite and metasedimentary rocks is post-Late Jurassic. Postcrystalline emplacement of the peridotite occurred during the post-Late Jurassic and Late Cretaceous. The differences in the style and complexity of deformation between the peridotite and the upper parts of the ophiolite imply tectonic uncoupling of the peridotite from the overlying rocks. The sequence of deformations may reflect changes in strain regime as the peridotite approached a subduction zone or was obducted. Parts of the peridotite may have been simultaneously subjected to different physical conditions. Geographic orientations of slip directions and of major axes of stress and strain ellipsoids inferred from this study may add little to our understanding of regional tectonics, owing to probable postcrystalline translations and rotations during emplacement.

## INTRODUCTION

The 130-km-long body of the Josephine Peridotite lies along the west boundary of the Klamath Mountains in southwestern Oregon and northwestern California (fig. 1). The fault along much of the west edge of the peridotite has been correlated with the South Fork Mountain fault and forms the boundary between the Coast Ranges on the west and the western Jurassic belt of the Klamath Mountains on the east. A 72-km-long segment of the peridotite in California and an adjoining 19-km-long segment in Oregon were studied. In addition to mapping of the peridotite and adjoining rocks in reconnaissance fashion and compilation of published and unpublished mapping (Evans, 1984), minor structures of the peridotite were studied to determine the deformational history of the peridotite. One goal was to test whether structural analytical techniques would provide a tool for prospecting for chromite in this peridotite. The structure of the chromite deposits is discussed by Evans and is not repeated here. Structural analysis was determined to be of possible limited use in locating chromite ore-bearing structures in the Josephine Peridotite. The present report is concerned with the deformational history of the peridotite, contains the detailed mesoscopic fabric data from which previously stated conclusions were drawn (Evans, 1984), and includes petrofabric studies.

*Acknowledgments.*—I was assisted in the field by E. Van Dohlen in fall 1977, by D. Huber in summer 1978, and by L. Fraticelli in spring 1979. Discussions with John Albers, Henry R. Cornwall, Russell G. Evarts, Robert A. Loney, and Norman J Page, all of the U.S. Geological Survey, and with Gregory D. Harper, State University of New York at Albany, aided in the formative stages of this report. Albers and Cornwall also visited me in the field during the 1979 field season for additional discussions.

## GEOLOGIC SETTING

The Josephine Peridotite, chiefly harzburgite, is the basal part of the Josephine ophiolite (Harper, 1980a, b; Harper and Saleeby, 1980). Harper (1984, p. 1011) restricted the name to the harzburgite tectonite part of the peridotite body. However, the original mapping of the peridotite by Wells and others (1949) includes rocks which have later been recognized as being of cumulate origin. In this report, the earlier usage is retained. The age of the Josephine Peridotite is Jurassic or older (more exactly, pre-Middle Jurassic) on the basis of K-Ar ages on diorite and gabbro dikes ranging from 83 to 167 million years (Ma) that intrude the peridotite (Dick, 1973).

The parts of the ophiolite above the peridotite are, in ascending order: a cumulate ultramafic-rock unit, gabbro, a dike complex, and a spilitic pillow-lava unit. All the contacts between the upper part of the ophiolite and the Josephine Peridotite are faulted. Detailed descriptions of these and other rock units of the area were given by Evans (1984) and the references cited by Evans, particularly Harper (1980a, b, 1983, 1984). The ophiolite (excluding the Josephine Peridotite) is assigned a Late Jurassic age on the basis of a concordant U-Pb age of 157 Ma (Harper and Saleeby, 1980; Saleeby and others, 1982) on plagiogranite dikes in the ophiolite (assuming that the plagiogranite is an intrusive phase related to the ophiolite), on the basis of a concordant U-Pb age of $151 \pm 2$ Ma (Saleeby and others, 1982) on a silicic dike that intrudes the ophiolite, and on the basis of a Late Jurassic age for the metasedimentary rocks overlying the ophiolite.

The metasedimentary rocks overlying the Josephine ophiolite consist of green radiolarian chert and red argillite at the base, succeeded by a monotonous sequence of interbedded graywacke, slate, rare conglomerate, and rare limestone. The minimum thickness in the study area is estimated at 2,500 m. Harper (1938) proposed that the metasedimentary rocks overlying the Josephine Peridotite are part of the same clastic wedge as the Galice Formation to the north of the study area. The Galice Formation, however, overlies the Late Jurassic mafic plutonic Chetco River complex of Hotz (1971), and the contact between that terrane and the Josephine ophiolite is a Late Jurassic thrust fault. Because the stratigraphic identification of the metasedimentary rocks is in doubt, no formational name for them is used in this report. The metasedimentary rocks are assigned a Late Jurassic age on the basis of occurrences of the pelecypod *Buchia concentrica* Sowerby a few hundred meters above the base in the area between the Middle and South Forks Smith River (Harper, 1980a, b), and on the basis of a concordant U-Pb age of $150 \pm 2$ Ma (Saleeby and others, 1982) on a sill that intrudes the metasedimentary rocks.

The Josephine Peridotite contains no marker horizons for determining megascopic internal structure. The chromite deposits, however, are interpreted to lie in a generally gently dipping zone, 300 m thick, within the upper part of the peridotite (Evans, 1984). According to this model, the peridotite is divided into three units: (1) peridotite below the chromite-bearing zone, (2) the chromite zone, and (3) peridotite above the chromite-bearing zone (fig. 2). The peridotite above the chromite-bearing zone may grade into cumulate ultramafic rocks. Segments of the chromite-bearing zone that are interpreted to dip 2°–55° define several megascopic folds: two anticlinal axes and a synclinal trough trend nearly east-

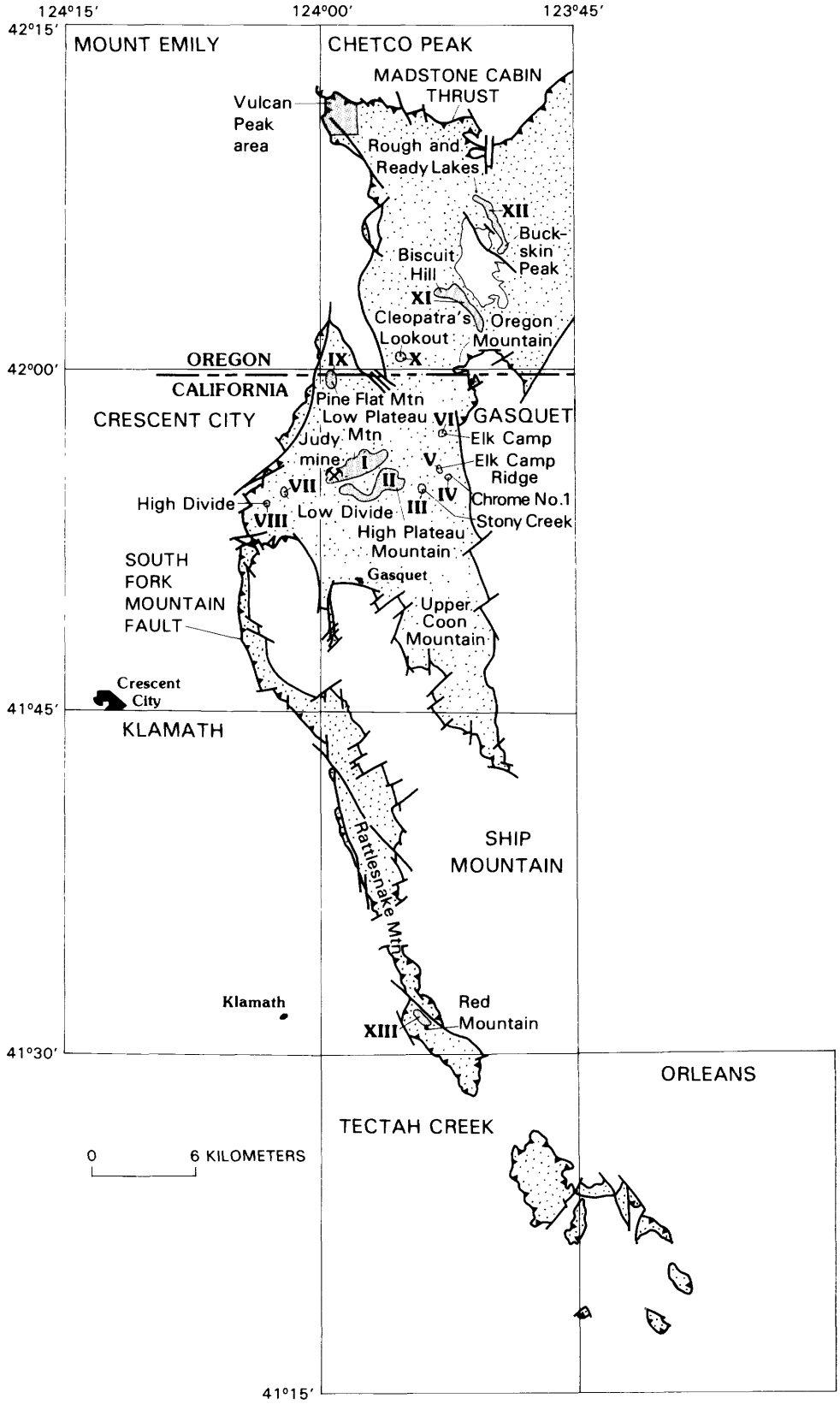


FIGURE 1.—Index map of northern California and southern Oregon, showing locations of areas of detailed study (fine-stippled areas denoted by roman numerals) within body of the Josephine Peridotite (coarse-stippled areas), and names and outlines of 15-minute quadrangles. See figure 2 for explanation of other symbols.

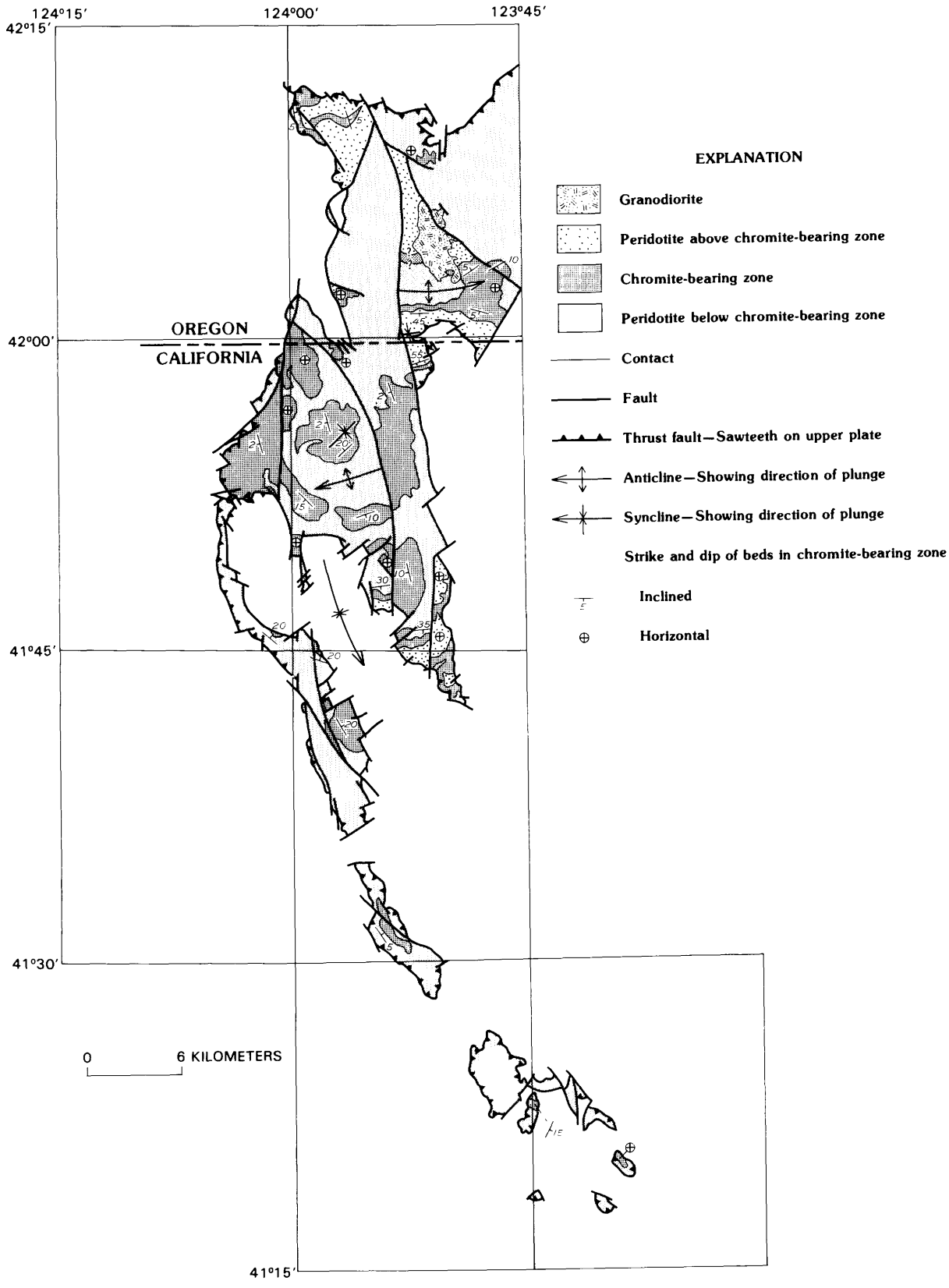


FIGURE 2.—Generalized geologic map of study area, showing internal macroscopic structure of the Josephine Peridotite.

west and are subhorizontal; a subhorizontal syncline trends northeast; and a synclinal trough, approximately coincident with a syncline in the upper parts of the ophiolite and overlying metasedimentary rocks, trends north-northwest and plunges south-southeast. The geometry and position of the chromite deposits imply that the chromitiferous dunite could have been emplaced contemporaneously with development of the overlying parts of the ophiolite. The chromite may have precipitated from chromitiferous dunitic magma over a particular range of pressure-temperature conditions not far below the gabbro.

The Josephine Peridotite and overlying rocks of the western Jurassic belt are interpreted from aeromagnetic data to compose a flat-lying sheet of rocks approximately 2.5 km thick (Evans, 1984; Griscom, 1984). Exposures of the base of the peridotite may be present in the Rattlesnake Mountain area and southeast of the mountain (Evans, 1984, pl. 1). This contact may be truncated by the South Fork Mountain fault.

The Josephine Peridotite is thrust over the Middle and Late Jurassic Rogue Formation (see Imlay, 1980, p. 55) and the Late Jurassic Chetco River complex (Hotz, 1971) along the Madstone Cabin thrust (Ramp, 1975). Juxtaposition occurred after the Late Jurassic and before emplacement of the Josephine ophiolite along the South Fork Mountain fault. Final emplacement of the ophiolite postdates the overridden Upper Jurassic and Lower Cretaceous rocks of the Coast Ranges called the Franciscan Complex in California and the Dothan Formation in Oregon. Irwin (1964, p. C9) assigned the thrusting to the Late Cretaceous Coast Range orogeny. Bailey and others (1970) concluded that the thrust at the west margin of the western Jurassic belt, possibly the South Fork Mountain fault, is continuous with the Coast Range thrust to the southeast.

## JOSEPHINE PERIDOTITE

The Josephine Peridotite, first named by Wells and others (1949, p. 9), is predominantly a medium- to coarse-grained, layered and foliated harzburgite tectonite, locally massive, containing less than 5 percent dunite, lherzolite, wehrlite, and orthopyroxenite in the study area. Layers of orthopyroxenite are as much as 10 cm thick, and of dunite as much as 30 cm. Another type of layering is formed by abrupt changes in the proportions of pyroxene and olivine in harzburgite and, locally, in dunite. The weak to conspicuous foliation in harzburgite is defined by planar arrays of enstatite grains. Detailed descriptions of parts of the peridotite, chiefly in southwestern Oregon, were given by Himmelberg and Loney (1973), Dick (1976), and Vail (1977). The following description is based on a study of the Vulcan Peak area (fig. 1) by Himmelberg and Loney (1973) and on observations of the peridotite south of their study area.

The harzburgite is predominantly xenoblastic granular and is composed chiefly of olivine and enstatite, with diopside and chromite as accessory minerals. Enstatite grains are as much as 4 mm long; some are subhedral, but most are anhedral with irregular or rounded shapes. They contain exsolution lamellae of clinopyroxene and kink bands. Some enstatite grains are embayed by olivine and contain rounded inclusions of olivine. These textures could suggest either an igneous or a pyrometamorphic origin (Pike and Schwarzman, 1977). Olivine grain size is difficult to determine because of serpentinization in most rocks; however, the grains appear to be generally anhedral and 1 to 5 mm long. Red-brown translucent and opaque varieties of generally anhedral intergranular chromite grains, about 1 mm across, are disseminated in amounts of less than 1 percent.

Although dunite makes up less than 5 percent of the peridotite, it is present in many exposures. The dunite occurs as irregular bodies, lenses, rods, and tabular bodies that are both concordant with and discordant to enstatite layering in harzburgite. In this report, the concordant bodies are referred to as layers, and the discordant bodies as dikes. The largest dike is 120 m wide, but most range in width from 1 to 50 cm. Chromite schlieren and chromite foliations, defined by planar arrays of chromite grains or by flattened chromite rods and nodules, occur in some dunite. These planar structures may be parallel to dunite-harzburgite contacts and to foliation in the harzburgite, or at an angle to the contacts and foliation. The presence of some chromite foliations that cut across dunite-harzburgite contacts and are visible in harzburgite as well as in dunite strongly suggests formation after establishment of the contacts. Alternatively, these relations might be produced by metasomatism of harzburgite to dunite, such as Dungan and Avé Lallemant (1977) described in the Canyon Mountain area. Although no clear evidence of metasomatism was found in the present study, origin of some of the dunite by this process cannot be ruled out for the Josephine Peridotite.

Olivine texture in dunite is generally hypidiomorphic granular. Grains are commonly 1 to 5 mm long, but some exceed 1 cm in length; at Red Mountain, southeast of Crescent City, Calif., some dunite contains olivine grains as large as 5 cm. Grains are subhedral, with rounded inclusions of olivine; other grains are anhedral and rounded. The olivine textures suggest a primary cumulate origin for the dunite. Kink bands are locally abundant in olivine. The chromite grains (generally smaller than 1 mm) are anhedral, subhedral, and

euhedral; some grains are intergranular to olivine, and some are inclusions in olivine. Some chromitiferous dunite exhibits chromite-net texture and occluded-silicate texture (fig. 3), terms introduced by Thayer (1969, p. 133–134). These textures, which are identical to primary textures in the Stillwater Complex (Jackson, 1961, figs. 9, 10, 30; Thayer, 1969, fig. 1), strongly suggest that some of the chromitiferous dunite originated as a cumulate ultramafic rock. Himmelberg and Loney (1973) recognized three kinds of dunite bodies in the Vulcan Peak area on the basis of chromite textures: (1) dunite containing euhedral chromite and occurring in irregular bodies, layers, and dikes; (2) dunite containing anhedral chromite and occurring in layers and irregular folded bodies; and (3) dunite containing disseminated subhedral chromite and poikilitic clinopyroxene that has rounded olivine inclusions and occurring in somewhat irregular dikes. These distinctions, however, were not made in this study.

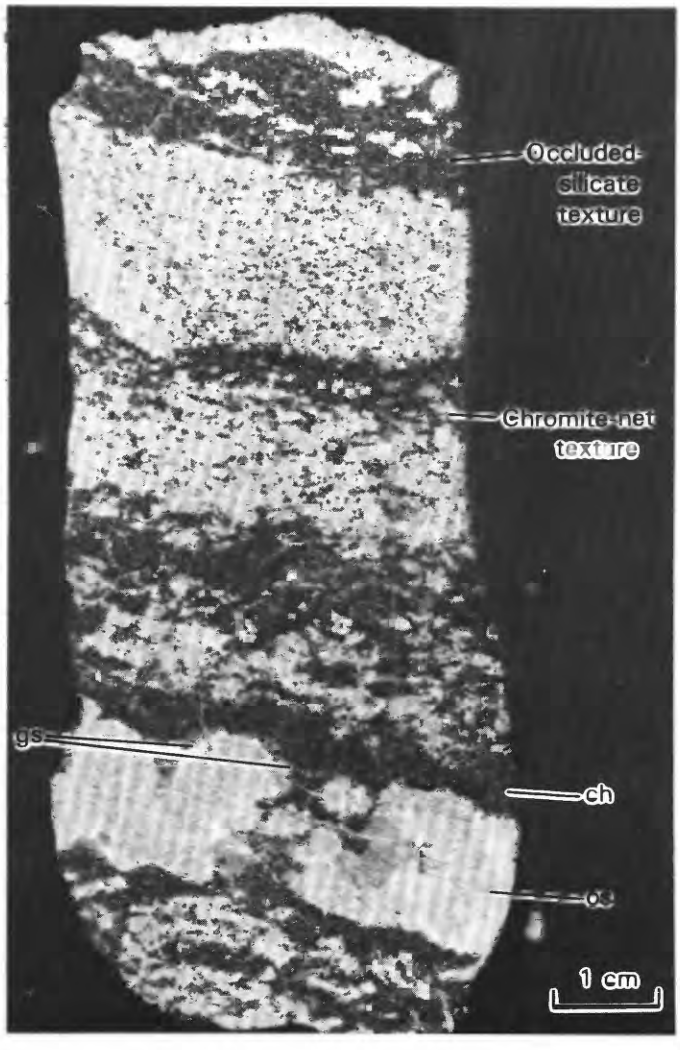


FIGURE 3.—Chromitiferous dunite, showing chromite-net and occluded-silicate textures. Light areas, olivine (serpentinized; os); gray areas, green serpentine (gs); dark areas, chromite (ch). Serpentinization of olivine occurs preferentially adjacent to chromite.

The chromitite occurs only in lenses and irregular bodies of dunite. These deposits, presently subeconomic, are scattered seemingly at random in the peridotite and in serpentinite derived from dunite. In the chromitite, chromite grains range in size from 1 to 5 mm and are either translucent red or opaque in thin section. They are anhedral intergranular to euhedral and occur chiefly with minor olivine, but also with enstatite and diopside. Some grains are rounded, with corroded cuspate boundaries, especially those in contact with enstatite; against diopside the chromite is euhedral. The corrosional texture resembles the reaction replacement textures described by Jackson (1961) for silicate minerals in the Stillwater Complex.

Himmelberg and Loney (1973, p. 1591–1595) obtained chemical analyses of harzburgite and dunite and electron-microprobe analyses of primary minerals from harzburgite, dunite, and chromitite. From these microprobe analyses, the olivine in harzburgite is uniformly $Fo_{91}$, in dunite $Fo_{91.9}$, and in chromite $Fo_{93.4}$. The most iron rich olivine is in dunite containing poikilitic clinopyroxene ($Fo_{87.8}$ from the dunite fraction, $Fo_{86.8}$ from an olivine inclusion in chromite). The following ratios and analysis fall within the range for orthopyroxenes and clinopyroxenes from other harzburgites: Mg/(Mg + Fe) ratio, 0.92; enstatite Mg/(Mg + Fe + Ca) ratio, 89–90; $Al_2O_3$ content, 1 to 3 weight percent. The chromite ranges considerably in the contents of Cr, Al, Mg, and $Fe^{2+}$. The grains are chemically inhomogeneous, and individual grains in each specimen vary in composition.

Two estimates of the temperature of formation of harzburgite in the Vulcan Peak area were presented by Himmelberg and Loney: 915 to 1,365 °C, averaging 1,150 °C, based on the distribution of Mg and Fe in coexisting orthopyroxene and clinopyroxene; and 950 to 1,015 °C, based on pyroxene compositions. The pressure of formation was estimated at 0.5 to 0.7 GPa at formation temperatures of 1,000 to 2,000 °C, using pyroxene compositions and experimentally determined stability fields.

No clear evidence was found bearing on the origin of the harzburgite as either a residuum of partial melting or a product of crystallization of an ultramafic or picritic magma in this study or in that by Himmelberg and Loney (1973). Dick (1976, p. 331; 1977a, b), however, cited textural, mineralogic, geochemical, and field data which he interpreted as evidence that the Josephine Peridotite underwent at least two periods of fractional melting. The chromite-net texture and the occluded-silicate texture of chromitiferous dunite, as well as the presence of

subhedral olivine grains containing rounded olivine inclusions, strongly suggest a magmatic stage in the formation of some of the dunite.

Orthopyroxenite dikes, ranging from 0.5 to 600 cm in width, occur in the peridotite. Their temperature of formation would be a minimum of 650 °C if they formed by hydrothermal alteration of olivine and addition of silica (Bowen and Tuttle, 1949), and about 1,300–1,400 °C if the dikes formed as a result of filter pressing of interstitial liquid from a peridotitic mush (Raleigh, 1965, p. 737). No evidence was found to favor either of these two hypotheses.

## STRUCTURAL ANALYSIS

### INTRODUCTION

The complexly deformed peridotite in the Vulcan Peak area was described by Loney and Himmelberg (1976). The present study attempts to characterize the internal structure of a 90-km-long segment of the Josephine Peridotite to the south and east of the Vulcan Peak area (fig. 1). For this purpose, data were gathered from 13 small areas of relatively well exposed peridotite; 12 of these areas are 6 to 30 km north of the town of Gasquet, and one area is at Red Mountain, 35 km south of Gasquet. Owing to limitations in exposure and field time, the number of data collected are few for such a large peridotite body; some of these areas provided much less information than others.

Less than 1 percent of the area underlain by peridotite was suitable for structural analysis (figs. 1, 4). Most good exposures are on or near ridgetops and at some chromite mines where removal of regolith is extensive. Also, 10 of the study areas are within the chromite-bearing zone of the peridotite, and so conclusions based on this information may be limited in application to this zone. Despite these obstacles to a definitive study of the structure of the peridotite, the field observations point to a complex sequence of structural events recorded by some consistent features in much of the peridotite. The following résumé and table 1 are presented as an aid to understanding the descriptions of structures and discussions of mesoscopic fabric below.

The Josephine Peridotite mainly consists of two phases—a predominant harzburgite tectonite and minor dunite. Some of the dunite has the characteristics of an igneous intrusion, some is a tectonite, some appears to be deformed igneous rock, and some may have a metasomatic origin.

The harzburgite tectonite typically exhibits layering defined by concentration of enstatite and foliations defined by planar arrays of enstatite, structures that are emphasized by layers of dunite parallel to the enstatite layering and foliation. Orientations of these planar structures may be uniform over a few square kilometers, as on Low Plateau Mountain, or may vary widely, as on Red Mountain, Calif. Well-defined marker units are absent, and so the macroscopic structure of the harzburgite cannot be easily determined. Clues to the internal structure are supplied by detached isoclinal-fold hinges and enstatite rods that have the profiles of detached fold hinges. Many of the isoclinal folds and enstatite rods plunge at low angles north-northwest. These minor tight fold hinges indicate extreme flattening in a plane parallel to the axial planes of the folds and to the foliation and layering in the harzburgite, which parallel the axial planes. During such a ductile deformation event, most preexisting structures would have been obliterated, greatly modified, or rotated. The deformation probably occurred under high-pressure/temperature conditions, possibly in a subcrustal environment (deformation 1, table 1).

Layering, foliation, and axial planes of isoclinal folds in harzburgite are folded about the axes of open folds, which plunge at low angles north-northwest (deformation 2, table 1). Even younger open folds appear to fall into three general groups based on the orientations of axes: plunging northeast and east-west at low angles, and steeply plunging (deformations 3, 4, and 5, respectively). Some of the folds, especially in the northeast-trending group, have well-developed axial-plane foliations that are defined by planar arrays of chromite grains in dunite.

The younger ages of the open folds relative to the early isoclinal folds are based on a probable sequence of deformation from a ductile to a less ductile folding,

FIGURE 4.—View northward from Red Mountain (foreground) toward Rattlesnake Mountain (center skyline). Outcrops on Rattlesnake Mountain are very poor, as is typical of most of the southern part of the peridotite. Distance from foreground to high part of Rattlesnake Mountain is 11 km; distance across flat part of Rattlesnake Mountain is 1.6 km. Top of Rattlesnake Mountain may be part of the Klamath peneplain (Diller, 1902, p. 15–18).

TABLE 1.—*Summary of structures, and the orientations and ages of structures, for deformations affecting the Josephine Peridotite*

| Deformation | Structures | Orientations | Age |
|---|---|---|---|
| 9 | South Fork Mountain and other faults. Postcrystalline emplacement-obduction | Generally strike N-S and dip at low angles E. | Late Cretaceous; Coast Range orogeny. |
| 8 | Madstone Cabin thrust. | Strikes E-W. and NE. and dips at low angles S. and SE. | Post-Late Jurassic. |
| 7 | Chromite zone in peridotite folded into a broad syncline. No mesoscopic structures in the peridotite. | Synclinal axis plunges at a low angle SSE. | Post-Late Jurassic, after deposition of metasedimentary rocks overlying the Josephine ophiolite. |
| 6 | Warping and faulting of orthopyroxenite dikes. | No data---------- | |
| 5 | Generally open folds. Locally, chromite foliation parallels axial planes. | Axial planes: varying strikes, steep dips; linear elements: varying trends, steep plunges. | Relation to deformations 3 and 4 not known; possibly more than one episode included. |
| 4 | Generally open folds. Flexural-slip mechanism. Local isoclinal folding and chromite rods in chromitiferous dunite. Local chromite foliation parallels axial planes. | Axial planes: varying strikes, steep dips; linear elements: plunges at low to moderate angles angles E. and W. | Late Jurassic, penecontemporaneous with parts of the Josephine ophiolite. |
| 3 | Generally open folds. Isoclinal folds and chromite rods in chromitiferous dunite. Chromite foliations are best developed parallel to axial planes of these folds. Dunite dikes parallel axial planes, with local brecciation. | Axial planes; strike NE, dip at low to high angles NW. and SE.; linear elements; plunge at low to moderate angles NE. Possible steep conjugate folds locally. | |
| 2 | Open folds. Flexural-slip mechanism | Axial planes; strike NW., dip steep, linear elements: subhorizontal, trend NW. | |
| 1 | Isoclinal folds. Orthopyroxenite and dunite rods. Pullapart layers. Axial planes parallel foliation and layering in harzburgite. | Planar elements; varying. linear elements; mostly plunge NNW. and NW. at low angles. | Pre-Middle Jurassic, predating gabbro and diorite dikes. |
| | Pre-episode 1: rock may have contained folds, dunite dikes, dunite and enstatite layering and deformational or primary cumulate textures. | No data ---------- | |

evidence of small-circle rotation of isoclinal folds about generally east-west trending axes, and the occurrence of open folds unaccompanied by northwest-trending isoclinal folds in certain northeast-striking chromitiferous dunite dikes.

Relative ages of the northeast- and east-west-trending folds are suggested by the parallelism of some dikes, containing both northeast- and east-west-trending minor folds, to the axial planes of northeast-trending folds in general. These dikes appear to be postkinematic with respect to some northeast-trending folds in harzburgite. The northeast-trending minor folds within the dikes suggest that dike emplacement may have taken place during a phase of strain relaxation or rebound in the deformation, or that these minor folds represent relatively minor, local deformation associated with dike emplacement. The east-west-trending minor folds may have formed during a subsequent deformation.

Evidence for the ages of steep folds relative to the other open folds is not definitive. In some outcrops, the steep folds are approximately perpendicular to northeast-trending folds and may constitute a conjugate set in a $B \perp B'$ tectonite. In one area, steep folds make up the dominant set and may represent a separate folding episode.

Subsequent episodes of deformation appear to have affected the earlier structure of the peridotite very little or only on a macroscopic scale. Warping and faulting of the late orthopyroxenite dikes that cut dunite dikes indicate late low-intensity strain (deformation 6, table 1). No mesoscopic structures are associated with folding of the chromite zone of the peridotite into a broad syncline plunging south-southeast (fig. 2; deformation 7, table 1). Later, the peridotite was emplaced during at least two events (deformations 8, 9) that included extensive serpentinization.

Standard techniques of structural analysis were used (Turner and Weiss, 1963; Ramsay, 1967). Attitudes, styles, and geometric relations of several types of planar and linear fabric elements were observed. The mesoscopic structures in each part of the study area were analyzed separately. Crystalline fabric elements, described below, were correlated between parts of the study area (areas I–XIII), and inferences were made regarding the deformational history of the peridotite. Petrofabric studies on eight samples were carried out and correlated with the mesoscopic fabrics.

The profile drawings of linear structures in this report are oriented with the top of the page as the up direction and the page surface perpendicular to the downward-plunging direction. Trends of minor structures, (small arrows) are referred to a 360° compass with 0° (north) at the top of the page and 90° (east) to the right; numbers at the heads of arrows are the angles of plunges.

Structural data were plotted as points on the lower hemispheres of equal-area projections. North is indicated by a short line pointing toward the top of the page, and vertical by a cross in the center of the primitive circle. Some of the structural data ($n>20$) were contoured by a method originally described by Kamb (1959), using a variable counting area; this area is a function of the number of data points and the frequency of significant deviations from a uniform spatial distribution. Contours are in intervals of $\sigma$ or $2\sigma$, where $2\sigma$ is the expected number of data points within a counting area for a uniform distribution across the entire stereogram. A point density greater than $3\sigma$ is considered to be a significant deviation from a random distribution. Pole-free areas indicate a possibly significant absence of data points.

The following descriptions of structures and structural analysis deal with deformations 1 through 6 because these episodes were inferred from minor structures in the relatively unserpentinized part of the peridotite. No minor structures were found to correspond to deformation 7, and deformations 8 and 9 are postcrystalline. The timing of the these last three deformations, however, is important in placing upper limits to the crystalline deformations and in understanding how these deformations fit into the regional tectonic development.

## DESCRIPTIONS OF MINOR STRUCTURES

### LAYERS AND FOLIATIONS

The most common structures in harzburgite are layers of dunite and of orthopyroxenite (chiefly enstatite and minor olivine), such as those shown in figure 5. Harzburgite layering, defined by changes in the proportions of enstatite and olivine, parallels orthopyroxenite layering. Some of the layers are traceable without change in thickness for several meters in a single outcrop; however, these layers generally are not sufficiently distinctive to be followed from one outcrop to another except for some dunite bodies mapped by J.P. Albers (unpub. data, 1977) and H.R. Cornwall (unpub. data, 1979). The layering could have formed by: (1) metamorphic differentiation, (2) precipitation from a magma, or (3) a combination of precipitation and differentiation.

Some layers in harzburgite consist of dunite or enstatite-poor harzburgite containing pods of coarse-grained (larger than 2 cm) orthopyroxenite (fig. 6). These types of layers parallel orthopyroxenite layers. The orthopyroxenite pods appear to be segments of formerly continuous orthopyroxenite layers. These layers were pulled apart in the plane of the layering; some of the segments were also plastically deformed. The large grain size of the orthopyroxenite suggests recrystallization, possibly accompanying disruption of the layers. The pullapart structures point to large extensional strain in the plane of the layering but do not clearly indicate the mechanism of deformation. These structures could have resulted from: (1) pervasive plastic deformation of the rock, in which visible effects of the

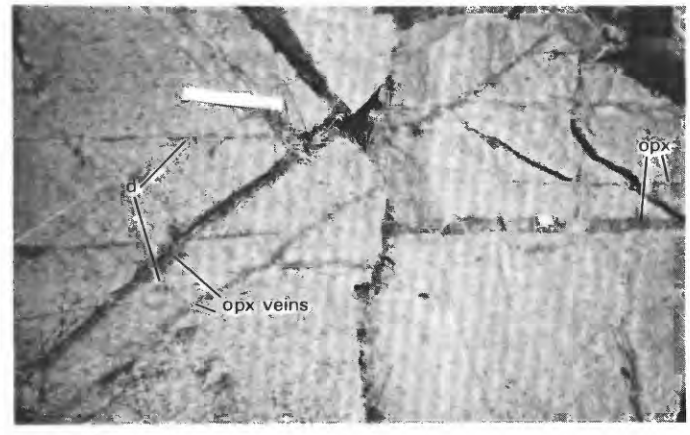


FIGURE 5.—Orthopyroxenite (opx) and dunite (d) layers in harzburgite. Layers are cut obliquely by orthopyroxenite veins. Scale is 20 cm long.

deformation were confined to selected zones containing mechanically inhomogeneous materials; (2) plastic deformation confined to narrow zones in the rocks; or (3) flow of a crystal mush having a composition of dunite or orthopyroxene-poor harzburgite and containing orthopyroxenite as a solid phase.

Chromite-rich layers or schlieren in dunite most commonly occur in the central parts of dunite layers. In places, chromite schlieren are near dunite-harzburgite contacts, and some are at a low angle to external contacts of the dunite body. Locally, as on Upper Coon Mountain (fig. 1), the chromite schlieren consist of angular fragmented chromite nodules indicating brecciation of the chromite.

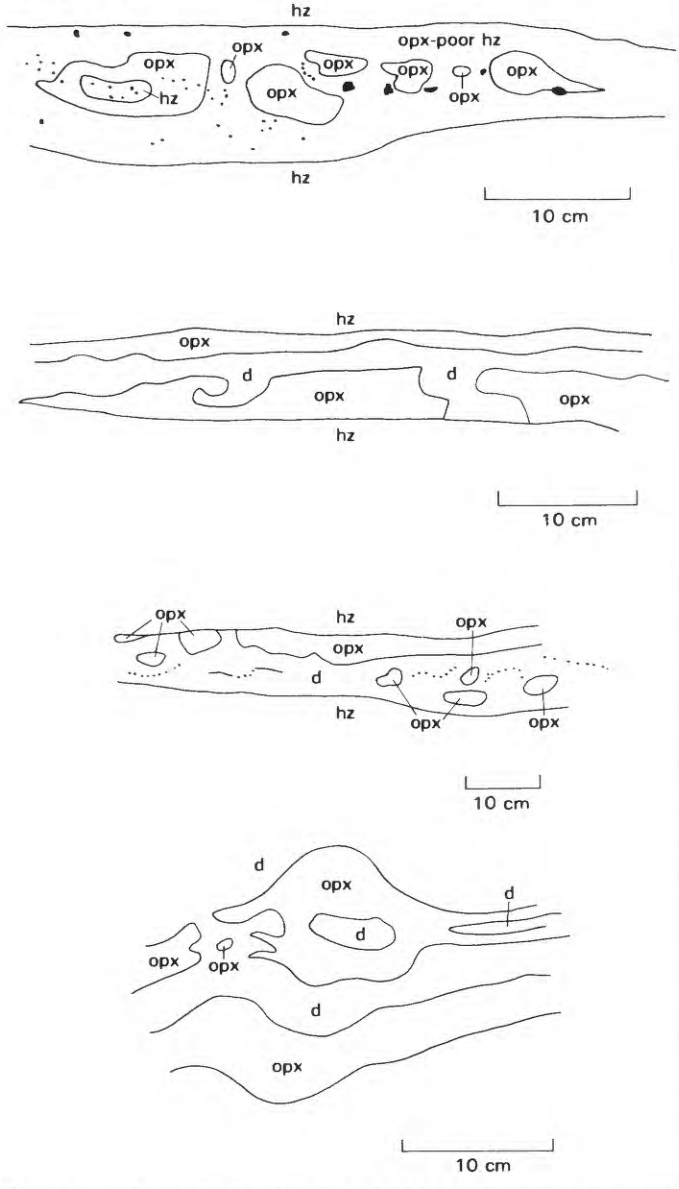


FIGURE 6.—Layers in harzburgite exhibiting pullapart structure. d, dunite; hz, harzburgite; opx, orthopyroxenite. Dots and dark line segments represent chromite grains and lenses, respectively.

A foliation defined by planar arrays of orthopyroxene grains is present in many places in harzburgite. Typically the foliation is subparallel to layering in the same outcrop and, locally, to the axial planes of isoclinal folds of layers. The orthopyroxene foliation and the layering are subparallel even in a comparison of the attitudes of the two types of fabric elements in nearby outcrops. This relation suggests that the layering and foliation formed contemporaneously, or that early layering was rotated into parallelism with the foliation.

Chromite schlieren in dunite locally contain an internal foliation defined by planar arrays of chromite grains or pods. Generally these chromite foliations are oriented at high angles to the chromite schlieren (fig. 7) and are commonly subparallel to the axial planes of nearby minor folds. Flattening of the outlines of olivine grains near axial chromite foliations in the plane of the foliation (fig. 8) indicates the orientation of the maximum principal compressive stress, $\sigma_1$, for the deformation at a high angle to the foliation. In places, the chromite foliation cuts across dunite-harzburgite contacts and parallels a foliation of accessory chromite in harzburgite, relations which would indicate that the chromite foliation postdates the dunite-harzburgite contacts, if metasomatism can be ruled out. The contacts, however, do not appear to be greatly affected by formation of the late chromite foliation; possible minor crenulations of the contacts may be the only mesoscopic effect. In some harzburgite, abundant magnetite forms

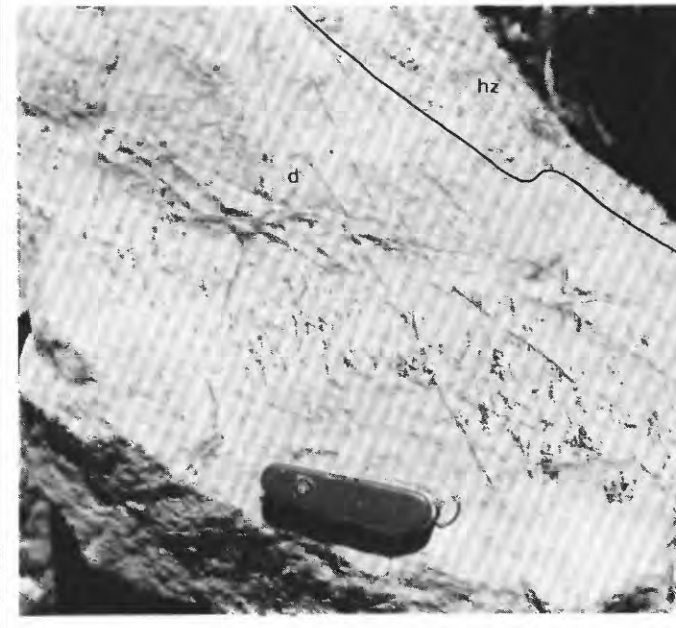


FIGURE 7.—Chromite foliation in dunite at a high angle to dunite (d)-harzburgite (hz) contact. Knife is 10 cm long.

foliations, the attitudes of which cannot be measured because of the strong magnetic effects of the magnetite.

Planar arrays of flattened chromite rods and nodules define a foliation in some dunite bodies. On Red Mountain, this type of foliation is subparallel to enstatite foliation in harzburgite and at an angle to the dunite-harzburgite contacts. The tonguelike form of the dunite in figure 9 suggests that the dunite intruded the harzburgite and that the flattened chromite-rod foliation postdates dunite emplacement.

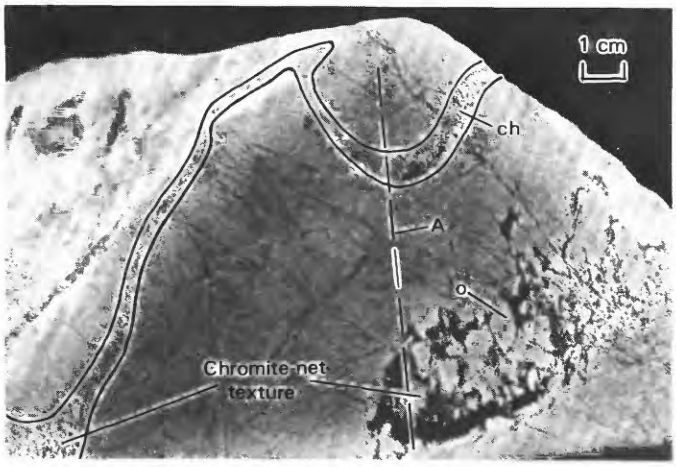


FIGURE 8.—Deformed chromite-net texture in dunite. Axial plane (A) of fold of chromitiferous layer (ch) dips steeply. Olivine grains (o) are flattened subparallel to axial plane. Chromite foliation is partially developed parallel to axial plane.

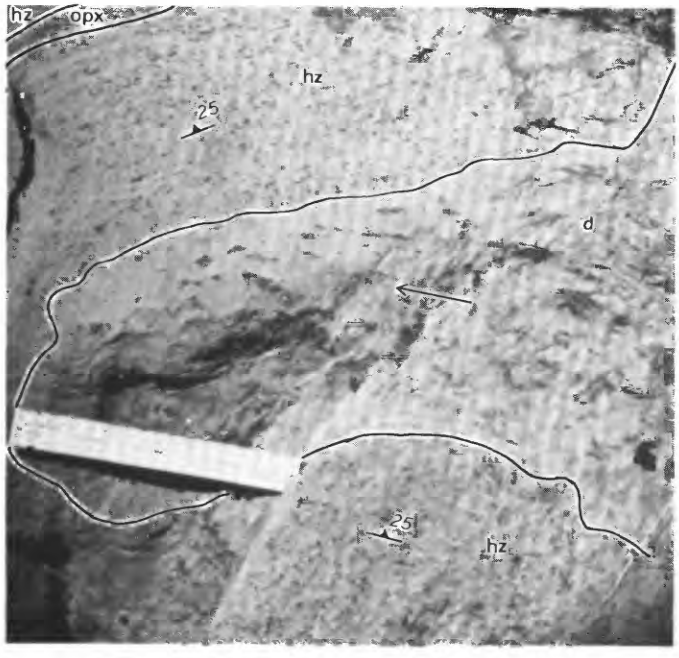


FIGURE 9.—Flattened rods of chromite in dunite, plunging 30°, N. 15° W., at an angle to dunite-harzburgite contact. Foliation, defined by planar array of flattened rods, is subparallel to enstatite foliation in harzburgite. d, dunite; hz, harzburgite; opx, orthopyroxenite. Arrow indicates direction of plunge of rods. Barb and line show dip and trace of harzburgite foliation. Scale is 20 cm long.

## FOLDS

Folds of dunite, enstatite, and chromite layers have amplitudes of generally 5 to 100 cm. Folds with amplitudes greater than 1 m are difficult to recognize because the fold hinges are not exposed. A few dunite folds with amplitudes of 50 m, however, were mapped by J.P. Albers on Low Plateau Mountain.

Isoclinally folded bodies, with greatly thickened hinge zones and detached hinges, probably represent the oldest type of fold in the peridotite (fig. 10; deformation 1, table 1). These folds generally plunge at low angles north-northwest and northwest; axial planes are subparallel to enstatite foliation and layering in adjacent harzburgite. The isoclinal folds and detached fold hinges indicate large extension in the plane of the harzburgite foliation. Although some extension occurred parallel to the fold axes, the axes are not clearly in the direction of maximum extension. Slip could have occurred at any angle, though not exactly parallel to the fold axes. Locally wide variation in the axes of detached isoclinal folds, as in area I (fig. 1), suggests (1) initial differences in fold orientations before the deformation, or (2) rotation of early folds as the deformation progressed. Axes of folds formed before

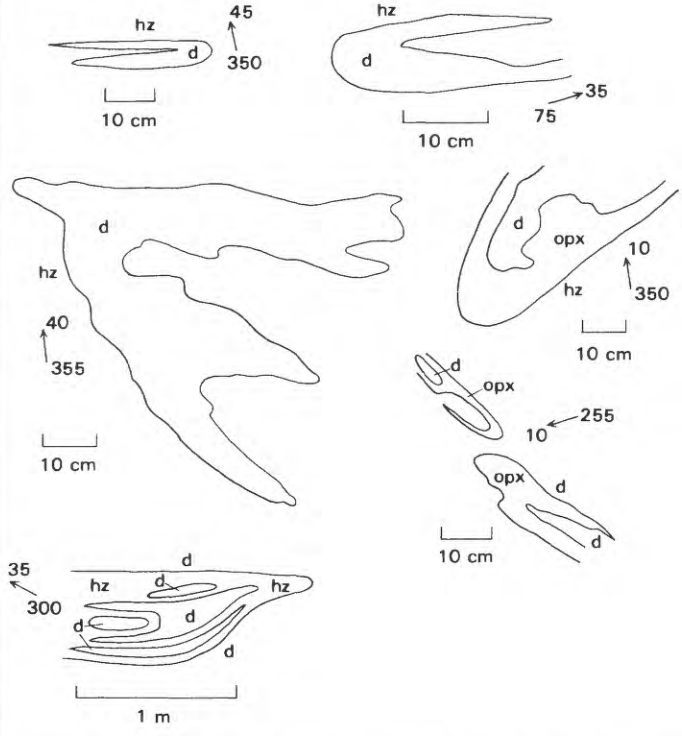


FIGURE 10.—Isoclinal folds in peridotite. d, dunite; hz, harzburgite; opx, orthopyroxenite. Arrows show orientation of hingelines.

flattening would be rotated into the plane of flattening, and the preexisting angular relations would be obliterated. Assuming that these structures formed by plastic deformation, the extreme flattening of the folds implies a maximum principal finite compressive strain and, possibly, maximum compressive stress oriented at a high angle to the axial planes (Ramsay, 1967, p. 429) and to the harzburgite foliation at some stage in the folding. This deformation could be (1) an early pervasive plastic deformation in which pretectonic structures were drastically modified or obliterated, or (2) a deformation confined to narrow zones in the peridotite. Similarity of the orientations of the axial planes of isoclinal folds to those of foliation and layering in harzburgite suggests that these planar fabric elements are related and is consistent with the pervasiveness of the deformation, even though isoclinal-fold hinges are not common everywhere in the harzburgite. The paucity of isoclinal-fold hinges in some parts of the peridotite may be due to the low probability of finding the narrow hinge zones in the poorly exposed terrain. However, hinges may also be rare in places, owing to their obliteration during the intense ductile deformation.

Other folds of dunite and enstatite layers are open in profile and generally exhibit little tectonic thinning or thickening of folded layers (figs. 11, 12). Folding of some axial planes of isoclinal folds in an open style about axes with nearly the same orientation as the isoclinal-fold axes (fig. 11) indicates a stage of less intense plastic deformation after the isoclinal folding (deformation 2, table 1). Other open folds (fig. 12) and the lineations parallel to them are divided into three groups on the basis of orientations: (1) plunging at low to moderate angles, mostly in the northeast quadrant (deformation 3, table 1); (2) plunging at low to moderate angles east and west (deformation 4); and (3) plunging steeply (deformation 5). These open folds probably postdate the early isoclinal folds because: (1) these open folds would be unlikely to have remained open after the early flattening deformation, unless the flattening affected only narrow zones of the peridotite; (2) early isoclinal folds are rotated about axes coincident with the axes of open folds in areas II and X (fig. 1); (3) axial planes of open folds are generally at large angles to the early harzburgite layering and foliation; and (4) dunite dikes cutting the layering and foliation in harzburgite contain folds correlated with the later open folds.

Minor structures in northeast-striking dunite dikes suggest that the northeast-trending folds probably predate the east-west-trending folds. The dikes, subparallel to the axial planes of northeast-trending folds in harzburgite, probably postdate these folds but also contain northeast- and east-west-trending minor folds. The northeast-trending minor folds in the dikes may

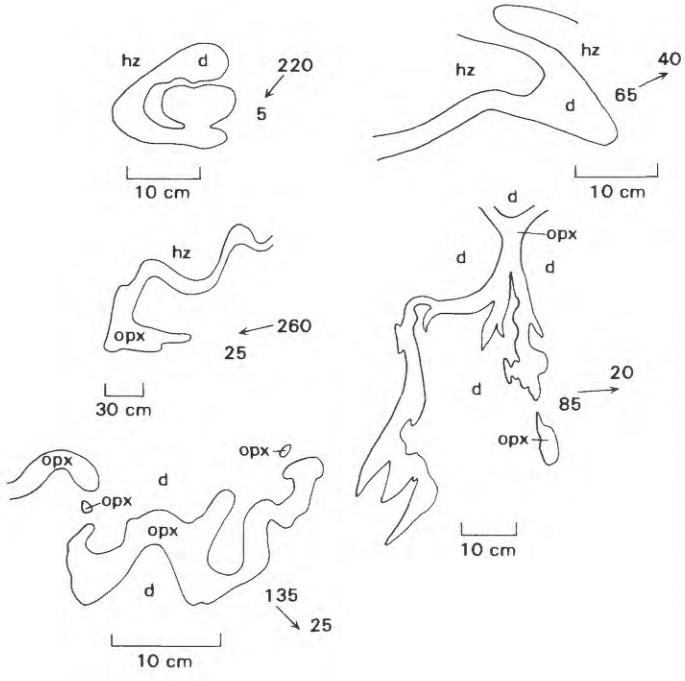


FIGURE 11.—Refolded early isoclinal folds in peridotite. Axes of refolding are subparallel to early isoclinal axes. d, dunite; hz, harzburgite; opx, orthopyroxenite. Arrows show orientation of hingelines.

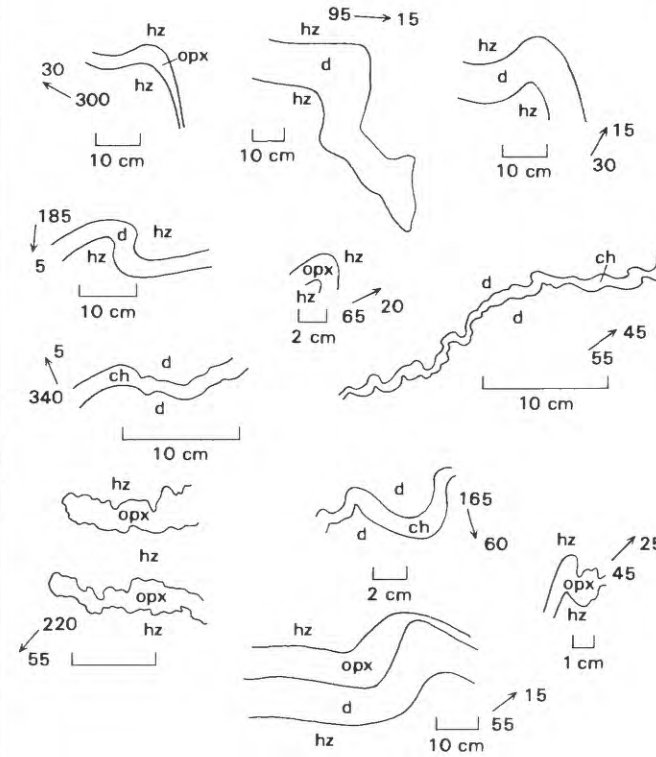


FIGURE 12.—Open folds in peridotite. ch, chromitite; d, dunite; hz, harzburgite; opx, orthopyroxenite. Arrows show orientation of hingelines.

have formed during or after dike emplacement and may reflect a final phase of deformation 3 or a local event related to emplacement. The east-west-trending minor folds in the dikes would most likely postdate these events.

Some steep folds are at nearly 90° to the northeast-trending folds in some outcrops and may be a conjugate set in a B⊥B′ tectonite. In area XII (fig. 1), steep folds make up the dominant set, possibly formed during a separate folding episode of unknown age relative to the other open folds.

Three of the macroscopic folds of the chromite zone shown in figure 2 are broad warps, the axes of which parallel the axes of minor northeast- and east-west-trending open folds. On this basis, these large folds may correlate with the deformations deduced from the minor folds.

The north-northwest-trending macroscopic syncline south of Gasquet is a very late stage fold affecting the chromite zone and the overlying sequence of ophiolite and metasedimentary rocks (deformation 7, table 1). No mesoscopic structures correlatable with this deformation were found in the peridotite.

Some of the open folds of dunite and orthopyroxenite layers in the harzburgite occur near chromitiferous dunite in which the chromite layers are isoclinally folded along axes subparallel to the open folds; limbs of the isoclinal folds are tectonically thinned and thickened and are pulled apart. These relations suggest that, internally, the chromitiferous dunite yielded in a very ductile manner, whereas the dunite and orthopyroxenite layers in harzburgite were much less ductile.

Another example of a ductility contrast occurs locally at High Plateau Mountain (subarea IIc, fig. 1), where plastically deformed chromitite layers are adjacent to angular and subangular blocks of dunite in a matrix of chromitite (fig. 13). Either minor deformation or, possibly, replacement of olivine by chromite has resulted in a mismatch of opposing edges of the dunite fragments. The fragments appear to be segments of a formerly continuous lens; however, no fault zone lies between the chromitiferous dunite deformed in the ductile mode and the segmented dunite. The compositional contrasts in this outcrop may be related to differences in the amounts of liquid phases present at the time of deformation; variations in these amounts could have influenced the mechanical properties and deformational mode of the rock. Boudier and Nicolas (1977, p. 75) noted no microstructural differences between unmelted lherzolite and that deformed with 5 to 10 percent of melt. Therefore, if a fluid phase is to enhance ductility, it may have to exceed 10 percent of the peridotitic mush at the time of deformation but not make up so large a fraction that most of the strain is absorbed by movement of the fluid phase alone (see George, 1978). In the case of the outcrop shown in figure 13, especially in the chromite, a substantial part of the fluid phase would presumably have had to be expelled during and after ductile deformation. What may be evident here is the result of crystal-mush flow, possibly in a mush containing nearly completely crystalline blocks (dunite lens), followed by filter pressing.

### RODS

Rods of dunite (max 1 m long), orthopyroxenite (max 2 m long), and chromitite (max 0.1 m long) have oval to irregular profiles, and some have profiles resembling folds that are interpreted as detached fold hinges. A few orthopyroxenite rods have dunite cores; some have dunite shells. Dunite and orthopyroxenite rods most commonly parallel the axes of early northwest-trending isoclinal folds (deformation 1, table 1) but also occur parallel the axes of other fold groups (deformations 3–5). Chromite rods parallel the fold axes of all fold groups but are the main type of rods parallel to the axes

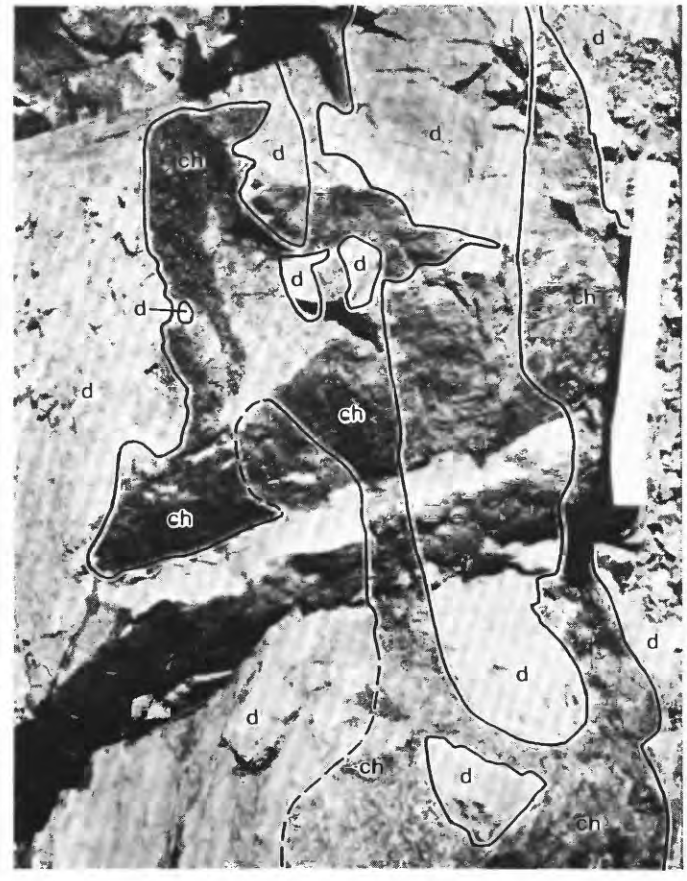


FIGURE 13.—Chromite (ch) in dunite (d). Solid lines, sharp dunite-chromitite contacts; dashed lines, gradational contacts between zones of disseminated chromite and nearly chromite free dunite. Scale is 20 cm long.

of open folds. These relations are consistent with a hypothesis that the chromitiferous dunite behaved more plastically than the other rock types during the episodes of open folding.

## MINERAL LINEATIONS

Lineations, defined by alignments of the long axes of enstatite grains, occur on a few of the rare surfaces weathered parallel to dunite-harzburgite contacts. Other lineations, defined by alignments of chromite grains, occur in some dunite bodies. These lineations are generally penetrative elements in the dunite and are visible on surfaces that cut the dunite at a low angle to the lineation.

## DIKES

Dunite dikes, ranging in width from 0.01 to 120 m, are most abundant in the Low Divide-High Divide area and on Red Mountain, Calif. (areas VII, VIII, XIII, fig. 1). Some irregular bodies may be dikes that were emplaced in harzburgite before the early isoclinal folding and formation of the foliation and layering (fig. 14). The presence of apophyses that intrude along orthopyroxene layering and foliation (fig. 15) suggests that some dunite "layers" may be intrusive in origin and not the products of metamorphic differentiation or cumulate processes. The central location of chromite schlieren in some dikes suggests that the dunite "layers" containing such schlieren may also be of intrusive origin. Some dikes contain folded chromite layers with fold axes correlated only with the three groups of open folds. These dikes must have been emplaced after the early episode of isoclinal folding but before development of the open folds; some of the dikes postdate some of the northeast-trending open folds. Dunite dikes cutting across others further indicate more than one episode of dunite emplacement (fig. 16). Dikes that appear to be unaffected by folding may have formed after much of the folding of the peridotite. The occurrence of several generations of dunite dikes is consistent with the suggestion by Dick (1977a) that magma generation in the mantle by fractional melting occurred sporadically and that the dunite dikes are the crystallized remnants of the magmas that passed through the peridotite to the crust.

Orthopyroxenite dikes, 0.5 to 300 cm thick, cut across layering and foliation in the harzburgite and across the dunite dikes. Crosscutting of some orthopyroxenite dikes by others indicates more than

FIGURE 14.—Irregular dunite body in harzburgite that may have been an early dike folded during early plastic deformation. Fold axes plunge 55°, N. 85° E. Hammer handle is 30 cm long.

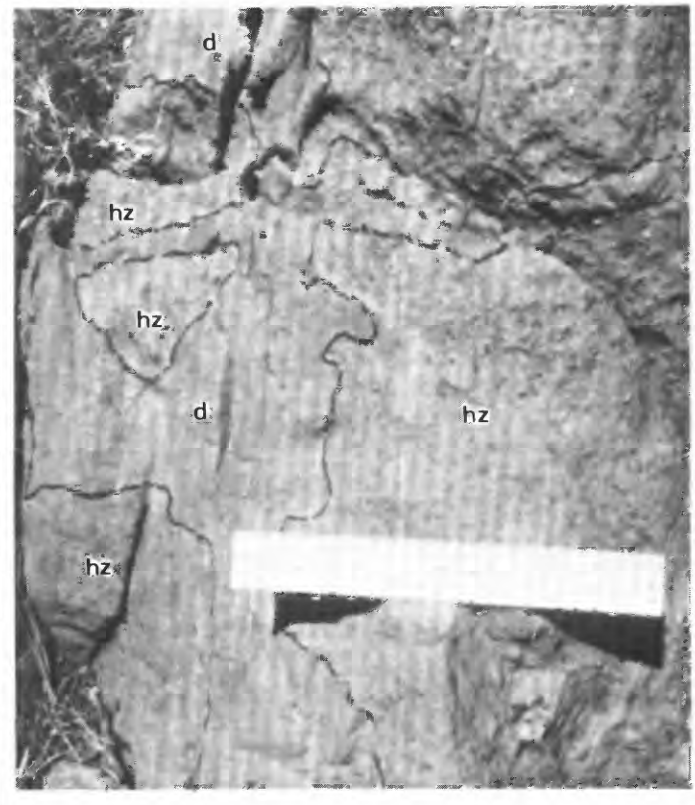


FIGURE 15.—Dunite (d) dike in harzburgite (hz). Subhorizontal dunite apophyses follow layering and foliation in harzburgite. Scale is 20 cm long.

one episode of emplacement. Broad warping and faulting of some dikes reflect low-intensity ductile and brittle deformation (figs. 17, 18).

Composite dunite-orthopyroxenite dikes, consisting of tabular segments of dunite separated by tabular segments of orthopyroxenite, intrude the harzburgite (fig. 19). No evidence was found to indicate whether the orthopyroxenite was emplaced after the dunite or vice versa, or whether the dike segments formed by intrusive, metasomatic, or fusional processes.

## SUMMARY

The Josephine Peridotite underwent an early ductile deformational event during which preexisting textures and structures of primary cumulate or tectonic origin were largely destroyed. The structures resulting from the flattening and rotation during this event are the enstatite and dunite layering, the enstatite foliation, and the detached isoclinal fold hinges with axial planes parallel to the layering and foliation (deformation 1, table 1). Most linear elements (folds, rods, mineral lineations) of this deformation plunge at low angles north-northwest. These structures were refolded around north-northwest-trending fold axes in an open style during a later, less intense deformation (deformation 2). Subsequent open folds, probably beginning with those plunging at low angles northeast (deformation 3), developed, and a chromite foliation formed parallel to the axial planes of these folds. Some steep folds may have been formed locally at this time in a conjugate ($B \perp B'$) relation to the northeast-trending folds. The open east- west-trending folds may postdate the northeast-trending folds (deformation 4). Some steep folds, with an unknown relation to other open folds, may represent a distinct and, possibly, local episode of deformation (deformation 5). A few chromite foliations were observed subparallel to the axial planes of east-west-trending and steeply plunging folds. Some macroscopic

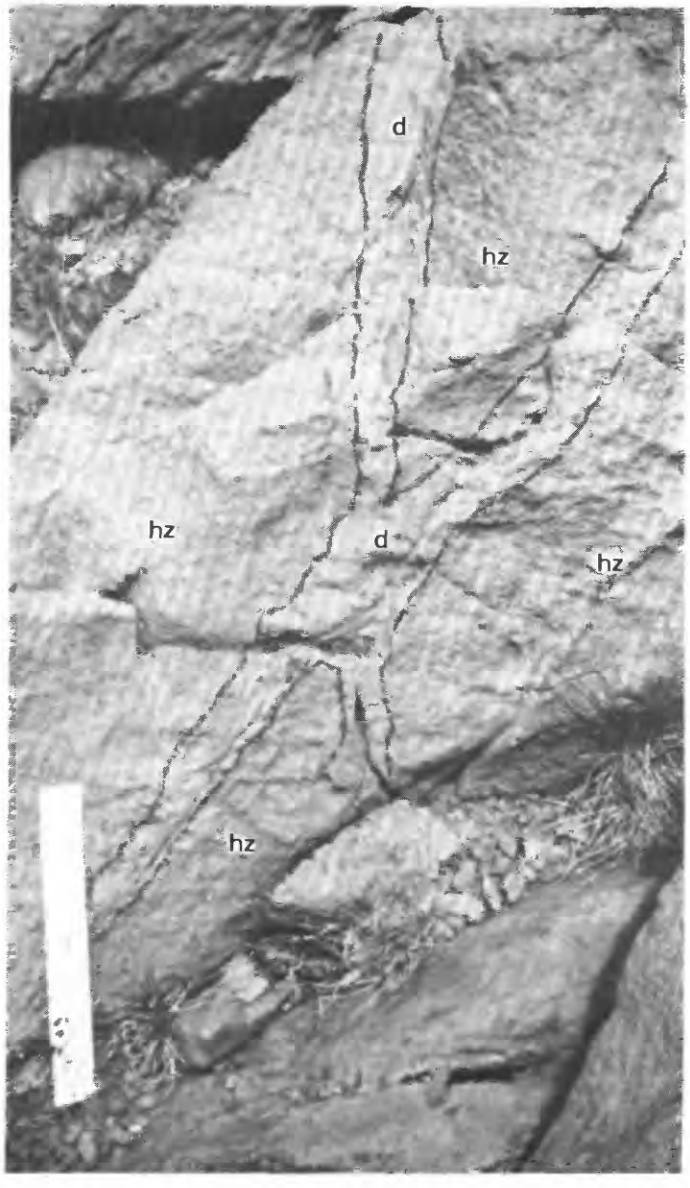


FIGURE 16.—Intersecting dunite (d) dikes in harzburgite (hz). Scale is 20 cm long.

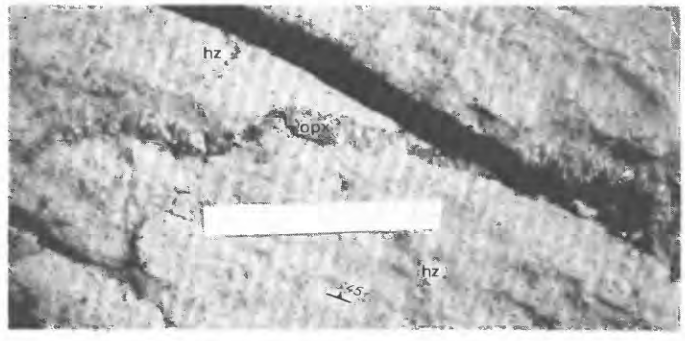


FIGURE 17.—Warped orthopyroxenite (opx) dike. Dike cuts across weakly defined orthopyroxene foliation in harzburgite (hz) at a low angle. Barb and line show dip and trace of foliation. Scale is 20 cm long.

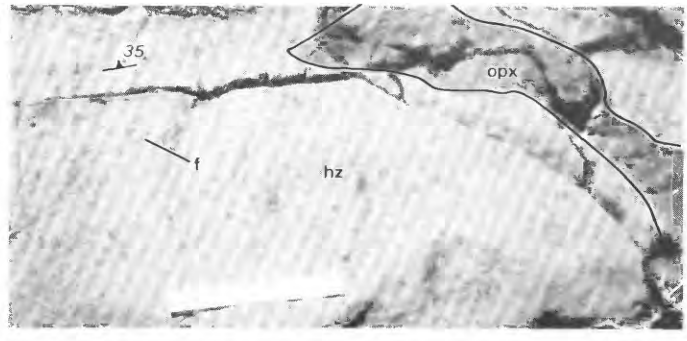


FIGURE 18.—Faulted (f) orthopyroxenite dike. Separation must be more than 15 cm because offset segment of dike was not found. hz, harzburgite; opx, orthopyroxenite. Barb and line show dip and trace of harzburgite foliation. Scale is 20 cm long.

folds of the chromite zone may correlate with the northeast- and east-west-trending folds. Warping and faulting of late orthopyroxenite veins (table 1, deformation 6) mark the latest event, during which minor structures formed in the unserpentinized peridotite. One large syncline, formed after development of the overlying ophiolite and sedimentary rocks (deformation 7), is not reflected in these minor structures.

Dunite dikes were probably emplaced throughout the structural development of the peridotite. Emplacement of some dikes can be crudely dated as: (1) before the early plastic deformation (deformation 1), (2) after the early plastic deformation, (3) postkinematic to some northeast-trending folds in harzburgite (deformation 3), and (4) after most of the open folding. In general, the orthopyroxenite dikes postdate the dunite dikes, although the presence of composite orthopyroxenite-dunite dikes suggests possible overlap of dunite and orthopyroxenite emplacement.

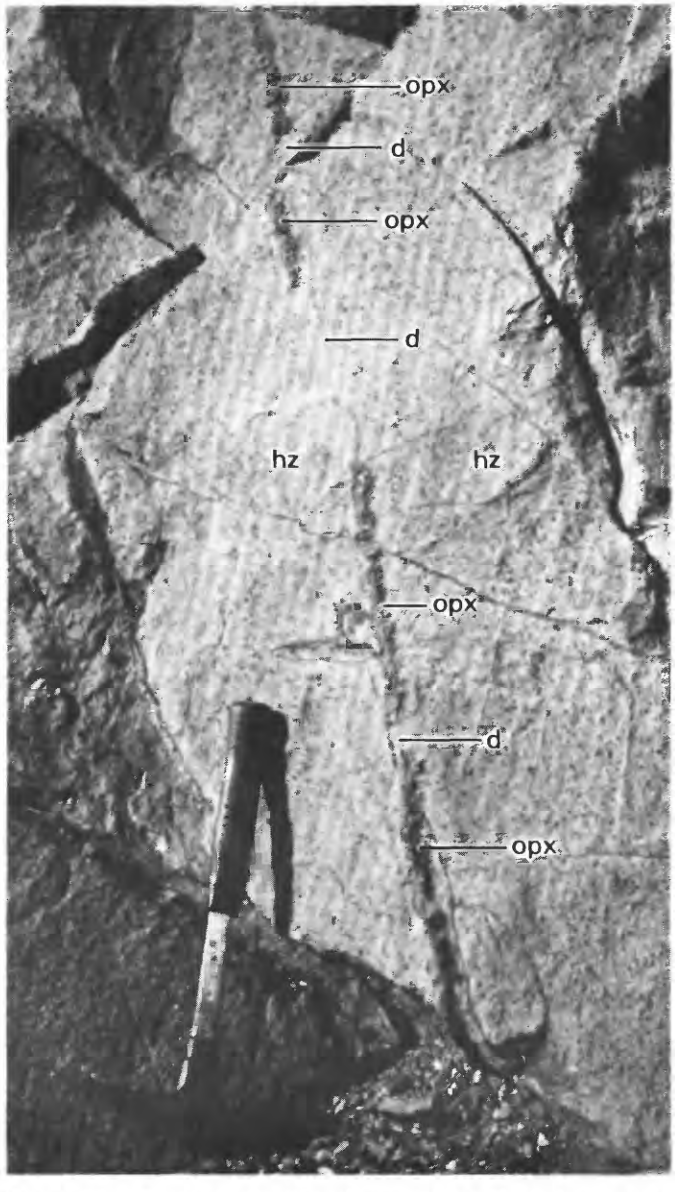


FIGURE 19.—Composite dunite-orthopyroxenite dike in harzburgite (hz). Dunite (d) occupies space between orthopyroxenite (opx) segments. Hammer handle is 30 cm long.

## MESOSCOPIC FABRIC

### AREA I: LOW PLATEAU MOUNTAIN

Area I is 17 km south of the California-Oregon State line, approximately in the center of the 15-km outcrop width of the Josephine Peridotite at this latitude (fig. 1). This area includes the top of Low Plateau Mountain and outcrops as much as 300 m below the summit. Flanks of the mountain are covered with landslide deposits and coarse regolith; the plateaulike top of the mountain is partly covered by laterite. J.P. Albers, assisted by E. Van Dohlen, mapped the area in detail in summer 1977.

The poles of orthopyroxenite layers, of dunite layers lacking chromite, and of dunite layers containing chromite were plotted on separate fabric diagrams and contoured to detect differences in the orientation patterns of these three types of layers (figs. 20*A*–20*C*). Enstatite

FIGURE 20.—Fabric diagrams for area I (fig. 1). *A*, Contour diagram of poles of orthopyroxenite layers in harzburgite. 78 points. Contours: 2σ, 4σ, 6σ, 8σ, and pole-free area (unlabeled contours). $\perp\bar{S}_A$, center of 8σ concentration, is pole of a plane striking N. 22° W. and dipping 21° NE. *B*, Contour diagram of poles of dunite layers lacking chromite in harzburgite. 31 points. Contours: 2σ, 4σ, 6σ, 8σ, and 10σ. $\perp\bar{S}_B$, center of 10σ concentration, is pole of a plane striking N. 52° E. and dipping 27° SE. *C*, Poles of dunite layers containing chromite (dots). 19 points. Circle $\perp\bar{S}_C$, approximate mean orientation of layers, is pole of a plane striking N. 46° W. and dipping 22° NE. Dashed great circle defines a β-axis (square) plunging 20°, N. 88° E. *D*, Detached isoclinal-fold hinges. *E*, Poles of axial planes of detached fold hinges. *F*, Contour diagram of linear elements measured in the field. 36 points. Contours: 2σ, 4σ, 6σ, and 8σ. $\bar{B}_1$, center of 8σ concentration, is mean axis of elements trending N. 52° E. and plunging 16° NE. $\bar{B}_2$, center of 8σ concentration, is mean axis of elements trending S. 88° W. and plunging 48° W. *G*, Poles of late chromite foliation. Dashed line, vertical great circle; squares, poles of great circle, a horizontal β-axis trending N. 30° E. *H*, Intersections of late chromite foliation and dunite layers. *I*, Intersecting linear elements. Circles, orthopyroxenite folds; small crosses, chromitite folds. Double-headed arrows indicate angles of intersection. *J*, Group I β-axes. 24 points. Contours: 2σ, 4σ, 6σ, 8σ, 10σ, and pole-free area. Dot $\bar{\beta}_1$, mean attitude of β-axes, trending N. 35° E. and plunging 30° NE. *K*, Contour diagram of group II β-axes. 32 points. Contours: 2σ, 4σ, 6σ, 8σ, 10σ, and pole-free area. Dot $\bar{\beta}_2$, mean attitude of β-axes, trending S. 75° E. and plunging 14° SE. *L*, Poles of axial planes of group I β-axes. Contours: 2σ, 4σ, 6σ, and pole-free area. 24 points. Dot $\perp\overline{A.P.}$, pole of mean attitude of axial planes, is pole of a plane striking N. 7° E. and dipping 65° E. Dashed line, great circle; square, pole of great circle, a β-axis trending N. 28° E. and plunging 40° NNE. *M*, Contour diagram of axial planes of group II β-axes. 32 points. Contours: 2σ, 4σ, 6σ, 8σ, and 10σ. Dot $\perp\overline{A.P.}$, center of 10σ concentration, is pole of mean of axial planes and represents a vertical plane striking N. 66° W.

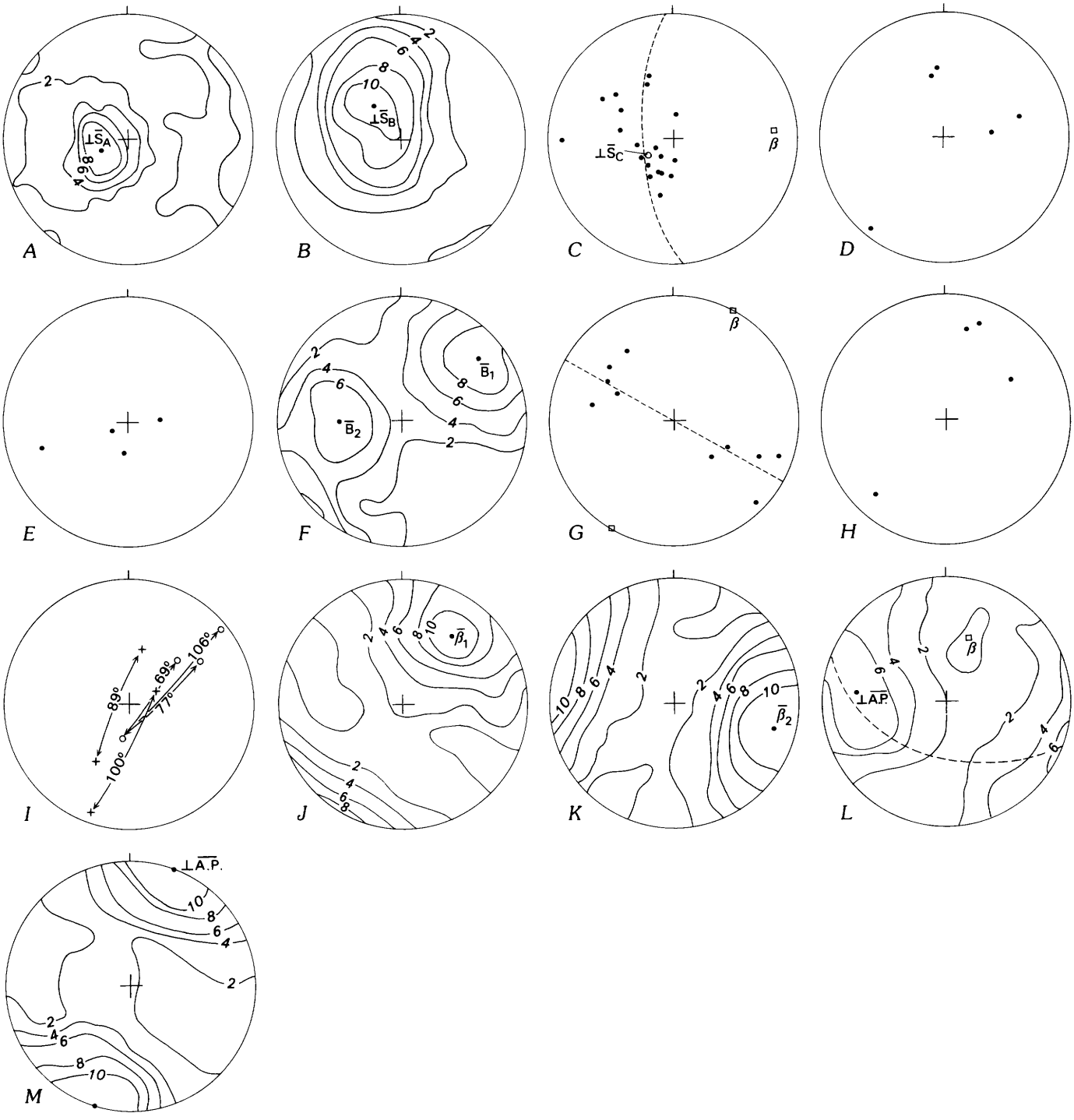
A
2
4
6
8
⊥S̄A
B
2
4
6
8
10
⊥S̄B
C
⊥S̄C
β
D
E
F
2
4
6
8
6
4
2
B̄1
B̄2
G
β
H
I
89°
69°
77°
106°
100°
J
2
4
6
8
10
β̄1
K
10
8
6
4
2
2
4
6
8
10
β̄2
L
β
⊥A.P.
2
4
6
M
⊥A.P.
10
8
6
4
2
2
4
6
8
10

foliations parallel the orthopyroxenite layering. The orthopyroxenite layers and the dunite layers lacking chromite have mean orientations ($\bar{S}_A$ and $\bar{S}_B$) 29° apart; the orthopyroxenite layers and the dunite layers containing chromite have mean orientations ($\bar{S}_A$ and $\bar{S}_C$) 5° apart. $\bar{S}_A$ strikes N. 22° W. and dips 21° NE.; $\bar{S}_B$ strikes N. 52° E. and dips 27° SE.; and $\bar{S}_C$ strikes N. 46° W. and dips 22° NE. The proximity of $\bar{S}_A$ and $\bar{S}_C$ indicates a close relation between these two sets of planar elements. The small difference between $\bar{S}_A$ and $\bar{S}_B$ may not be significant because of the large overlap in the orientations of these two sets. The conclusion that the three types of layers are related neither contradicts nor supports any of the hypotheses listed above regarding the origin of these layers.

Detached fold hinges (fig. 20*D*) plunge at low to moderately steep angles north-northwest, east-northeast, and southwest. The axial planes of these folds parallel layering and foliation in the harzburgite (fig. 20*E*).

Folds of dunite-harzburgite contacts and of chromite schlieren measured in the field fall into two groups on the contour diagram (fig. 20*F*): an 8σ concentration trending northeast and a 6σ concentration trending east-west. These folds are mostly open, although a few nearly isoclinal folds occur in both groups.

Chromite foliations dip steeply to moderately steeply northwest and southeast (fig. 20*G*) and have a horizontal β-axis trending N. 30° E. Constructed intersections of these foliations with the enclosing dunite layers plunge at low angles northeast and southwest (fig. 20*H*). These relations suggest that the chromite foliations are geometrically equivalent to the axial planes of the northeast-trending folds and may have formed contemporaneously with the northeast-trending folds.

Figure 20*I* plots five pairs of intersecting chromite folds in dunite at two localities. The fold pairs intersect at acute angles ranging from 69° to 89° and averaging 78°. The approximate perpendicularity of these pairs suggests that these folds represent members of conjugate sets in a $B \perp B'$ tectonite: one set trends northeast; the other set, plunging steeply, is not defined on the contour diagram (fig. 20*F*).

Using the field data of J.P. Albers (unpub. data, 1977), β-axes were constructed from the attitudes of layers in adjacent outcrops; these axes were then compared with the orientations of measured fold axes. The subparallelism of minor folds and β-axes presumably indicates that the β-axes represent axes of macroscopic folds that are not exposed.

Two groups of β-axes were determined: group I, trending generally northeast (fig. 20*J*), and group II, trending west-northwest (fig. 20*K*). The mean of group I, $\beta_I$, trends N. 35° E. and plunges 30° NE., 18° from the mean of measured northeast-trending folds, $\bar{B}_1$ (fig. 20*F*). β-axes and measured northeast-trending linear elements largely coincide. These relations are consistent with the hypothesis that the group I β-axes are axes of macroscopic folds. If the group I β-axes are large folds, the group II β-axes also probably represent the axes of macroscopic folds. However, the angle between $\bar{B}_2$, the mean of measured east-west-trending folds, and $\beta_{II}$, the mean group II β-axes, is 64°. Either the macroscopic fold axes in this case differ systematically in orientation from the mesoscopic ones, or the measured east-west-trending folds are not a representative sample of east-west-trending linear elements in area I (fig. 1). Whatever the explanation for the difference in orientation between these two fabric elements, the east-southeast-plunging 10σ concentration of group II β-axes seems too strong to be fortuitous.

Axial planes for groups I and II β-axes were constructed, assuming an axial angle of more than 90°. Axial planes of group I β-axes generally dip steeply east (fig. 20*L*), as do half the measured chromite foliations (fig. 20*G*). Poles of the axial planes have a diffuse great-circle distribution, the pole of which defines a β-axis trending N. 22° E. and plunging 36° NE., close to $B_I$ (fig. 20*J*). These relations suggest either a large variation in axial-plane orientation or refolding of some northeast-trending folds about northeast-trending axes.

Axial planes of group II β-axes are generally steep and strike predominantly northwest.

At the Judy mine (fig. 1), a chromitiferous dunite body intrudes harzburgite at a 25° angle to dunite layering and weak foliation in the harzburgite. Folds of the chromite layers trend northeast and east-west, parallel to the two main groups of linear elements in area II (figs. 1, 21*B*). These relations indicate that the dunite was emplaced after formation of the foliation and layering, but before the formation of some of the northeast-trending folding.

## AREA II: HIGH PLATEAU MOUNTAIN

Area II is immediately south of area I (fig. 1) and separated from it by Peridotite Canyon. Outcrops examined are along the top of the mountain (subarea IIa), on the lower jeep trail (subarea IIb) to the abandoned lookout, and along the western spur (subarea IIc). Laterite covers much of the central part of the mountaintop.

In subarea IIa, near the summit of the mountain, the dunite layers, dunite-harzburgite contacts, and harzburgite foliations dip generally west (fig. 21*A*). The mean orientation of the planar fabric elements, $\bar{S}$, strikes N. 0° E. and dips 43° W. The poles lie along a

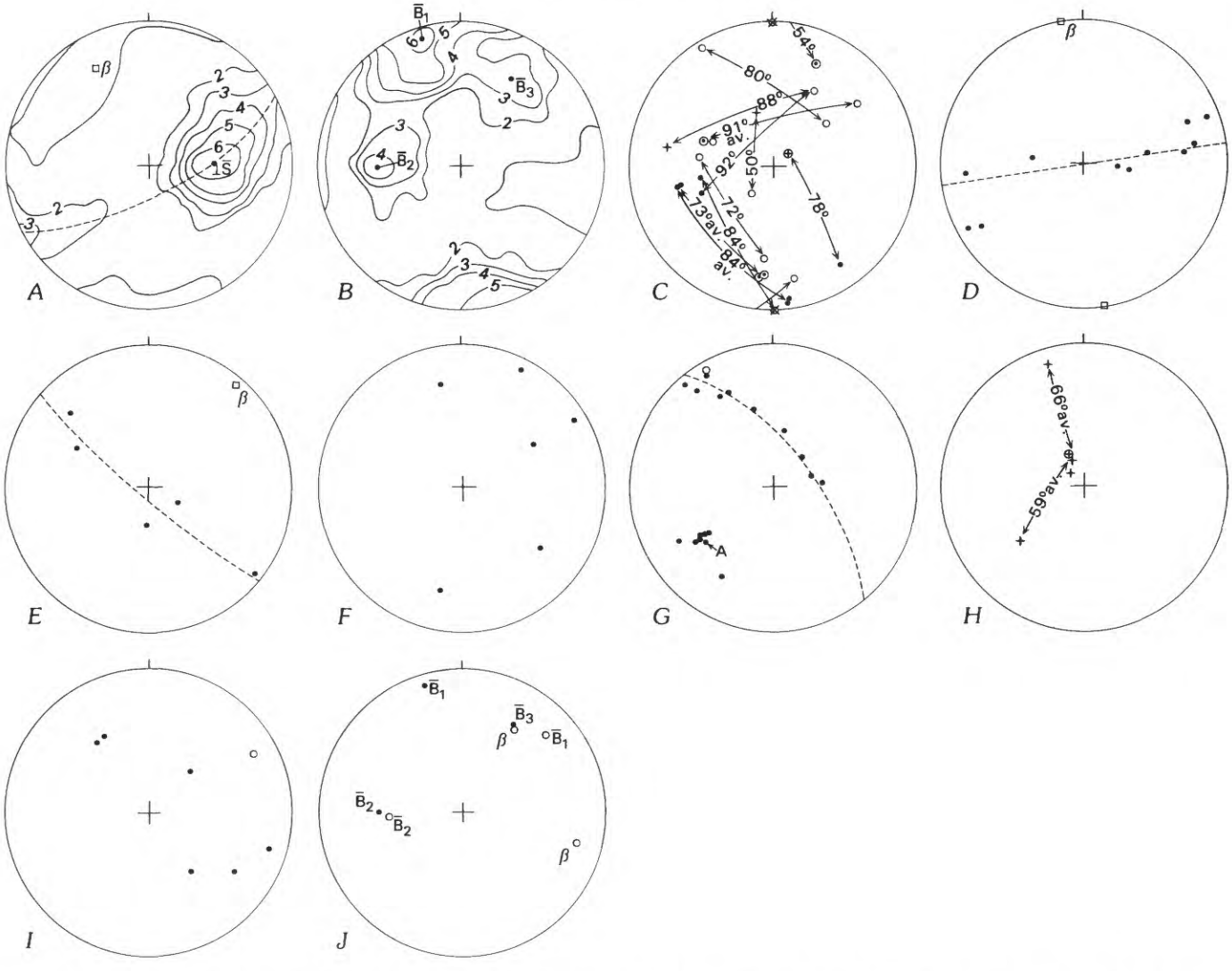


FIGURE 21.—Fabric diagrams for subarea IIa. *A,* Contour diagram of poles of dunite layers, dunite-harzburgite contacts, and foliation in harzburgite. 44 points. Contours: 2σ, 3σ, 4σ, 5σ, 6σ, and pole-free area (unlabeled contours). Dot ⊥S̄, mean attitude of layering and foliation, striking north-south and dipping 43° W. Dashed line, great circle; square, pole of great circle, a β-axis trending N. 25° W. and plunging 20° NW. *B,* Contour diagram of linear elements. 53 points. Contours: 2σ, 3σ, 4σ, 5σ, 6σ, and pole-free area (unlabeled contour). Dot $\bar{B}_1$, center of 6σ concentration, trending N. 15° W. and plunging 10° NW.; dot $\bar{B}_2$, center of 4σ concentration, plunging 38° W.; dot $\bar{B}_3$, center of 3σ lobe, trending N. 32° E. and plunging 30° NE. *C,* Intersecting linear elements. Dots, dunite folds; circles, orthopyroxenite folds; small crosses, chromitite folds; circled dot, dunite rod; circled cross, chromite rod; X'ed circle, pyroxene rod. Double-headed arrows indicate angles of intersection. *D,* Poles of axial planes of folds, plunging north-northwest and south-southeast. Dashed line, vertical great circle; squares, pole of great circle and a horizontal β-axis trending N. 10° W.. *E,* Poles of axial planes of folds, plunging northeast. Dashed line, great circle; square, pole of great circle, a β-axis plunging 5°, N. 40° E. *F,* Poles of axial planes of folds, plunging east-west. *G,* Multiply folded outcrop. Dots, fold axes; circle, axis of early fold. Dot A, rotation axis of an 80° small circle (dashed line), trending S. 55° W. and plunging 35° SW. *H,* Linear elements in dunite of multiply folded outcrop. Small crosses, chromite folds; circled cross, chromite rod. Double-headed arrows indicate angular separations of elements. *I,* Poles of axial planes of some folds in figure 21*G*. Dots, axial planes of late folds; circle, axial plane of early fold. *J,* Comparison of linear elements in subarea IIa (dots) (fig. 21*B*) and area I (circles) (figs. 20*F,* 20*J,* 20*K*).

great circle, the pole of which is a β-axis trending N. 25° W. and plunging 20° NW.

The linear elements in subarea IIa fall into three groups on the contour diagram (fig. 21*B*): (1) a 6σ concentration plunging at a low angle north-northwest ($\bar{B}_1$, N. 15° W., 10° NW.); (2) a 4σ concentration plunging at a moderate angle west ($\bar{B}_2$, 38° W.); and (3) a 3σ lobe plunging at low to moderate angles northeast ($\bar{B}_3$, N. 32° E., 30° NE.). The northeast- and east-west-trending linear elements are similar in attitude to the main fold groups in area I (fig. 1).

Pairs of intersecting linear elements occur at some localities (fig. 21*C*). Elements trending northeast and east-west are about 90° apart, as are $\bar{B}_2$ and $\bar{B}_3$. Therefore, the subfabric including northeast- and east-west-trending linear elements has the symmetry of a $B \perp B'$ tectonite, a relation suggesting possible contemporaneity of these two groups of elements. A few steep folds that do not fall into one of these three fold groups have orientations that place them outside the 2σ contour of figure 21*B*.

Orientations of axial planes for each of the three main groups of folds vary widely. Folds trending north-northwest are isoclinal and have axial planes dipping at low to steep angles and striking north-south (fig. 21*D*). Most of these orientations are close to the attitudes of layering and foliation in the harzburgite. Refolding of these isoclinal folds is reflected in the girdle distribution of axial planes, similar to layering, about a north-northwest-trending axis. The northeast-trending folds have axial planes that strike generally northeast and range from steeply dipping to nearly flat lying (fig. 21*E*). The poles lie along a great circle, the pole of which is a β-axis plunging 5°, N. 40° E., 23° from $\bar{B}_3$. These relations suggest refolding of the northeast-trending folds about a northeast-trending axis. The axial planes of folds trending east-west dip steeply in many directions (fig. 21*F*).

An outcrop of multiply folded peridotite was found near the summit of High Plateau Mountain (figs. 22, 23). The tight early fold hinge trends N. 30° W. and plunges 5° NW. The rotated straight-line segments of the hinge lie along a small circle with axis plunging 35°, S. 55° W., parallel to the axes of later open folds (fig. 21*G*). This evidence indicates that the southwest-plunging folds are younger than the northwest-trending fold hinge and that the later folding was predominantly by flexural slip.

Although the fabric data from the multiply folded peridotite can be explained by a flexural-slip model, the concept of flexural slip occurring in peridotite is difficult to envisage because the rock does not, at first, appear to contain surfaces that can slip past one another. Instead, the peridotite appears to be mechanically isotropic. Even where layered and foliated, the rock breaks as easily across as along these planar structures. Very few natural fractures occur parallel to the layering or foliation. The mineralogic compositions of dunite and harzburgite layers do not differ greatly; olivine is the dominant constituent of both rock types. In addition, phyllosilicate and double-chain anhydrous inosilicate

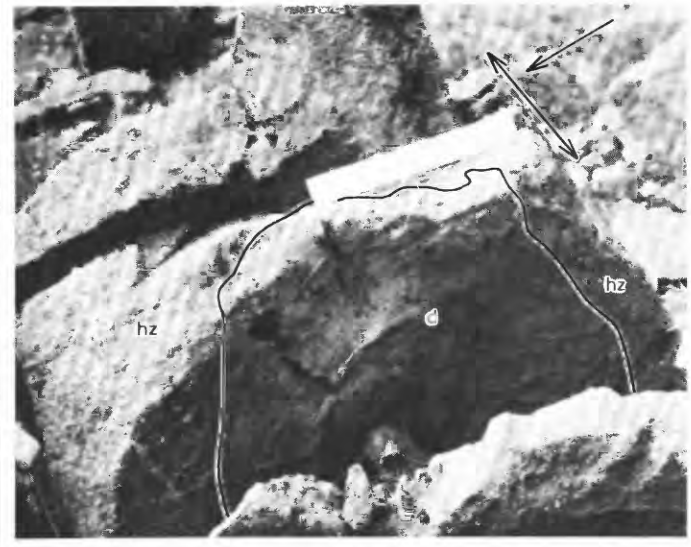


FIGURE 22.—Multiply folded peridotite. d, dunite; hz, harzburgite. Arrow along right side of outcrop parallels early-fold hinge (orientation, N. 30° W., 5° NW.); arrow pointing to right side of outcrop parallels later-fold hinge (average orientation, N. 60° W., 35° SW.). Black spots in dunite are folded chromite lenses. Scale is 20 cm long.

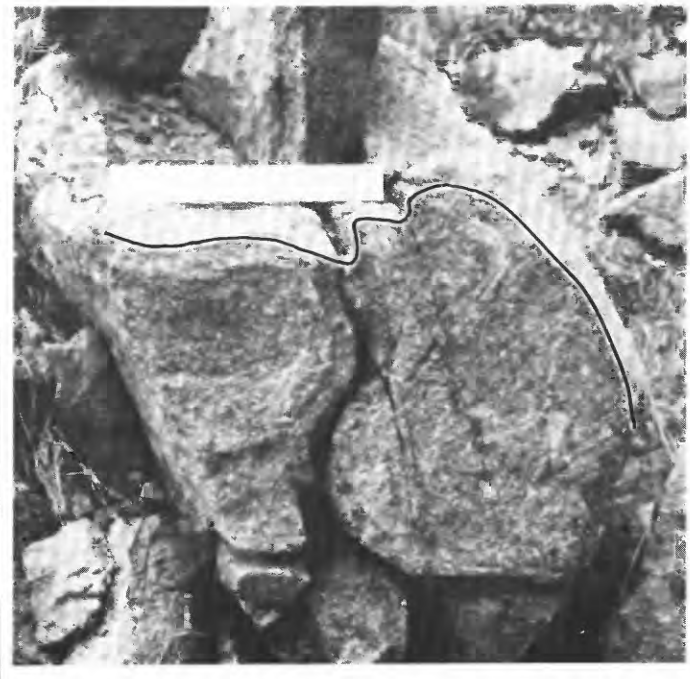

FIGURE 23.—Multiply folded peridotite, viewed along late-fold hinge. Black line shows refolding of early-fold hinge. Scale is 20 cm long.

minerals, the presence of which may facilitate slip parallel to layering, were absent in the rocks during the crystalline deformations because these types of minerals are not developed in association with the structural elements under discussion. Nevertheless, a flexural-slip model need not be discarded for the peridotite, nor the fabric data suggesting this model discarded as fortuitous—an unlikely conclusion.

Clearly, the peridotite underwent stages in its development during which physical conditions differed considerably from its present surface environment. Apparently, during some stages of deformation the physical state of the rock may have favored flexural slip. The local development of chromite foliations parallel to the axial planes of open folds does not contradict at least a modified flexural-slip model because the style of yielding varied throughout the rock. Flexural slip may more easily be accepted as a possible folding mechanism, given the presence of a fluid phase, as would be implied by Dick's (1976, 1977a, b) hypothesis of partial melting of the peridotite. The presence of a fluid phase, however, is not clearly a necessary condition for flexural-slip folding in these rocks. Intrusion of dunite dikes parallel to orthopyroxenite layering and foliation in harzburgite (fig. 15) and parallel to the axial planes of northeast-trending folds implies that planar fabric elements are potentially planes of relative weakness in the peridotite. The evidence, therefore, points to the planar fabric elements behaving as mechanically active elements under certain conditions of relatively high pressure and temperature and, possibly, in the presence of a fluid phase, even though other fabric elements consistent with this model, such as cleavage or schistosity parallel to layering, are absent. A flexural-slip model was also suggested for one episode of deformation in the Canyon Mountain Complex (ophiolite), Oreg. (Avé Lallemant, 1976, p. 37).

Chromite rods and folds in the dunite core of the fold hinge fall into three groups: (1) plunging 10°, N. 15° W., subparallel to the fold hinge; (2) plunging 35°, S. 50° W., subparallel to the late folds; and (3) plunging 70°–80° NW. (fig. 21*H*). The steep folds could have formed penecontemporaneously with either of the other two groups of folds, or they could belong to another folding episode. Like the steep folds shown in figure 21*C*, the age relations of these folds to other groups of folds are not known.

The axial plane of the early-fold hinge dips steeply southwest (fig. 21*G*); axial planes of late folds generally dip steeply southeast and northwest. One of these axial planes dips moderately southwest; its orientation was possibly influenced by the shape of the dunite core of the early fold.

In subarea IIb, dunite layers, dunite-harzburgite contacts, and foliations in harzburgite have a great-

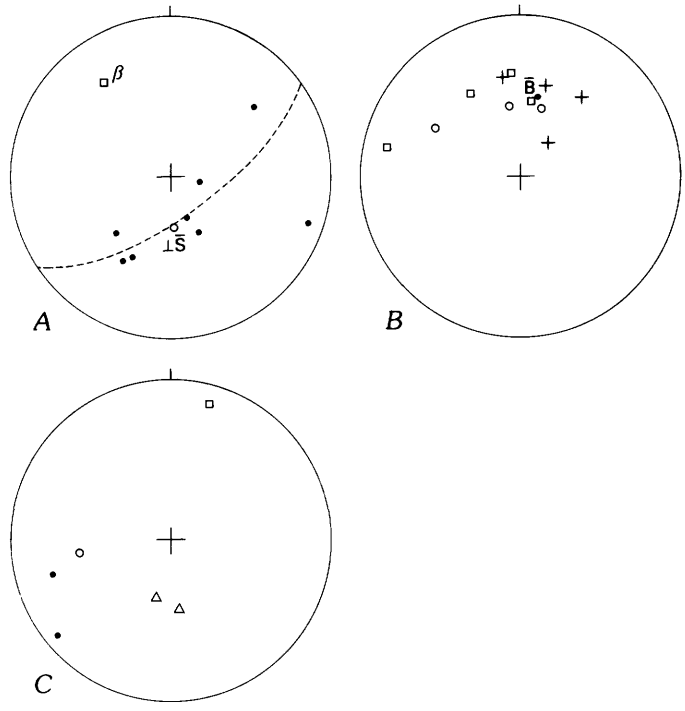


FIGURE 24.—Fabric diagrams for subarea IIb. *A*, Poles of dunite layers, dunite-harzburgite contacts, and foliation in harzburgite. Dashed line, great circle; square, pole of great circle, β-axis plunging 25°, N. 35° W. ⊥S̄, approximate mean pole of planar elements. *B*, Linear elements. Small circles, orthopyroxenite folds; small crosses, chromitite folds; squares, β-axes; dot B̄, mean orientation of northeast-trending linear elements. *C*, Poles of axial planes. Dots, northeast-trending folds; square, west-northwest-trending fold; triangles, north-northwest-trending folds; circle, pole of chromite foliation.

circle distribution (fig. 24*A*) that defines a β-axis plunging 25°, N. 35° W., like that in subarea IIa. Folds plunge at low to moderate angles west, at moderate angles north-northwest and northeast, and steeply northeast (fig. 24*B*). Axial planes of two folds trending north-northwest dip at a low angle north subparallel to layering and foliation in harzburgite (fig. 24*C*). Axial planes of two folds trending northeast dip steeply northeast. A chromite foliation subparallel to one of the axial planes indicates the geometric equivalence of these two fabric elements. The axial plane of a west-northwest-trending fold dips steeply south-southwest.

In subarea IIc, poles of dunite layers and foliation in harzburgite approximate a β-axis plunging 5°, N. 80° E. (fig. 25*A*). At least two groups of linear elements are present (fig. 25*B*), one group trending generally northwest and the other northeast. Axial planes of two folds trending northeast dip steeply southeast (fig. 25*C*); the axial plane of a west-northwest-trending fold dips steeply southwest.

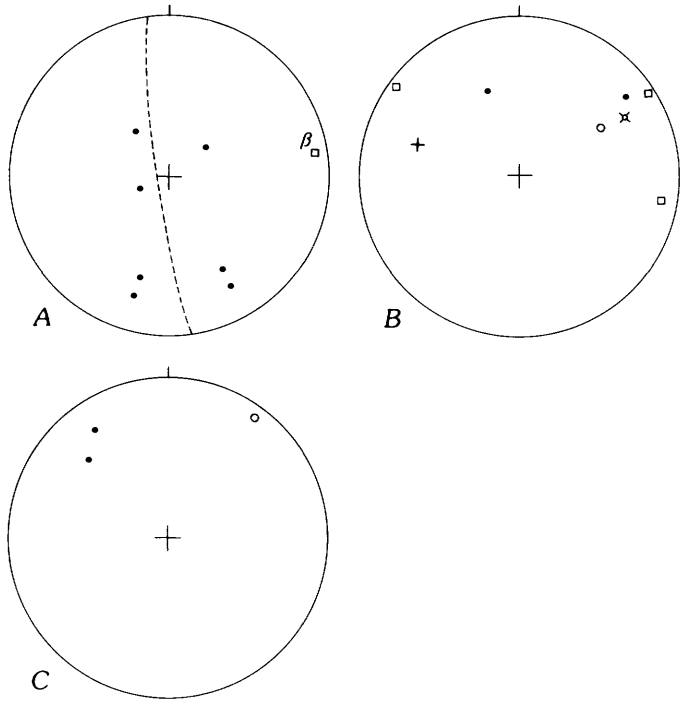


FIGURE 25.—Fabric diagrams for subarea IIc. *A*, Poles of dunite layers and foliation in harzburgite. Dashed line, great circle; square, pole to great circle, a β-axis plunging 5°, N. 80° E. *B*, Linear elements. Dots, dunite folds; circle, orthopyroxenite fold; X'ed circle, orthopyroxene rod; small cross, chromitite fold; squares, β-axes. *C*, Poles of axial planes. Dots, northeast-trending folds; circle, northwest-trending fold.

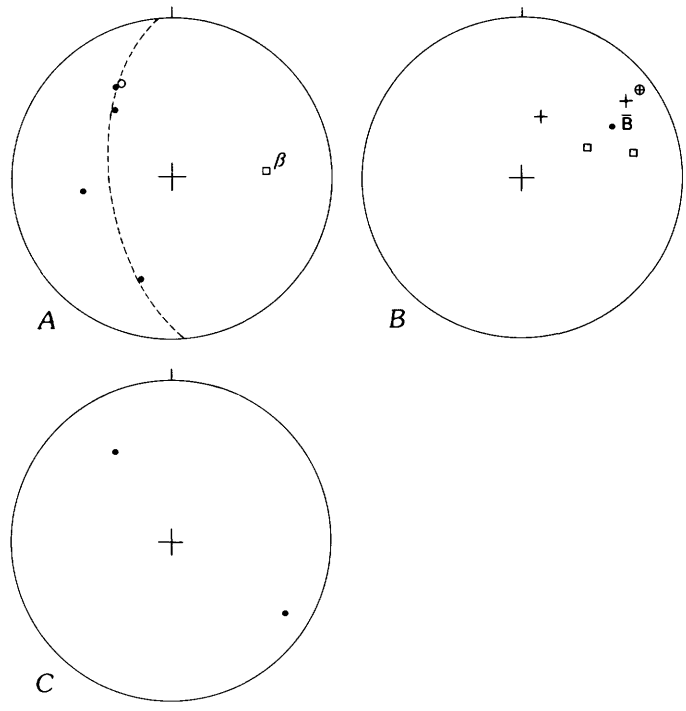


FIGURE 26.—Fabric diagrams for area III (fig. 1). *A*, Poles of chromite schlieren in dunite (dots) and a dunite-harzburgite contact (circle). Dashed line, great circle; square, pole to great circle, a β-axis plunging 35°, N. 85° E. *B*, Linear elements. Small crosses, chromite folds; circled cross, chromite lineation; squares, β-axes; dot B̄, mean orientation of linear elements, plunging 32°, N. 62° E. *C*, Poles of axial planes of chromite folds.

### AREA III: STONY CREEK

Area III is 1.5 km east of area II, in the upper Stony Creek drainage (fig. 1). Chromitiferous dunite, minor harzburgite, and sheared, chromite-bearing serpentinite are exposed in mines and prospects. Poles to chromite schlieren and layers and to a dunite-harzburgite contact lie along a great circle, the pole of which defines a β-axis plunging 35°, N. 85° E. (fig. 26*A*). Linear elements measured in the field plunge at low to steep angles northeast and east-northeast (fig. 26*B*). At least some of the northeast-trending linear elements probably correlate with the northeast-trending fold group in area II. Axial planes of two of the folds dip steeply northwest and southeast (fig. 26*C*).

### AREA IV: CHROME NO. 1

Area IV consists of two open pits, 4 km east of area II, excavated in chromitiferous dunite (fig. 1). Poles of chromitite layers lie near a great circle that defines a β-axis plunging 3°, N. 15° W. (fig. 27*A*). Chromite folds plunge at low angles north-northwest subparallel to the β-axis, north-northeast, steeply northwest and southeast (fig. 27*B*). Folds trending north-northwest intersect folds that plunge steeply northwest. The axial plane of a fold trending north-northwest is vertical and strikes N. 20° W., close to the orientation of some chromitite layers (fig. 27*C*). The axial plane of a fold trending north-northeast dips at a low angle northeast, also close to the orientation of some chromitite layers. Axial planes of three folds plunging steeply northwest and southeast strike northwest; two dip steeply, and one is vertical.

### AREA V: ELK CAMP RIDGE

Area V, 3 km east of area II, is along part of the crest of Elk Camp Ridge (fig. 1). Poles to layering and foliation in harzburgite dip north and south at moderate to steep angles and define a nearly east-west trending horizontal β-axis (fig. 28*A*). Linear elements plunge in many directions, and more than one fold group may be represented (fig. 28*B*). Axial planes of two folds plunging southeast dip steeply south and are subparallel to layering and foliation (fig. 28*C*). These southeast-plunging folds may be correlated with the earliest folds described in area I and subarea IIa. The east-west-trending folds

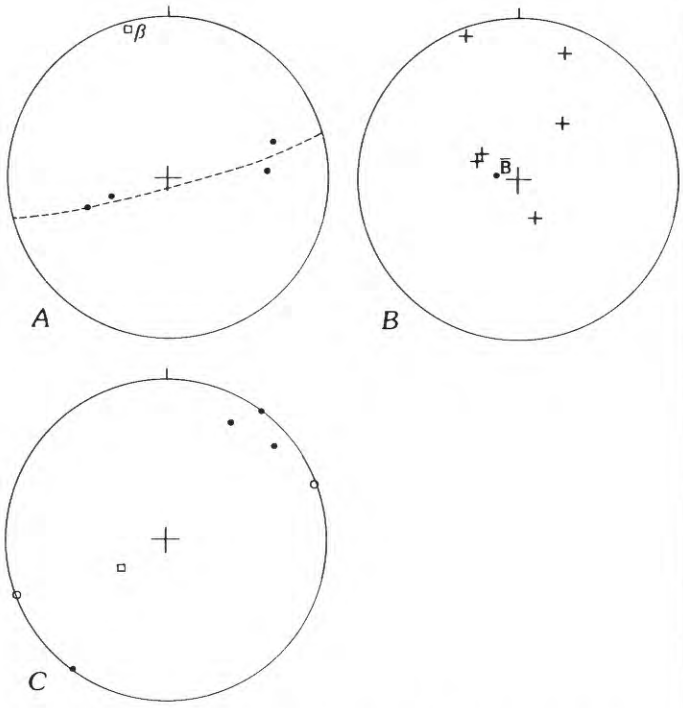


FIGURE 27.—Fabric diagrams for area IV (fig. 1). *A*, Poles of chromite layers. Dashed line, great circle; square, pole to great circle, a β-axis plunging 3°, N. 15° W. *B*, Axes of chromite folds (small crosses). Dot $\bar{B}$ mean orientation of steep folds, plunging 80°, N. 85° W. *C*, Poles of axial planes. Dots, steeply plunging folds; circles, north-northwest-trending fold; square, north-northeast-trending fold.

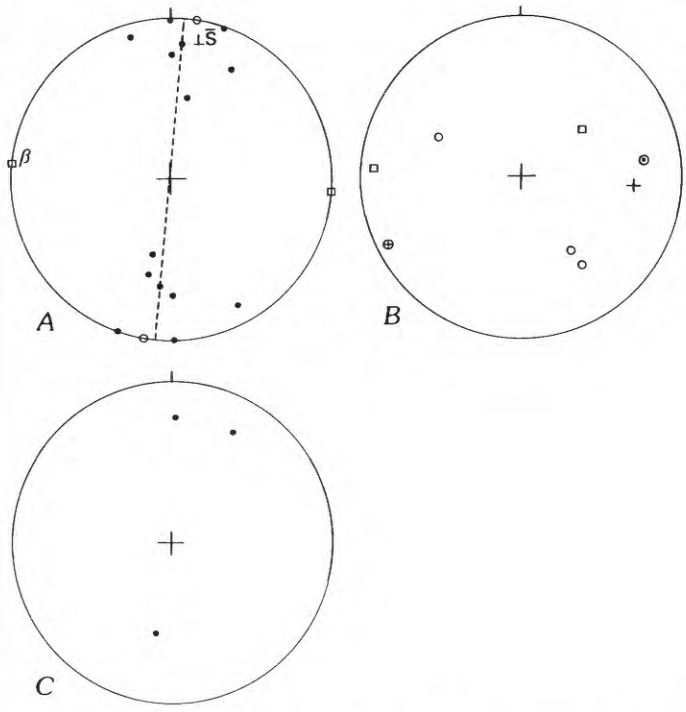


FIGURE 28.—Fabric diagrams for area V (fig. 1). *A*, Poles of dunite and orthopyroxenite layers in harzburgite and of chromite schlieren in dunite. Dashed line, great circle; squares, pole of great circle, a horizontal β-axis trending N. 85° W.; circle ⊥S̄, pole of mean attitude of layers and schlieren. *B*, Linear elements. Small circles, orthopyroxenite folds; small cross, orthopyroxene rod; squares, β-axes; circled dot, axis of dunite pod; circled cross, chromite lineation. *C*, Poles of axial planes of southeast-plunging folds.

and linear elements in area V may be equivalent to the east-west-trending elements in area I and subarea IIa.

### AREA VI: ELK CAMP

Area VI is on Elk Camp Ridge, 4 km northwest of area I (fig. 1). The area has natural exposures of dunite and harzburgite, as well as some open pits in partially serpentinized dunite. Poles of layers define a steep β-axis plunging 70°, S. 10° E. (fig. 29*A*). Linear elements plunge mostly east and northeast, but also steeply southwest and at low angles southeast (fig. 29*B*). At one locality, a β-axis and a chromite fold are 78° apart, a relation suggesting that more than one group of folds is present. Axial planes of folds trending northeast dip steeply east and southeast (fig. 29*C*); axial planes of folds plunging steeply southwest dip steeply southwest. Axial surfaces of folds plunging southeast dip at a low angle southeast. A late chromite foliation dips steeply northeast and is not close to any group of axial planes.

### AREA VII: LOW DIVIDE

Area VII is 3.5 km west of area I and 2 km from the west edge of the peridotite (fig. 1). The area is in a dunite dike, 45 to 120 m wide by 365 m long. The dunite is partly capped and underlain by harzburgite and appears to have been emplaced as an irregular cylindrical body plunging at a low angle north-northeast (Evans, 1984). Harzburgite pods (fig. 30) in the dunite are elongate north-northeast. The contacts of these pods with dunite are partly concordant with and partly discordant to dunite layers in the pods. The harzburgite pods can be interpreted either as boudins or xenoliths.

Planar fabric elements are divided into three groups, which are discussed separately here: (1) dunite layers in harzburgite and a harzburgite foliation, (2) chromite schlieren in dunite and chromitiferous dunite veins, and (3) dunite-harzburgite contacts. Most dunite layers in harzburgite dip at low angles northerly (fig. 31*A*). The mean orientation of dunite layers, $\bar{S}_A$, strikes N. 78° W. and dips 32° NNE. A local harzburgite foliation in a harzburgite block differs greatly in orientation from the dunite layers and may have been rotated. Poles of dunite layers lie near a great circle that defines a β-axis plunging 24°, N. 22° W., possibly related to north-north-

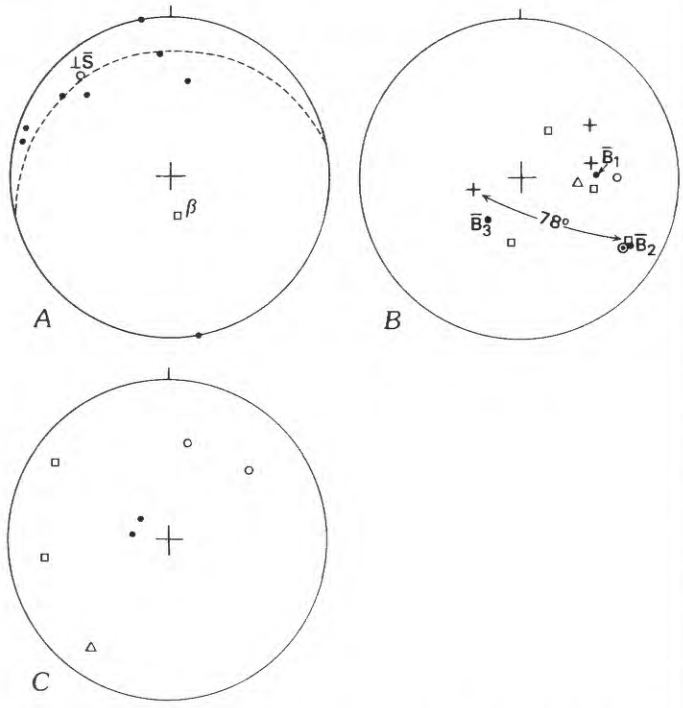


FIGURE 29.—Fabric diagrams for area VI (fig. 1). *A*, Poles to dunite layers and foliation in harzburgite. Dashed line, great circle; square, pole of great circle, a β-axis plunging 70°, S. 10° E.; circle ⊥S̄, pole of mean attitude of layers and foliation. *B*, Linear elements. Circle, orthopyroxenite fold; squares, β-axes; triangle, intersection of dunite layer and late chromite foliation; small crosses, chromitite folds; circled dot, axis of dunite pod; dot $\bar{B}_1$, mean orientation of east-northeast- and east-plunging elements, plunging 50°, N. 80° E.; dot $\bar{B}_2$, mean orientation of southeast-plunging elements, plunging 20°, S. 56° E.; dot $\bar{B}_3$, mean orientation of southwest-plunging elements, plunging 57°, S. 50° W. *C*, Poles of axial planes. Dots, southeast-trending linear elements; circles, steep elements trending north-south and northeast; squares, northeast-trending folds; triangle, pole of chromite foliation.

west-trending folds in some other parts of the study area, such as subarea IIa.

Poles of chromite schlieren in dunite dip at low to steep angles generally east and northeast (fig. 31*B*). The mean orientation of chromite schlieren, $\perp S_B$, strikes N. 38° W. and dips 30° NE. Most of the poles lie near a great circle that defines a β-axis plunging 20°, N. 2° E. One chromitiferous dunite vein is subparallel to chromite schlieren; another has its pole along the great circle that defines the north-plunging β-axis. This evidence suggests a possible close relation between the schlieren and veins; the veins could have been emplaced along planes of weakness parallel to the schlieren, or the veins may be a type of schlieren.

Dunite-harzburgite contacts vary widely in orientation. The contour diagram of poles of the contacts (fig. 31*C*) shows two 4σ concentrations with mean attitudes representing (1) a plane striking N. 28° E. and dipping 80° NW., subparallel to the north-northeastward trend of the dunite dike; and (2) a plane striking N. 85° W. and dipping 57° S. Near-parallelism of set 1 with the trend of the dike suggests that the dunite-harzburgite contacts are fractures and that the two sets of contacts can be interpreted as conjugate sets of faults, the mean attitudes of which are 78° apart. The dunite body could be interpreted to be either (1) a dunite intrusive that was emplaced along fractures (the harzburgite pods would be xenoliths) or (2) a metasomatic body formed by alteration of enstatite in harzburgite to olivine by percolation of an aqueous fluid along fractures (Dungan and Avé Lallemant, 1977). The sharp dunite-harzburgite contacts and the presence of chromitiferous dunite exhibiting chromite-net and occluded-silicate textures favor a magmatic origin for the dunite.

Folds plunge chiefly east and northeast at low to steep angles (fig. 31*D*). The centers of two 5σ concentrations represent means of groups of linear elements: $\bar{B}_1$, trending N. 49° E. and plunging 54° NE.; and $\bar{B}_2$, trending S. 73° E. and plunging 44° SE. Neither group is close in attitude to the β-axes in figures 31*A* and 31*B*.

Axial planes of chromite folds trending north-northeast strike northwest and dip steeply or are vertical (fig. 31*E*). Axial planes of folds trending nearly east-west dip at moderate to steep angles north. The axial plane of a fold trending northeast strikes northeast and dips northwest.

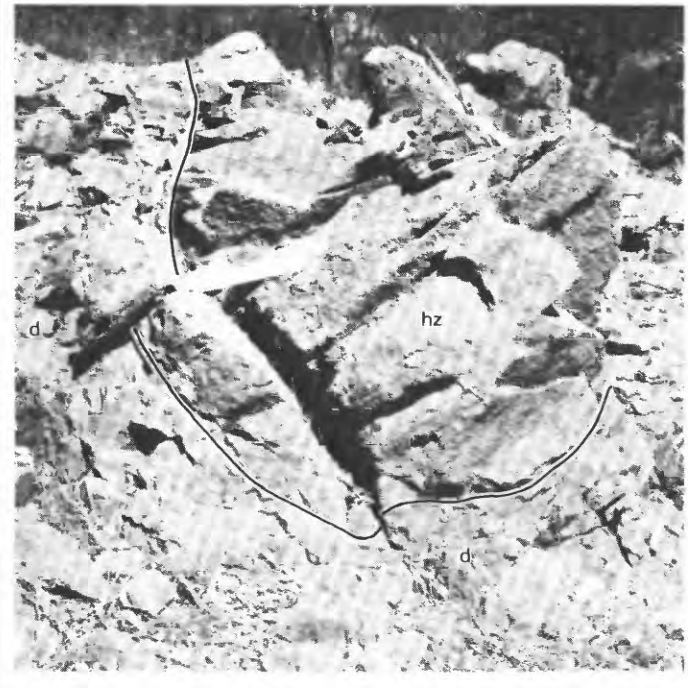


FIGURE 30.—Harzburgite (hz) pod in dunite (d). Scale is 20 cm long.

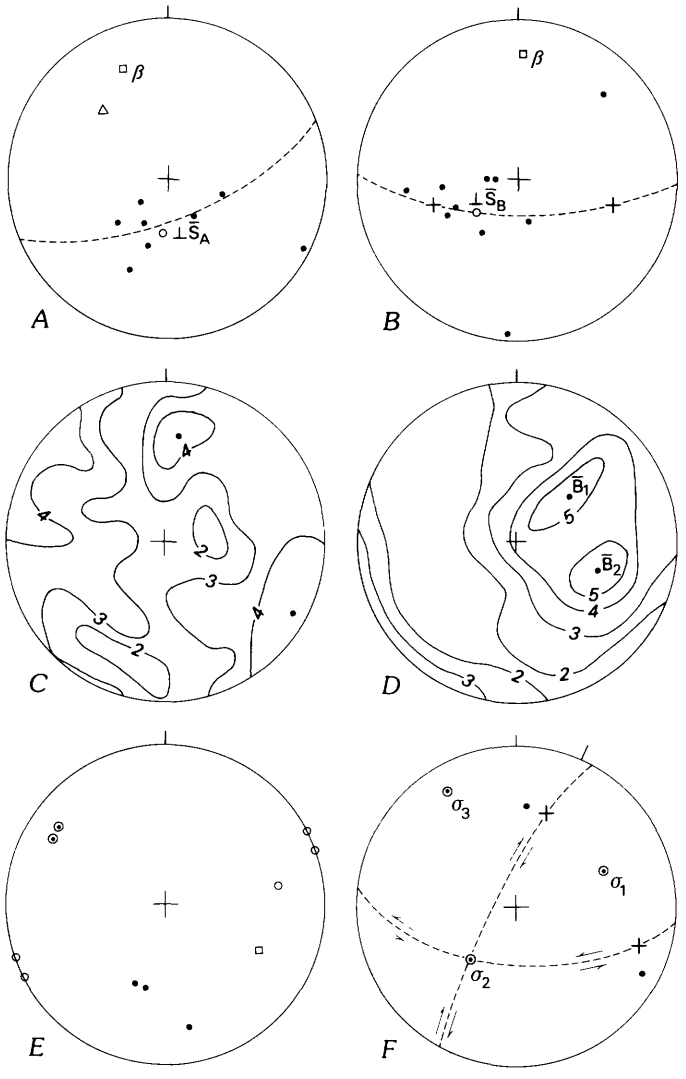


FIGURE 31.—Fabric diagrams for area VII (fig. 1). *A*, Poles of dunite layers in harzburgite (dots). Circle $\perp\bar{S}_A$, pole of mean orientation of layers, striking N. 78° W. and dipping 32° NNE.; triangle, harzburgite foliation; square, β-axis, plunging 24°, N. 22° W.; dashed line, great circle. *B*, Poles of chromite schlieren in dunite (dots). Circle $\perp\bar{S}_B$, pole of mean orientation of schlieren, striking N. 38° W. and dipping 30° NE.; small crosses, chromitiferous dunite veins; square, β-axis plunging 30°, N. 2° E.; dashed line, great circle. *C*, Contour diagram of poles of dunite-harzburgite contacts. 35 points. Contours: 2σ, 3σ, and 4σ. Dots, centers of 4σ concentrations, are mean attitudes of two groups of contacts: (1) N. 28° E., 80° NW., and (2) N. 85° W., 57° S. *D*, Contour diagram of linear elements. 28 points. Contours: 2σ, 3σ, 4σ, and 5σ. Dots $\bar{B}_1$ and $\bar{B}_2$, centers of 5σ concentrations, are mean axes of two groups of elements: $\bar{B}_1$, trending N. 49° E. and plunging 54° NE.; and $\bar{B}_2$, trending S. 73° and plunging 44° SE. *E*, Poles of axial planes of folds. Dots, dunite folds trending east-west; circles, chromitite folds trending north-northwest; circled dots, orthopyroxenite folds plunging steeply east; square, dunite fold trending northeast. *F*, Interpretation of dunite-harzburgite contacts. Dashed lines, mean attitudes of two groups of contacts in figure 31*C*; dots, poles to dashed great circles. Line pointing north-northeast on primitive circle shows strike of large dunite dike. Circled dots, principal stress axes; small crosses, inferred slip directions. Arrows indicate inferred sense of slip on mean surfaces.

Dynamic interpretation of the dunite-harzburgite contacts rests on theoretical conclusions regarding the relations of fault planes and the stress ellipsoid (Anderson, 1951). In the case of compressional stress, the acute dihedral angle between conjugate slip surfaces encloses the maximum principal stress $\sigma_1$; the intermediate stress axis $\sigma_2$ parallels the axis of intersection of the slip surfaces. In area VII (fig. 1), the mean $\sigma_1$, which may have resulted in the fracturing, plunges 37°, N. 68° E.; $\sigma_2$ plunges 50°, S. 41° W.; and $\sigma_3$, the minimum principal stress, plunges 14°, N. 32° W. (fig. 31*F*). Mean slip directions would plunge 37°, N. 20° E., and 18°, S. 73° E. Oblique slip with large strike-slip components would occur on both sets of faults. The sense of movement on fractures parallel to the dike trend would be upward on the southeast wall.

Although the theoretical stress orientation and slip directions are deducible from a theory of brittle fracture, the validity of the fracture criteria described above or even of the existence of a brittle-fracture mechanism of any kind in the upper mantle, presumably where the peridotite originated, is open to question because of expected ductile yielding in the upper mantle. Seismic focal mechanisms in the upper mantle are explainable by plastic rather than brittle deformation (see Avé Lallemant and Carter, 1970, p. 2217). Nevertheless, under conditions of unusually large strain rate, possibly associated with rapid plate movement, and (or) localized dunite intrusion, a brittle-fracture mode of deformation may be possible in the upper mantle. Alternatively, the peridotite, at the time of dunite emplacement, may have been at a level at which brittle fracturing could occur. Under these conditions, emplacement of the dunite could have caused fracturing, or the dunite may have intruded a preexisting fracture zone in harzburgite. Heating and partial recrystallization of the harzburgite xenoliths may have resulted in the elimination of much of the harzburgite foliation in these rocks. Subsequent folding of the chromite schlieren in the dunite crystal mush and of dunite apophyses in harzburgite xenoliths would contrast greatly in deformational mode with the initial brittle deformation.

Fracturing may also be controlled by the effective stress in the rock (see Fyfe and others, 1978, p. 200–204). If the pore spaces of the rock are filled with a fluid that cannot move, an external compression will result in a fluid pressure developing in the pores. The net effect of this pore pressure is to reduce the effectiveness of the applied stress; the material behaves as though it is subject to an effective stress, which can be much smaller than the external stress. One result can be brittle failure under higher confining pressures than might be expected in "dry" rock. Water, the most common fluid in crustal rocks, would probably not be pres-

ent in amounts large enough to affect pore pressure in peridotite, especially at great depths. However, fluid from partial melting of a peridotite mantle might be present in significant amounts during some phases of harzburgite evolution. Enough of the melt fraction might be present in places to permit localized brittle deformation in a subcrustal environment.

If the dunite body follows a zone of weakness that developed during formation of northeast-trending folds (deformation 3, table 1), the dunite must postdate that folding. However, the presence in the dunite of northeast-trending minor folds suggests either a final pulse of the deformation or local strain, possibly related to dunite emplacement. The east-west-trending minor folds (deformation 4) seem to be unrelated to any other fabric elements and probably postdate all the northeast-trending folds in area VII.

### AREA VIII: HIGH DIVIDE

Area VIII is 1.5 km southwest of area VII and 0.5 km west of the large north-northeast-trending dunite dike described above (fig. 1). Dunite layers and dikes make up about 40 percent of the terrain. As in area VII, dunite-harzburgite pods in dunite appear to be either boudins or xenoliths.

Most poles of foliations in harzburgite dip at low angles north (fig. 32*A*). The mean orientation of the foliation strikes N. 80° E. and dips 22° NNW. The poles appear to lie near a great circle that defines a β-axis plunging 9°, N. 57° E. Poles of dunite-harzburgite contacts range widely in orientation (fig. 32*B*); the mean orientation is estimated to strike N. 84° W. and dip 33° NNE., close to the mean orientation of harzburgite foliations. Many dunite-harzburgite contacts appear to parallel the harzburgite foliation. Most of these contacts lie near a great circle that defines a β-axis plunging 30°, N. 20° E. This β-axis, on the basis of more data than for the more northeasterly one, is probably the more reliable axis. Tabular dunite bodies generally dip steeply and strike northeast, like the large dunite body in area VII (fig. 31*C*). Chromite schlieren subparallel to dunite dikes suggest flow layering in a dike. Here, as in area VII, an intrusive origin for some of the dunite-harzburgite contacts is favored. Their orientations were influenced in part by the stress regime during emplacement and in part by preexisting planar anisotropies in the harzburgite host.

Linear elements (axes of dunite and orthopyroxene pods, chromite folds, chromite rods, and a β-axis) trend northeast and northwest (fig. 32*D*). Intersecting linear elements suggest that at least two groups of elements are present. The northeast-trending elements correspond to the northeast-trending elements in area VII; the northwest-trending elements are preserved in the harzburgite and may be related to the earliest deformation of the harzburgite (deformation 1, table 1).

Axial planes of northeast-trending linear elements dip southeast and northwest (fig. 32*E*). Axial planes of linear elements that trend northwest dip northwest and northeast.

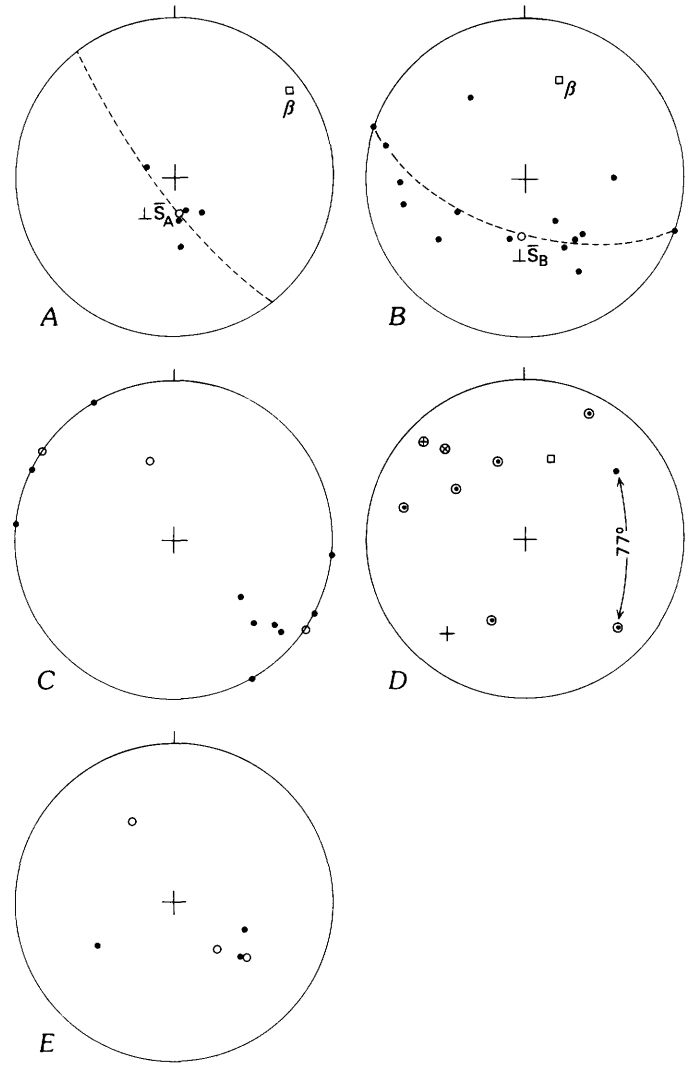


FIGURE 32.—Fabric diagrams for area VIII (fig. 1). *A*, Poles of foliations in harzburgite (dots). Circle $\perp\bar{S}_A$, mean of foliations, striking N. 80° E. and dipping 22° NNW.; square, β-axis plunging 9°, N. 57° E. Dashed great circle is perpendicular to β-axis. *B*, Poles of dunite-harzburgite contacts (dots). Circle $\perp\bar{S}_B$, mean of foliations, striking N. 84° W. and dipping 33° NNE.; square, β-axis plunging 30°, N. 20° E. Dashed great circle is perpendicular to β-axis. *C*, Poles of dunite dikes (dots) and chromite schlieren (circles). *D*, Linear elements. Dot, dunite fold; square, β-axis; circled dots, axes of dunite pods; small cross, chromitite fold; circled cross, chromite rods; circled X, axis of orthopyroxenite pod. Double-headed arrow indicates angle of intersection of linear elements. *E*, Poles of axial planes. Dots, northwest-trending folds; circles, northeast-trending folds.

Subparallelism of the dunite bodies with the axial planes of northeast-trending folds suggests that these two structural elements are related. Dikes were emplaced along planar weaknesses parallel to the axial planes; some dikes were emplaced along the early harzburgite foliation. In these respects, the fabric of area VIII resembles that of area VII.

### AREA IX: PINE FLAT MOUNTAIN

Area IX is 5 km north of area I, on the north end of Pine Flat Mountain (fig. 1). Layering and foliation in harzburgite dip at low to steep angles predominantly northeast (fig. 33*A*); the mean orientation, $\bar{S}$, strikes N. 42° W. and dips 50° NE. Distribution of poles suggests a β-axis plunging 30°, N. 42° E. Linear elements trend north-northwest through west-northwest and plunge at low to steep angles (fig. 33*B*). Intersecting linear elements suggest the presence of at least two groups, one trending north-northwest and the other northeast; steep and east-west-trending groups may also be represented. Axial planes of folds trending northeast dip moderately to steeply north and west (fig. 33*C*). Axial planes of folds plunging east dip moderately to steeply north and south.

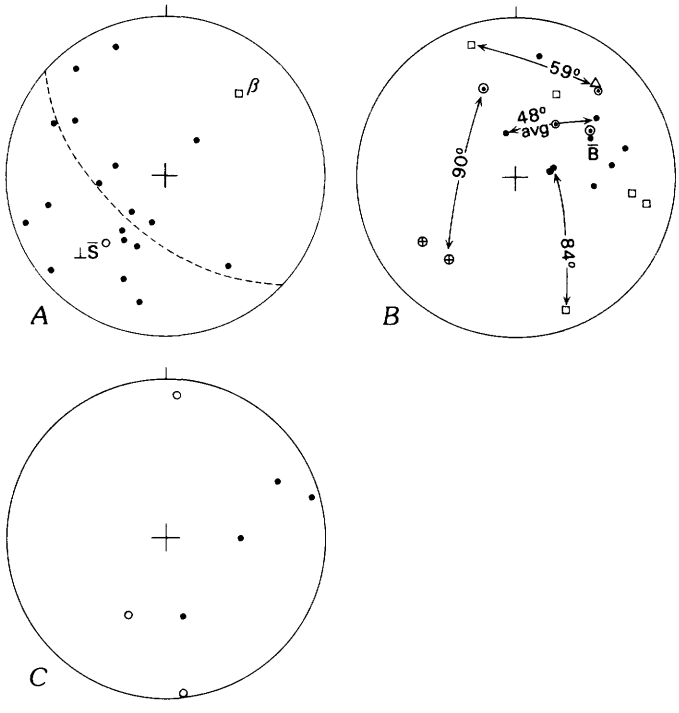


FIGURE 33.—Fabric diagrams for area IX (fig. 1). *A*, Poles of dunite and orthopyroxenite layers and foliation in harzburgite. 18 points. Circle ⊥$\bar{S}$, pole of mean attitude of layering and foliation, striking N. 48° W. and dipping 44° NE.; dashed line, great circle; square, pole to great circle, a β-axis plunging 30°, N. 41° E. *B*, Linear elements. Dots, orthopyroxenite folds; circles, axes of orthopyroxenite pods; circled dots, orthopyroxenite rods; triangle, orthopyroxene lineation; circled cross, chromite rods; squares, β-axes; dot $\bar{B}$, mean of northeast-trending linear elements. Double-headed arrows indicate angles of intersection of linear elements. *C*, Poles of axial planes. Dots, northeast-trending folds; circles, east-west-trending folds.

### AREA X: CLEOPATRA'S LOOKOUT

Area X is 8 km north of area I and 1 km north of the California-Oregon State line (fig. 1). Layering in harzburgite dips steeply north-northeast and south-southwest (fig. 34*A*), orientations that are atypical for most of the peridotite. The mean orientation, $\bar{S}$, strikes N. 71° W. and dips 70° SW. Linear elements plunge predominantly at low to moderate angles west-northwest, west-southwest, and east-southeast (fig. 34*B*). Most of these elements appear to lie on a small circle with axis plunging 9°, N. 82° W. This geometry is consistent with the observed refolding of isoclinal folds in the area. The small-circle rotation of linear elements suggests a predominantly flexural slip mechanism of latest folding in which slip occurred parallel to compositional

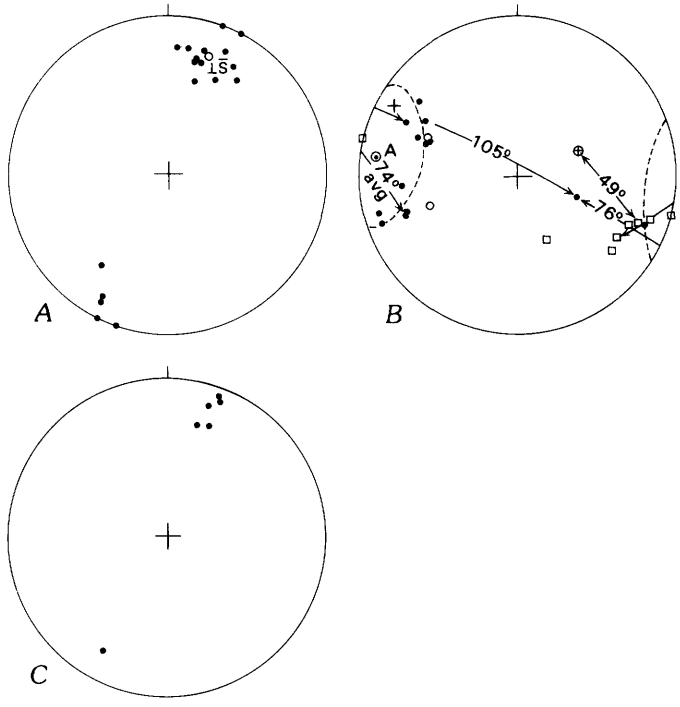


FIGURE 34.—Fabric diagrams for area X (fig. 1). *A*, Poles of orthopyroxenite and dunite layers. Circle ⊥$\bar{S}$, pole of mean layering, striking N. 71° W., dipping 70 SW. *B*, Linear elements. Dots, orthopyroxenite folds; squares, β-axes; circles, orthopyroxenite rods; small cross, chromitite fold; circled cross, chromite lineation; circled dot A, axis of 28° small circle (dashed line), plunging 9°, N. 82° W. Double-headed arrows indicate angles of intersection of linear elements. *C*, Poles of axial planes.

layering (see subsection above entitled "Area II"). Other steeply plunging linear elements are also present. Axial planes of isoclinal folds dip steeply north-northeast and south-southwest, subparallel to layering (fig. 34*C*).

Correlation of generally east-west trending linear elements in area X with the elements in other areas is unclear. Early isoclinal folds in area X could have been rotated from north-northwestward trends, as suggested by the atypical orientations of layering in this area. The fabric may approximate that in multiply folded peridotite near the summit of High Plateau Mountain (subarea IIa), where early folds were rotated about a later fold axis correlated with late east-west-trending folds.

### AREA XI: BISCUIT HILL

Area XI lies along Cook Road (Chetco Divide Road), from 2.5 to 5 km north of the California-Oregon State line, and includes outcrops along the jeep trail to Biscuit Hill, 3 km west of the road (fig. 1). Layers and foliations in harzburgite dip in many directions (fig. 35*A*). The mean orientation of planar elements, $\bar{S}$, strikes N. 9° W. and dips 67° E. Poles tend to lie near the great circle, the pole of which defines a β-axis plunging 50°, S. 41° E. Linear elements (dunite, orthopyroxenite and chromitite folds, axes of dunite pods, chromite lineations, and β-axes) tend to occur near a great circle striking N. 8° W. and dipping 80° E. (fig. 35*B*), close to $\bar{S}$. An 8σ concentration of nearly horizontal linear elements trends north-northwest ($\bar{B}$ plunges 6°, S. 6° E.). Intersecting linear elements suggest that more than one set of elements is present (fig. 35*C*). Groups suggested by figure 35*C*: (1) plunge generally north and south at low angles, (2) plunge moderately steeply southeast parallel to the β-axis, (3) plunge steeply, (4) trend northeast, and (5) trend west-northwest. The axial plane of a fold plunging southeast (group 2) dips steeply northeast (fig. 35*E*). The axial plane of a fold plunging northeast (group 4) dips steeply northwest. Axial planes of folds plunging at low angles west-northwest and east-southeast (group 5) dip steeply south. Two chromite foliations dip steeply northeast (fig. 35*E*), subparallel to the axial plane of the southeast-plunging fold representing group 2 folds. This relation suggests that the axial plane and chromite foliations are geometrically equivalent fabric elements.

### AREA XII: BUCKSKIN PEAK

Area XII is 9 to 14.5 km north of the California-Oregon State line, astride the ridge dividing Josephine and Curry Counties (fig. 1); access is by a jeep trail that leads to chromite mines in the Vulcan Peak area. Structures in the harzburgite are progressively less discernible northward in this area. About 1 km south of Rough and Ready Lakes, just north of the area, the rock is a monotonous, massive harzburgite. The expanse of mesoscopically structureless harzburgite from Rough and Ready Lakes southward, which contrasts with so

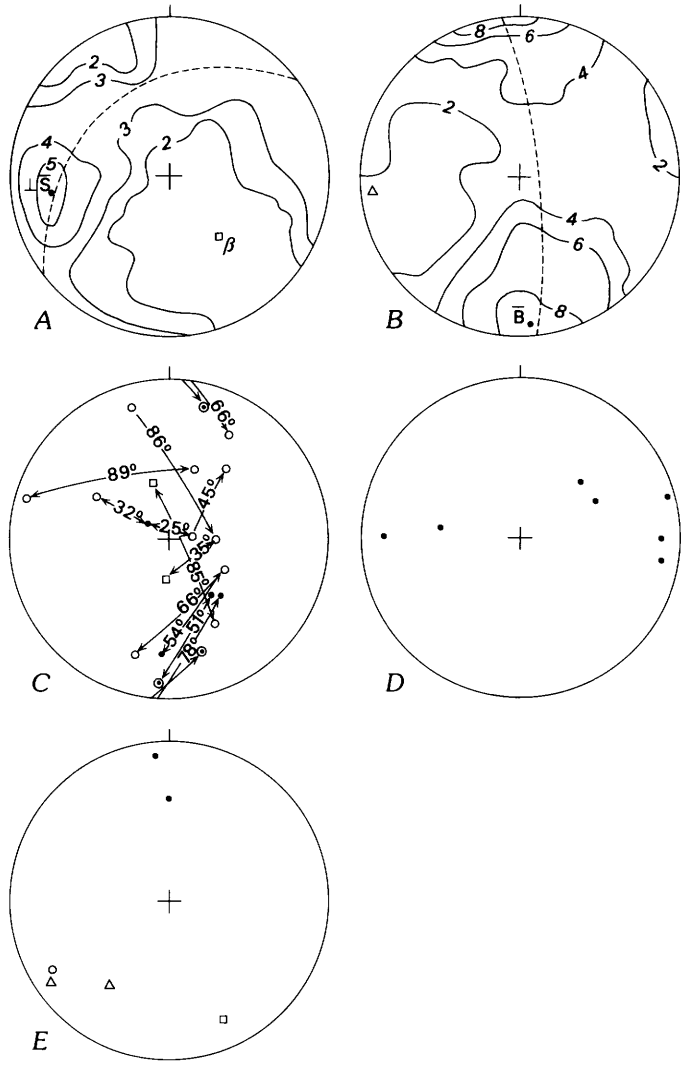


FIGURE 35.—Fabric diagrams for area XI (fig. 1). *A*, Contour diagram of poles of orthopyroxenite and dunite layers and of foliation in harzburgite. 21 points. Contours: 2σ, 3σ, 4σ, and 5σ. Dot ⊥$\bar{S}$, mean attitude of layering and foliation, striking N. 9° W. and dipping 67° E.; dashed line, great circle; square, pole to great circle, a β-axis plunging 50°, S. 41° E. *B*, Contour diagram of linear elements. 37 points. Contours: 2σ, 4σ, 6σ, and 8σ. Dot $\bar{B}$, center of 8σ concentration, is mean fold axis, trending N. 6° W. and plunging 6° SSE.; dashed line, great circle; triangle, pole to great circle, possibly a rotation axis of folds. *C*, Intersecting linear elements. Circles, orthopyroxenite folds; dots, dunite folds; circled dots, axes of dunite pods; squares, β-axes. Double-headed arrows indicate angles of intersection of linear elements. *D*, Poles of axial planes of folds plunging at low angles generally north and south. *E*, Poles of axial planes of folds trending east-west (dots), northwest (circle), and northeast (square), and poles of chromite foliations (triangles).

much of the harzburgite farther to the south, suggests that (1) localized recrystallization obliterated the foliation and other structures sometime in the history of the rock, or (2) the massive harzburgite may not have been deformed so intensely or in the same way as harzburgite to the south.

The dunite, chromite, and orthopyroxene layers and dunite-harzburgite contacts are subparallel at most localities and are plotted together here. In the contour diagram (fig. 36*A*), they dip predominantly east but have a multimodal distribution. The dominant, east-dipping group lies along a great circle that defines a β-axis plunging 40°, S. 80° E.; the subordinate group lies along a great circle that defines a β-axis plunging 10°, N. 80° W. The population of planar elements appears to be essentially bimodal with respect to the β-axes.

Linear elements, (including folds of dunite, orthopyroxene, and chromite layers, orthopyroxene and chromite rods, axes of dunite and orthopyroxene pods, chromite lineations, and β-axes), fall into four groups on

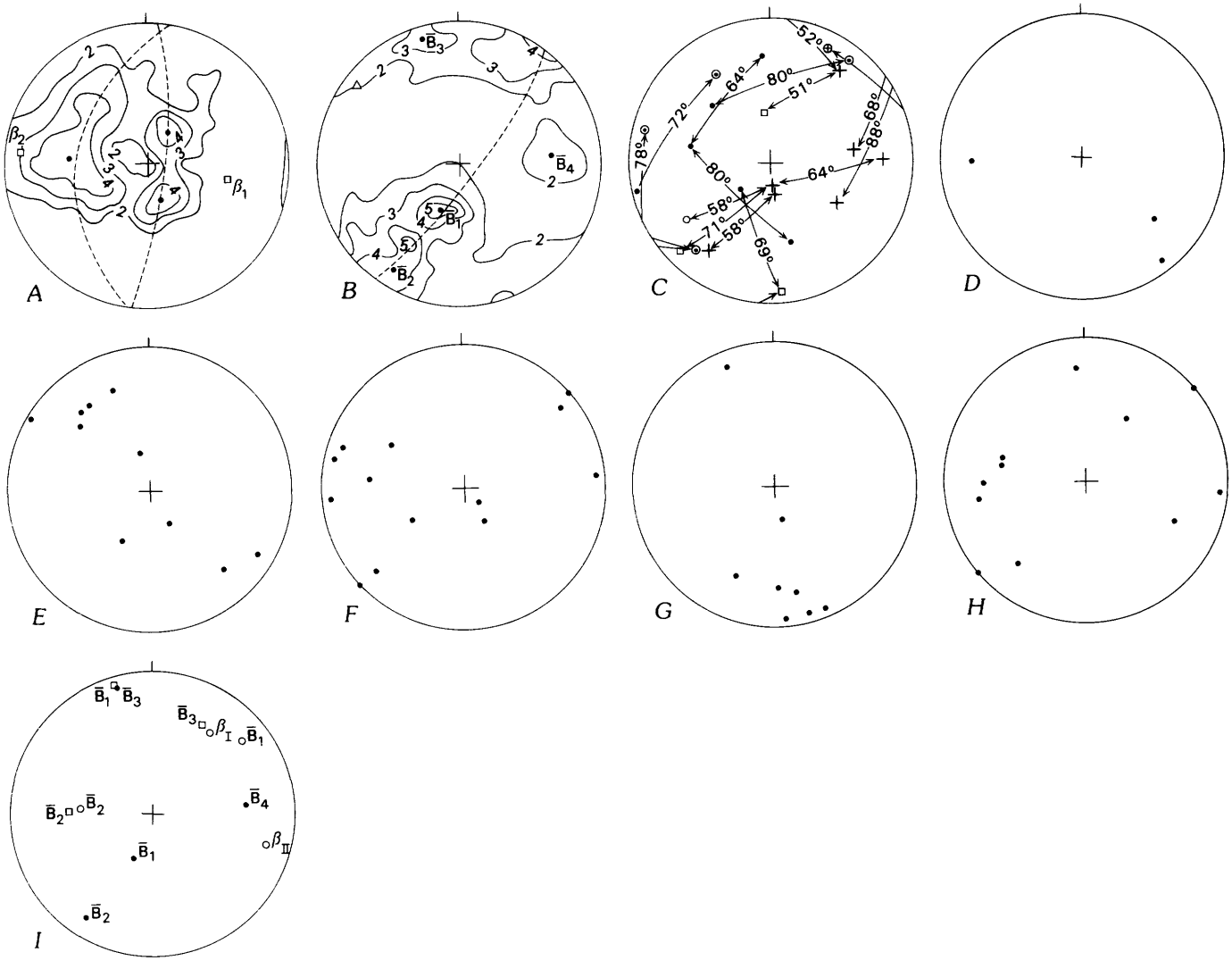


FIGURE 36.—Fabric diagrams for area XII (fig. 1). *A*, Contour diagram of poles of dunite, chromite, and orthopyroxenite layers and dunite-harzburgite contacts. 104 points. Contours: 2σ, 3σ, and 4σ. Dots, approximate centers of 4σ concentrations, are poles of mean attitudes of subpopulations; dashed lines, great circles; squares, poles of great circles and β-axes: $\beta_1$, plunging 40°, S. 80° E. and $\beta_2$, plunging 10°, N. 80° W. *B*, Contour diagram of linear elements. 60 points. Contours: 2σ, 3σ, 4σ, and 5σ. Dashed line, great circle; triangle, pole of great circle; dots, approximate mean axes of four groups of elements: $\bar{B}_1$, plunging 58°, S. 24° W.; $\bar{B}_2$, plunging 12°, S. 33° W.; $\bar{B}_3$, plunging 11°, N. 14° W.; and $\bar{B}_4$, plunging 30°, N. 86° E. *C*, Intersecting linear elements. Dots, dunite folds; circled dots, axes of dunite pods; circle, orthopyroxenite fold; circled cross, axis of orthopyroxenite pod; small crosses, chromitite folds; squares, β-axes. Double-headed arrows indicate angles of intersection of linear elements. *D*, Poles of axial planes of $\bar{B}_1$-type folds. *E*, Poles of axial planes of $\bar{B}_2$-type folds. *F*, Poles of axial planes of $\bar{B}_3$-type folds. *G*, Poles of axial planes of $\bar{B}_4$-type folds. *H*, Poles of chromite foliations. *I*, Comparison of linear elements in area XII (dots), area I (circles), and area II (squares).

the contour diagram (fig. 36*B*): (1) a 5σ concentration plunging steeply south-southwest; (2) a 4σ concentration with a small 5σ maximum, plunging at low to moderate angles chiefly southwest; (3) a 3σ concentration plunging at a low angle north-northwest; and (4) a 2σ concentration plunging moderately east, close to the more strongly defined β-axis. The dashed great circle represents a plane near which most linear elements occur. The pole to this plane lies close to, but outside, the 2σ contour on figure 36*A*, a relation suggesting that this plane is not closely related to layering; the plane may have another significance or be fortuitous. Orthopyroxenite rods, evidence of intense local strain, occur only in group 3 linear elements. Axes of dunite pods trend north-northwest (group 3) and northeast (group 2). Chromite lineations are absent only in the east-west-trending group (group 4). Intersecting linear elements (fig. 36*C*) support the division of the linear elements into at least four groups like those listed above.

Axial planes of group 1 folds are steep (fig. 36*D*). Axial planes of group 2 folds strike predominantly northeast and dip at low to steep angles (fig. 36*E*). Nearness of the β-axis of these axial planes to $\bar{B}_2$ suggests that this group of folds may have been refolded about an axis subparallel to $\bar{B}_2$. Axial planes of group 3 folds vary widely in orientation (fig. 36*F*); they crudely define a β-axis subparallel to $\bar{B}_3$, consistent with the field observation of refolding of northwest-trending isoclinal folds. Axial planes of group 4 folds mostly dip steeply north (fig. 36*G*). Chromite foliations vary widely in orientation (fig. 36*H*); subparallelism of foliations to the axial planes of all four fold groups indicates that these foliations are not uniquely related to any single folding episode.

Figure 36*I* compares the orientations of linear elements in area XII with those of elements in area I and subarea IIa. Elements of group 2 in area XII resemble the north-northwest-trending elements in area II and, like them, include many structures indicative of intense strain (isoclinal folds, rods). Elements of group 4 coincide in part with east-west-trending β-axes of area I but are far from measured linear elements in area I and subarea IIa. Elements of group 1 do not have major counterparts in area I and subarea IIa, but may correlate with steep folds in other areas and may represent a separate episode of deformation of local significance. Evidence in area XII does not indicate the relative ages of the linear elements.

### AREA XIII: RED MOUNTAIN

Area XIII is 50 km south of the California-Oregon State line and 10 km east of the town of Klamath (fig. 1). Harzburgite foliation and dunite and orthopyroxene layers subparallel to foliation dip at low to steep angles predominantly north and northwest (fig. 37*A*). The poles lie near a great circle, the pole of which defines a β-axis plunging 10°, S. 80° W. Dunite and orthopyroxene layers in nonfoliated harzburgite have a similar orientation pattern (fig. 37*B*), with predominantly northwest dipping layers and a slightly steeper β-axis. Dunite layers containing measurable linear elements have similar orientations (fig. 37*C*). All these subpopulations of planar elements could have been subparallel before folding.

Linear elements (orthopyroxenite and chromitite folds, the axis of a dunite pod, orthopyroxene and chromite rods) generally plunge at low to moderate angles north-northwest through south-southwest (fig. 37*D*). Sets of chromite rods parallel adjacent tightly folded chromite layers. The linear elements seem to make up at least two groups, as suggested by the 44° to 60° spread in intersecting linear elements; one group trends northwest, and the other east-west through northeast. β-axes of planar elements are subparallel to the second group. A few other folds plunge at low to moderate angles east and northeast.

Axial planes of east-west-trending folds are subparallel to layers and foliations in harzburgite (fig. 37*E*). Many of these east-west-trending folds are isoclinal, indicating flattening at high angles to the layers. The axial planes, like the layers and foliations, lie near a great circle, the pole of which defines a β-axis plunging 30°, S. 70° W., subparallel to the β-axes of the other planar elements. These relations suggest refolding of east-west-trending isoclinal folds about an east-northeast-trending axis. Refolding was also noted in outcrop. The axial plane of a fold plunging northeast dips moderately northwest, like some of the other axial planes.

Chromite foliations that cross dunite-harzburgite contacts are at low angles to dunite layers and dip moderately south-southwest (fig. 37*E*). Two chromite foliations, defined by arrays of flattened chromite rods, strike northeast; one dips moderately northwest, and the other is vertical. The chromite foliations are close in orientation to some axial planes of east-west-trending folds and may be geometrically equivalent to the axial planes of these folds, a relation consistent with interpretation of some chromite rods as detached fold hinges.

Late dunite dikes do not have a clearly defined orientation pattern. However, many of them seem to be close in orientation to the layering and foliation in harzburgite (fig. 37*F*), a relation that may reflect a mechanical anisotropy parallel to the layering and foliation. Orthopyroxenite dikes dip at moderate angles chiefly south, southwest, and west (fig. 37*G*), in no apparent relation to any planar anisotropy in the rock.

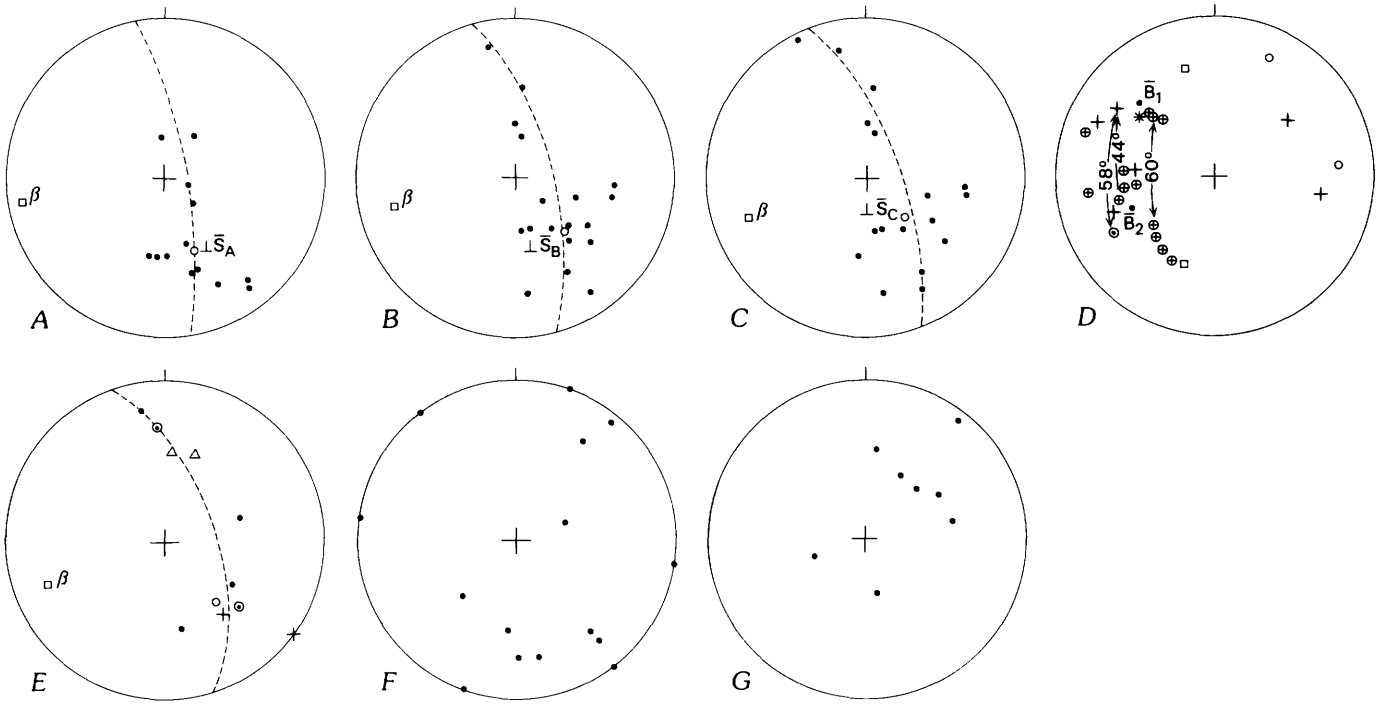


FIGURE 37.—Fabric diagrams for area XIII (fig. 1). *A*, Poles of foliation in harzburgite and of orthopyroxenite and dunite layers parallel to foliation. 13 points. Dashed line, great circle; square, pole of great circle, a β-axis plunging 10°, S. 80° W.; circle $\perp \bar{S}_A$, pole of mean attitude of layers and foliation. *B*, Poles of orthopyroxenite and dunite layers, not clearly parallel to a harzburgite foliation. 18 points. Dashed line, great circle; square, pole of great circle, a β-axis plunging 20°, S. 75° W.; circle $\perp \bar{S}_B$, pole of mean attitude of layers. *C*, Poles of dunite layers containing chromite and orthopyroxenite rods or folds. 17 points. Dashed line, great circle; square, pole of great circle, a β-axis plunging 20°, S. 70° W.; circle $\perp \bar{S}_C$, pole of mean attitude of layers. *D*, Linear elements. 25 points. Circles, orthopyroxenite folds; circled dot, axis of dunite pod; small crosses, chromitite folds; circled crosses, chromite rods; squares, orthopyroxenite rods; asterisk, axis of chromitite boudin; dot $\bar{B}_1$, mean orientation of northwest-plunging folds; dot $\bar{B}_2$, mean orientation of southwest- and west-plunging folds. Double-headed arrows indicate angles of intersecting linear elements. *E*, Poles of axial planes. Circle, northeast-plunging fold; dots, east-west-trending folds; circled dots, axial surface of dunite pod; triangles, chromite foliation; small crosses, chromite foliation defined by flattened chromite rods; dashed line, great circle; square, pole of great circle, a β-axis plunging 30°, S. 71° W. *F*, Poles of dunite dikes. *G*, Poles of orthopyroxenite dikes.

## SUMMARY

The mean poles of layers and foliations in harzburgite in parts of the study area (areas I, II, and V–XIII) are plotted in figure 38. In certain areas, subpopulations of these planar elements were defined, and the mean of each of these subpopulations was included on the plot. The resulting preferential representation of planar fabric elements from certain areas was judged to be preferable to ignoring the subpopulations.

The mean attitudes vary widely. Many of these means lie near a great circle that defines a β-axis plunging 10°, N. 38° E. This regional fold axis for the peridotite reflects the pervasive northeast-trending folds observed in many areas.

Mean attitudes of subpopulations of linear elements were determined for most of the 13 areas (fig. 1); the data are summarized in figure 39. No mean orientations were determined for those areas in which the linear subfabrics do not constitute moderately well defined sets. The means are divided into four groups, defined in part by orientation and in part by fold style, that correspond to the fold groups described above: (1) early folds, generally trending north-northwest and northwest (fig. 39*A*); (2) northeast-trending folds (fig. 39*B*); (3) east-west-trending folds (fig. 39*C*); and (4) steep folds plunging in several directions (fig. 39*D*). Variation in the attitudes of mean orientations of each group of linear elements could be due to random rotation of large blocks of peridotite by faulting, either during or after Late Cretaceous thrusting, as well as to broad-scale heterogeneity of the deformations.

Refolding of early isoclinal folds is indicated in outcrop and is implied in the suggested small-circle dispersion of the mean attitudes of linear elements of group 1 (fig. 39*A*). The axis of the small circle is horizontal and trends N. 45° W. Therefore, early isoclinal folding (deformation 1, table 1) was followed by flexural-slip folding on a broad as well as a minor scale (deformation 2). Large folds of this kinds are not mappable owing to the

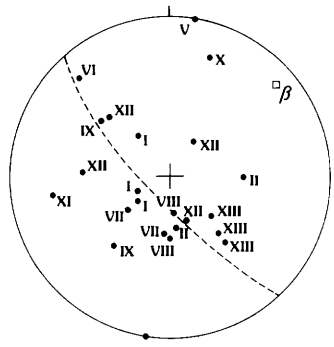

FIGURE 38.—Poles (dots) to mean attitudes of subpopulations of layering and foliations in areas I, II, and V through XIII (fig. 1). Dashed line, great circle; square, pole to great circle, a β-axis plunging 10°, N. 49° E.

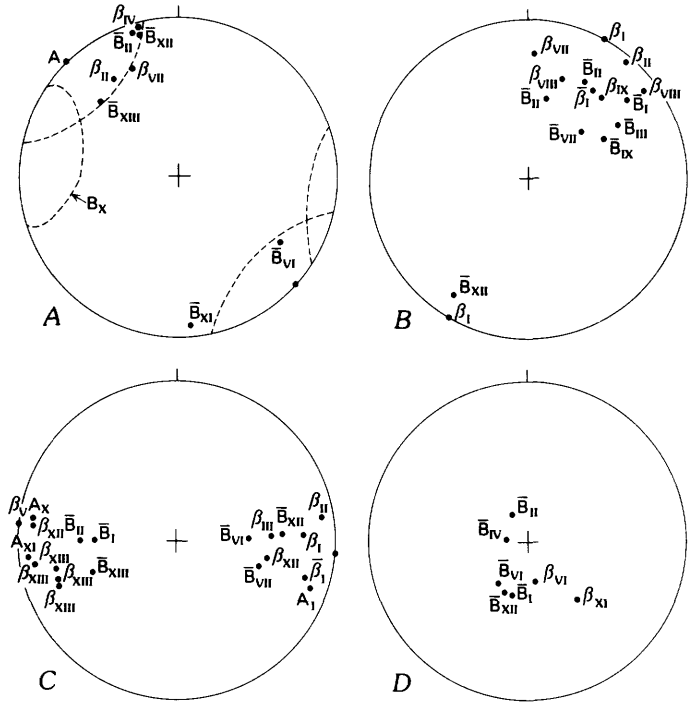


FIGURE 39.—Synopsis of linear elements in areas I through XIII (fig. 1). Dot B̄, mean orientation of a group of linear elements; dot β, β-axis; dot β̄, mean orientations of a group of β-axes; dot A, rotation axis. *A*, Linear elements trending northwest and north-northwest. Dashed circle $B_X$, distribution of early linear elements in area X. *B*, Linear elements trending northeast. *C*, Linear elements trending east-west. *D*, Steeply plunging linear elements.

absence of marker horizons in the harzburgite. Broad-scale folding of layers and foliations about this northwest-trending axis may account for some of the wide spread of poles in figure 38.

A β-axis, approximated from the distribution of poles to mean orientations of planar elements, plunges northeast (fig. 38), like the folds of group 2 above. This relation points to a broad-scale folding of peridotite during formation of later, northeast-trending folds (deformation 3). This event does not appear to have affected some domains in which poles of layering and foliation are far from the broad northwest-southeast band of poles (see areas V and X), and was not strong enough to alter greatly the orientations of early, northwest-trending folds.

Mean attitudes of subpopulations of linear elements with generally east-west trends (fig. 39*C*; deformation 4) show a large scatter along a steep east-west great circle. In some areas (area I), mean attitudes of the subpopulations differ greatly, possibly owing to systematic differences in orientation between large and small folds or, to heterogeneity of the deformation. The fabric data in area XII and subarea IIa indicate that early, northwest-trending folds were rotated in small circles about axes correlated with east-west-trending linear elements and thus that these east-west-trending elements are the youngest of the three groups, and suggest a flexural-slip mechanism of folding for the deformation.

Subpopulations of steep linear elements occur in only seven of the areas (fig. 39*D*). Relative development of steep linear elements varies from area to area in the peridotite. At some localities in area I, steep folds may be a conjugate set at right angles to northeast-trending folds (B ⊥ B′ tectonite), and contemporaneous with those folds (deformation 3). In area XII, steep elements constitute the dominant set and are not clearly related to any other group of elements. These steep linear elements may include elements formed during more than one episode of deformation; the episodes need not correspond to episodes of formation of northwest-, northeast-, or east-west-trending folds and may constitute a separate deformation (5).

## FABRIC OF THE VULCAN PEAK AREA

The structure of the Josephine Peridotite in the Vulcan Peak area (fig. 1) was studied by Loney and Himmelberg (1976). Dunite layers there are postulated to have originated by metamorphic differentiation, as well as by transposition of older layers into parallelism with the harzburgite foliation. The harzburgite foliation is predominantly horizontal or dips slightly northwest and southeast. Chromite layering in dunite is subparallel to the harzburgite foliation. The mean orientations of the subpopulations of foliations resemble those of layering for many of the areas I through XIII (compare fig. 22 with Loney and Himmelberg, 1976, fig. 9). Furthermore, the foliation at Vulcan Peak has a great-circle distribution that defines a β-axis plunging at a low angle southwest, subparallel to some measured fold axes. At Vulcan Peak, the earliest deformation, clearly the most intense one, created the dominant harzburgite foliation and a few isoclinal and nearly isoclinal folds. Some of these folds have disrupted limbs and detached

fold hinges, and show evidence of refolding. Axes of these early folds trend northwest through northeast and plunge at low angles. Harzburgite foliation and dunite layering were broadly warped later.

A late, weakly developed foliation, defined by closely spaced arrays of ridges on weathered surfaces, resembles a cleavage. Locally, this foliation grades into closely spaced fractures or joints. The foliation strikes north-south and dips steeply or is vertical. Orientations suggest that this foliation could be equivalent to some axial planes of late northeast-trending folds and some chromite foliations in areas I through XIII.

The mesoscopic fabric of peridotite in the Vulcan Peak area is broadly similar to the fabric of peridotite in areas I through XIII. Major differences are in the apparently more intense, late open folding exhibited in areas I through XIII.

## PETROFABRIC STUDIES

### INTRODUCTION

Eight oriented rock samples (J1–J8) were taken for petrofabric analysis: one of harzburgite, six of dunite, and one of wehrlite. The samples were selected from what seemed relatively unserpentinized outcrops that exhibited lineations, minor folds, and (or) planar structures. The hardness of most outcrops and the intense serpentinization of much of the more highly fractured peridotite precluded sampling more rocks for analysis and thus limited the selection. The eight rock samples are serpentinized to varying degrees (15–75 percent), but enough unserpentinized material remains in the most altered samples for petrographic study. The study plan was to measure the orientations of the principal axes of the optical indicatrix of 50 grains from each of three thin sections in each sample, olivine grains in samples J1 through J7 and diopside grains in sample J8. The thin sections are approximately mutually perpendicular and several centimeters apart. The 50-grain samples for each rock were compared to estimate degree of homogeneity of the subsamples before the data were compiled and contoured.

The petrofabric data described in this section indicate that, in much of the Josephine Peridotite, the olivine fabrics developed by syntectonic recrystallization. Homotactic or nearly homotactic orthorhombic and suborthorhombic microfabrics and mesoscopic fabrics formed during each major deformation. In rocks that underwent more than one deformation, the orthorhombic fabrics of the earlier deformations were locally overprinted rather than destroyed. These superposed subfabrics have triclinic symmetry because the deformations were not coaxial. A possible primary cumulate olivine fabric occurs in one chromitiferous dike showing textural evidence of a cumulus stage. A suborthorhombic diopside fabric in wehrlite is tentatively interpreted to have formed mainly by cumulus processes.

### DESCRIPTION OF MICROFABRICS

#### SAMPLE J1

Sample J1, a harzburgite, is from the doubly folded outcrop in the central part of subarea IIa (figs. 1, 22, 23). About 50 percent of the rock is serpentine, primarily along anastomosing veins; the enstatite is almost completely serpentinized. Olivine textures are difficult to identify in thin section (fig. 40). The generally anhedral olivine grains are as much as 5 mm long; apparent elongation is as much as 1.5:1 parallel to a weakly defined foliation. Some olivine embays enstatite. Many large olivine grains are polygonized. The enstatite grains, as inferred from the serpentinized pseudomorphs, were anhedral, as much as 4 mm long, poikilitic, and contained rounded inclusions of olivine. A few kink bands occur in relict enstatite grains. Chromite occurs as anhedral masses. The serpentine veinlets contain opaque iron oxides, possibly magnetite.

The degree of homogeneity of the optical fabric elements X, Y, and Z varies. The Z fabric is strongly homogeneous, the X fabric homogeneous but weaker than Z, and the Y fabric is somewhat heterogeneous:

*X fabric (fig. 41A).*—A girdle approximately perpendicular to the axial plane of the early isoclinal fold hinge; the 8σ maximum on the girdle is perpendicular to the axial plane.

*Y fabric (fig. 41B).*—A girdle approximately coincident with the X-girdle and containing two maxima (8σ and 6σ).

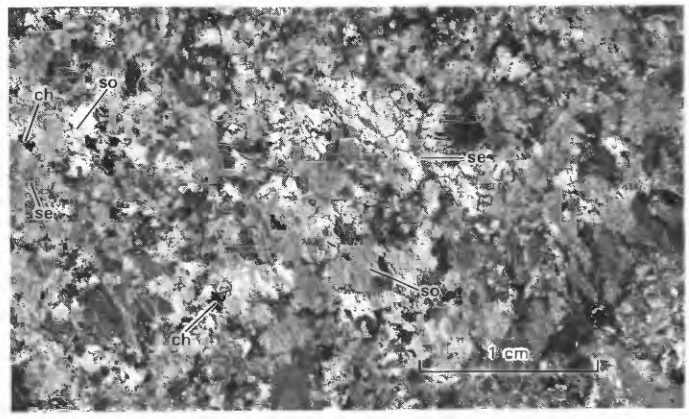


FIGURE 40.—Thin section of sample J1, a harzburgite. ch, chromite; se, serpentinized enstatite; so; serpentinized olivine. Serpentinization is concentrated along anastomosing veins at a large angle to long dimension of thin section. Grains are inferred to have been anhedral before serpentinization.

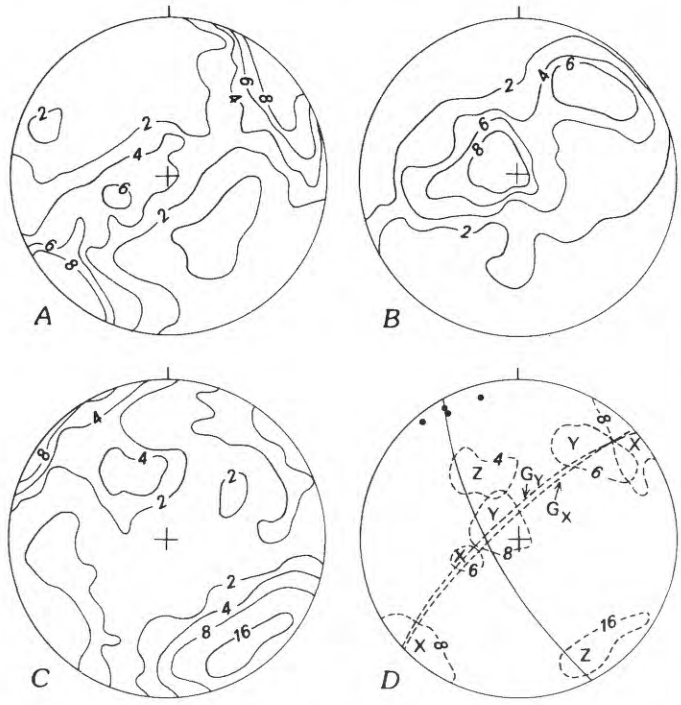


FIGURE 41.—Olivine-fabric diagrams for sample J1, a harzburgite. 148 points. Contours: 2σ, 4σ, 6σ, 8σ, 16σ, and pole-free area (unlabeled contours). *A*, X-axes. *B*, Y-axes. *C*, Z-axes. *D*, Synopsis of fabric features. Dashed lines, concentrations of X-, Y-, and Z-axes and girdle distributions (*G*) of X and Y; solid line, axial plane of early fold; dots, early-fold axes.

*Z fabric (fig. 24C).*—One maximum (16σ) at a high angle to the X- and Y-girdles and close to early-fold axes, and another maximum (4σ) unrelated to other fabric elements.

The fabric elements are summarized in figure 41*D*. The fabric has orthorhombic symmetry. The 16σ Z maximum is close to the north-northwest-trending folds referred to the earliest discernible deformation (1, table 1) in the peridotite. Because that deformation appears to have been pervasive in the harzburgite, the fabric illustrated by sample J1 may be typical of the harzburgite. Rotation of the early mesoscopic fold axis about an east-northeast-trending axis has not affected the harzburgite microfabric of the sample.

### SAMPLE J2

Sample J2 is from a dunite dike containing flattened chromite rods in area XIII (fig. 1). Planar arrays of the rods define a foliation in the dunite. The dunite contains 15 percent serpentine in a boxwork of veinlets cutting olivine (fig. 42). Very thin, anastomosing serpentine veinlets along olivine grain boundaries obscure olivine textures. Most olivine grains are anhedral; a few grains are subhedral. Grains range in size from 0.5 to 15 mm, with an apparent elongation of as much as 2.5:1, chiefly in the plane of the chromite-rod foliation. Two populations of olivine grains are suggested by the absence of gradation in size between large and small grains: (1) grains greater than 5 mm long, and (2) grains less than 2 mm long. Olivine is altered to iddingsite and a colorless amphibole (tremolite?) along veins. Kink bands were observed in a few olivine grains. Chromite grains are anhedral, angular, oval, and surrounded by shells of serpentine.

The degree of homogeneity of the optical fabric elements varies: Z and X are moderately homogeneous, and Y is somewhat inhomogeneous:

*X fabric (fig. 43A).*—A girdle at a high angle to the chromite-rod foliation; an 8σ maximum perpendicular to the foliation, and another 8σ maximum in the foliation.

*Y fabric (fig. 43B).*—A girdle nearly coincident with the X-girdle; one maximum (6σ) nearly perpendicular to the foliation, and another maximum (12σ) in the foliation.

*Z fabric (fig. 43C).*—A maximum (22σ) lying in the foliation and close to the chromite rods; a partial girdle at a high angle to the foliation.

The fabric elements are summarized in figure 43*D*. The total fabric, which has orthorhombic symmetry, points to contemporaneity of both the microscopic and mesoscopic fabric elements. Analysis of the mesoscopic fabric elements in area XIII suggests correlation of the fabric of sample J2 with the deformation during which the east-northeast-trending group of folds formed (deformation 4, table 1). The dunite dike was emplaced just before or during this deformation, or else earlier fabric elements were obliterated by the deformation.

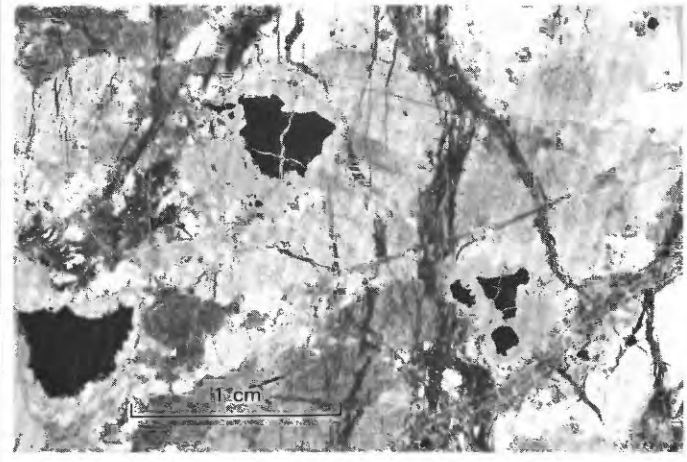


FIGURE 42.—Thin section of sample J2, a dunite. Light- and dark-gray grains, olivine; dark veins, serpentine; black grains, chromite with shell of gray serpentine. Olivine grains are mostly anhedral. Elongation of chromite masses not shown.

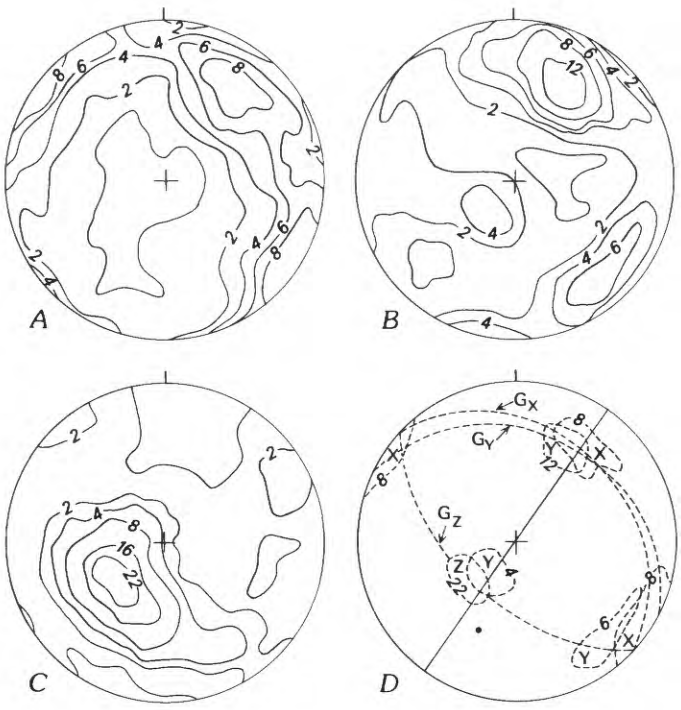


FIGURE 43.—Olivine-fabric diagrams for sample J2, a dunite. 163 points. Contours: 2σ, 4σ, 6σ, 8σ, 12σ, 16σ, 22σ, and pole-free area (unlabeled contours). *A*, X-axes. *B*, Y-axes. *C*, Z-axes. *D*, Synopsis of fabric features. Dashed lines, concentrations of X-, Y-, and Z-axes and girdle distributions (*G*) of X, Y, and Z; solid line, foliation defined by flattened chromite rods (dot).

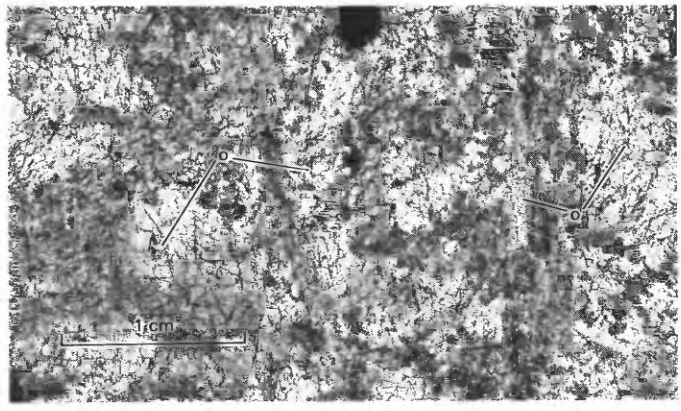


FIGURE 44.—Thin section of sample J3, a dunite. Large (5–10 mm) olivine grains (o) are fragmented by serpentine veinlets (network of fine lines). Some grains appear to be subhedral and equant and to contain recrystallized zones in which subhedral grains are 1 to 3 mm across. Two conspicuous zones oriented perpendicular to long dimension of section contain grains elongated as much as 3:1.

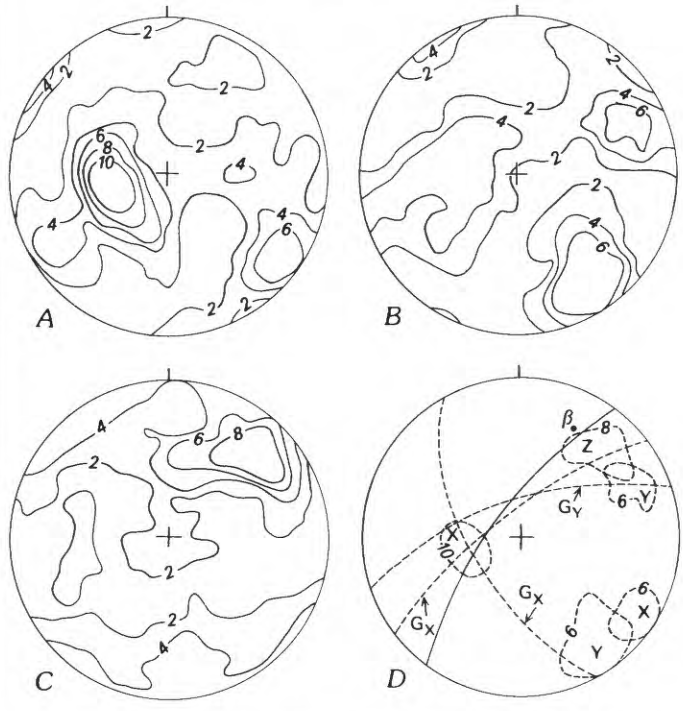


FIGURE 45.—Olivine-fabric diagrams for sample J3, a dunite. 150 points. Contours: 2σ, 4σ, 6σ, 8σ, 10σ, and pole-free area (unlabeled contour). *A*, X-axes. *B*, Y-axes. *C*, Z-axes. *D*, Synopsis of fabric features. Dashed lines, concentrations of X-, Y-, and Z-axes and girdle distributions (*G*) of X and Y; solid line, mean attitude of dunite dikes in area VIII (fig. 1); β, β-axis near sample site.

### SAMPLE J3

Sample J3 is from a dunite dike intruding harzburgite in area VIII (fig. 1). The rock contains 25 percent serpentine in veinlets that obscure the textural relations of the olivine (fig. 44). Olivine grains range in length from 0.1 to 15 mm, with apparent elongation as much as 3:1, though not consistently in the same direction or plane. No kink bands were seen. Anhedral chromite masses make up less than 1 percent of the rock, are disseminated in olivine, and, locally, contain what appear to be olivine inclusions.

Fifty-grain samples of X, Y, and Z are somewhat inhomogeneous:

*X fabric (fig. 45A).*—A possible partial girdle at a high angle to the mean attitude of the dunite dikes in the area, and a subordinate partial girdle at a low angle to the mean of dikes; one maximum (6σ) perpendicular to the mean of dikes, and another maximum (10σ) in the plane of the mean of dikes.

*Y fabric (fig. 45B).*—A girdle at a small angle to the mean attitude of dunite dikes; one maximum (6σ) approximately perpendicular to the mean of dikes, and another maximum (6σ) plunging east-northeast.

*Z fabric (fig. 45C).*—A maximum (8σ) near the mean attitude of dunite dikes and nearly coincident with the northeast-trending β-axes in area VIII.

The fabric elements are summarized in figure 45*D*. The nearly orthorhombic total fabric of sample J3 suggests a close relation between both the mesoscopic and

microscopic fabric elements. The dikes, including the one from which sample J3 was taken, postdate some northeast-trending folds in harzburgite. The Z maximum, however, is close to a northeast-trending β-axis that has been correlated with northeast-trending open folds (deformation 3, table 1). These relations can be explained in the same way as the northeast-trending folds in the large dunite dike in area VII, as reflecting a separate phase of deformation related to deformation 3 or as related to local deformation in the dike.

## SAMPLE J4

Sample J4 is from a dunite layer, 25 cm thick, in harzburgite in area XII (fig. 1). The layer contains chromite schlieren, folds, and lineations. A foliation, defined by planar arrays of chromite grains in chromite schlieren, parallels the axial planes of chromite folds. The rock is 75 percent serpentine; serpentinization is particularly intense around the anhedral chromite grains (fig. 46). Olivine textures are obscure. Extinction of unserpentinized olivine fragments, however, suggests that the grains were originally subhedral to anhedral, as much as 6 mm long, elongate as much as 2.5:1 in several directions, and locally at a high angle to chromite schlieren.

Fifty-grain samples of Z-axes are somewhat homogeneous; subsamples of X- and Y-axes are somewhat heterogeneous, and X more heterogeneous than Y:

*X fabric (fig. 47A).*—Two possible partial girdles at small angles to the plane of chromite schlieren; four maxima, one 4σ, two 6σ, and one 8σ.

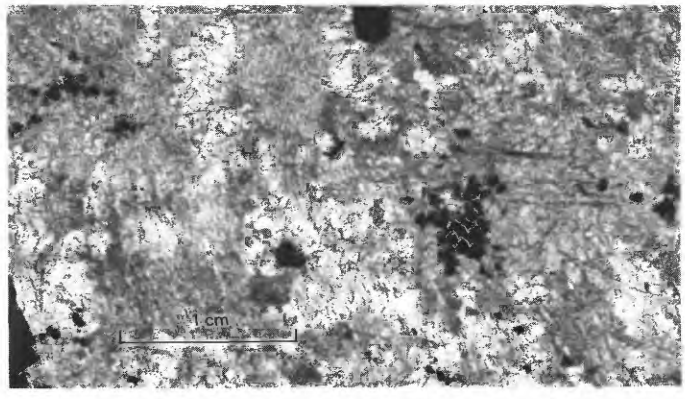


FIGURE 46.—Thin section of sample J4, a dunite. Olivine grains (white areas) were originally subhedral to anhedral. Serpentinization (gray areas) is especially intense in vicinity of chromite grains (black areas).

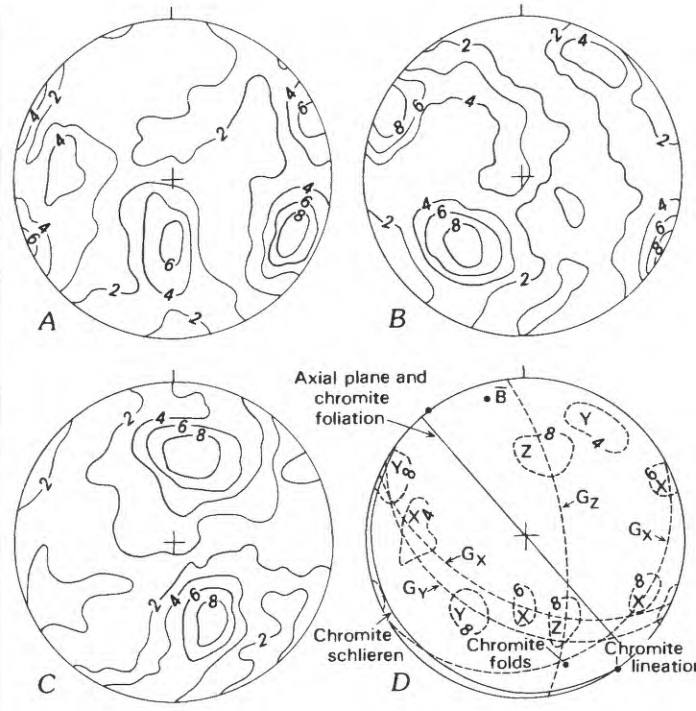


FIGURE 47.—Olivine-fabric diagrams for sample J4, a dunite. 144 points. Contours: 2σ, 4σ, 6σ, 8σ, and pole-free area (unlabeled contours). *A*, X-axes. *B*, Y-axes. *C*, Z-axes. *D*, Synopsis of fabric features. Dashed lines, concentrations of X-, Y-, and Z-axes and girdle distributions (*G*) of X, Y, and Z; dot B̄, mean of northwest-trending folds in area XII (fig. 1).

*Y fabric (fig. 47B).*—A possible partial girdle; three maxima, one 4σ and two 8σ.

*Z fabric (fig. 47C).*—Two maxima, 8σ each, one subparallel to the chromite fold axis and lineation and along the axial plane of the fold, and the other plunging north-northeast, perpendicular to one of the X-girdles and the partial Y-girdle.

The fabric elements are summarized in figure 47*D*. The total fabric is triclinic. The numerous maxima and the crossed X-girdles suggest that the total fabric is a resultant of superposed fabrics. The southeast-plunging Z maximum subparallel to chromite folds and lineations lies in the axial plane of the folds and has characteristics like the fabric of sample J1. The northwest-trending mesoscopic linear elements may be correlated with the early, northwest-trending isoclinal folds (deformation 1, table 1) or with the somewhat later episode of refolding of these folds (deformation 2). The northeast-trending Z maximum and possibly associated partial girdles of X and Y resemble the fabric of sample J3, which is interpreted to have developed along the northeast-trending folds (deformation 3).

SAMPLE J5

Sample J5 is from a dunite body, at least 5 m thick, in harzburgite in area III (fig. 1). About 15 percent of the rock is serpentine veinlets, which obscure the textures of the olivine (fig. 48). Olivine grains appear to be subhedral to euhedral; some large grains contain inclusions of olivine. Some of the olivine is anhedral and interstitial. These textures may be remnants of primary cumulate textures. Many grains have shadowy extinction, but few kink bands were seen. Grains range in size from 0.5 to 7 mm and are elongate parallel to chromite schlieren as much as 3:1. Chromite nodules are anhedral and have serpentine shells. Some nodules have oval serpentine cores, probably representing either altered olivine grains enclosed in aggregates of chromite grains or chromite masses deeply corroded by olivine (see chromite nodule in upper right corner, fig. 48). Chromite lineations are emphasized by the serpentine shells, which appear as serpentine rods in outcrop.

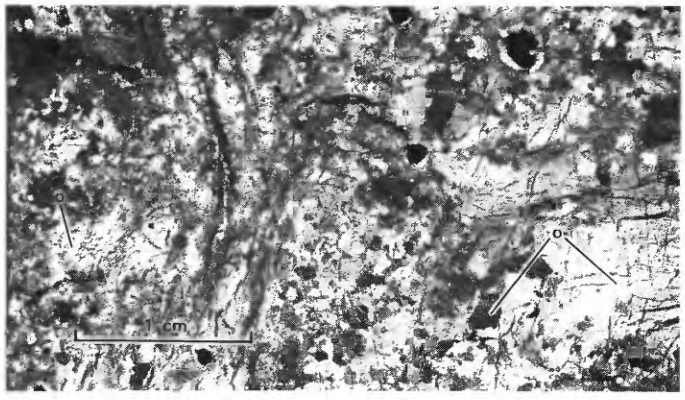


FIGURE 48.—Thin section of sample J5, a dunite. Serpentine is concentrated in dark veinlets and in light zones surrounding chromite grains (black areas). Olivine grains (o) are euhedral to subhedral; some large grains enclose smaller grains of olivine.

All three optical fabric elements are homogeneous in 50-grain samples:

*X fabric (fig. 49A).*—Possible partial girdles at small and large angles to chromite schlieren; two maxima, one 10σ at a high angle to chromite schlieren and one 6σ at a high angle to the axial plane of a northeast-trending chromite fold.

*Y fabric (fig. 49B).*—A partial girdle close to the planes of chromite schlieren; two maxima, one 10σ close to the chromite rods and a fold axis, and one 4σ.

*Z fabric (fig. 49C).*—A partial girdle close to the planes of chromite schlieren; two maxima, one 10σ close to the chromite schlieren and one 4σ at a large angle to the schlieren.

The fabric elements are summarized in figure 49*D*. The total fabric of the rock has triclinic symmetry. The subfabric consisting of the chromite schlieren, rods, and a fold axis plunging gently northeast, with Z- and Y-girdles and a 10σ Y maximum, appears to be orthorhombic. This subfabric may correlate with the episode of formation of northeast-trending folds (deformation 3, table 1), or have a cumulate origin. Although the 6σ X maximum, the axial plane of a chromite fold, the 4σ Z maximum, and, possibly, the steep northeast-trending fold axis all have nearly orthorhombic symmetry and may be related fabric elements, these elements are not easily correlated with any of the deformations recognized from mesoscopic data.

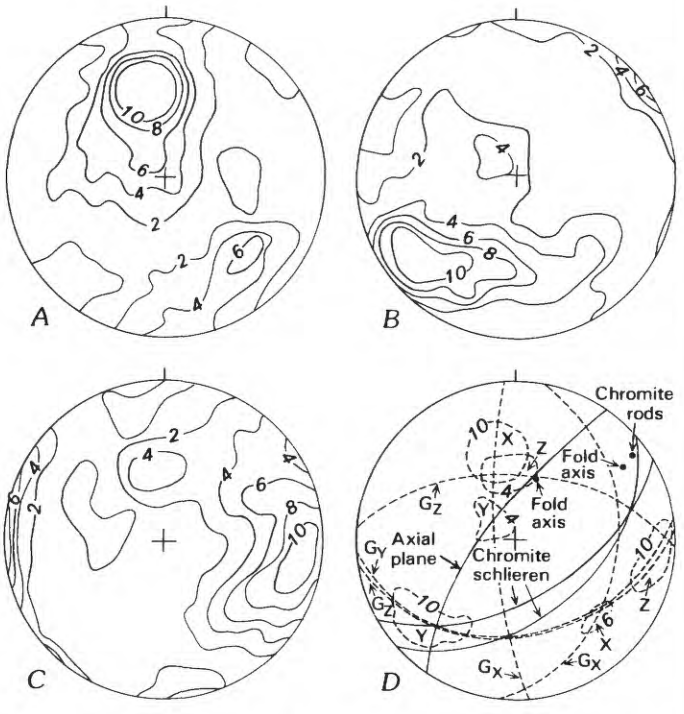


FIGURE 49.—Olivine-fabric diagrams for sample J5, a dunite. 141 points. Contours: 2σ, 4σ, 6σ, 8σ, 10σ, and pole-free area (unlabeled contours). *A*, X-axes. *B*, Y-axes. *C*, Z-axes. *D*, Synopsis of fabric features. Dashed lines, concentrations of X-, Y-, and Z-axes and girdle distributions (*G*) of X, Y, and Z.

SAMPLE J6

Sample J6 is from the thickest part (3 m) of the dunite dike in harzburgite at the Judy mine in area I (fig. 1). The dunite is massive. About 30 percent of the rock is serpentine veinlets, which obscure the textural relations of the olivine (fig. 50). Grain shapes vary: many grains are euhedral to subhedral, and others anhedral with angular and rounded shapes; these forms may be relict primary textures. Olivine grains range in size from 0.1 to 10 mm, with no preferred plane of grain

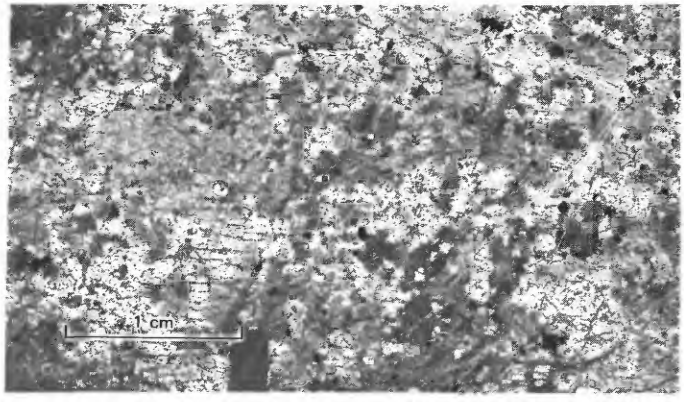


FIGURE 50.—Thin section of sample J6, a dunite. Olivine grains (light- and dark-gray areas) are cut by a network of serpentine veinlets. Grains are euhedral to subhedral and anhedral, with angular and rounded shapes. A possible preferred plane of flattening of olivine grains is at a high angle to long dimension of thin section. Black grains are chromite.

flattening. No kink bands were seen. The sample contains about 1 percent disseminated subhedral chromite.

The optical fabric elements are moderately homogeneous in 50-grain samples:

*X fabric (fig. 51A).*—A girdle at a large angle to the dunite lens; two maxima, one 8σ in the girdle and one 4σ at a large angle to the girdle.

*Y fabric (fig. 51B).*—A partial Y-girdle at an angle to the dunite lens; two maxima, one 12σ in the girdle and one 4σ at a large angle to the girdle.

*Z fabric (fig. 51C).*—Five maxima, two 4σ, one 5σ, and two 6σ, some of which are close together and possibly related.

Most of the Z maxima seem to be associated with mesoscopic linear elements (fig. 51*D*). The triclinic symmetry and the numerous optical fabric maxima and girdles suggest superposed fabrics.

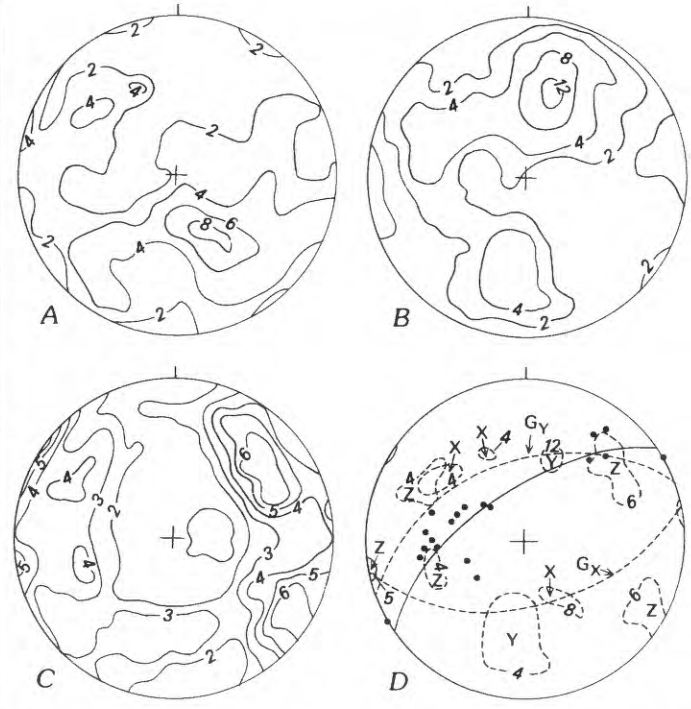


FIGURE 51.—Olivine-fabric diagrams for sample J6, a dunite. 148 points. Contours: 2σ, 3σ, 4σ, 5σ, 6σ, 8σ, 12σ, and pole-free area (unlabeled contours). *A*, X-axes. *B*, Y-axes. *C*, Z-axes. *D*, Synopsis of fabric features. Dashed lines, concentrations of X-, Y-, and Z-axes and girdle distributions (*G*) of X and Y. Dots, linear elements (fold axes and rods); solid great circle, plane of dunite lens.

## SAMPLE J7

Sample J7 is from a dunite dike, 60 cm thick, cutting harzburgite foliation and layering in area I (fig. 1). About 75 percent of the rock is serpentine (fig. 52). Original olivine textures are obscure; however, judging from the simultaneous extinction of numerous olivine fragments, some grains may have exceeded 1 cm in size. No grain elongation was noted, and no kink bands were observed. Subhedral to anhedral chromite, making up less than 1 percent of the rock, is disseminated. Some of the grains contain olivine inclusions, a possible relict primary texture.

Optical fabric elements are distinctly heterogeneous in 50-grain samples:

*X fabric (fig. 53A).*—One girdle at a high angle to the dunite dike, and another girdle at a low angle to the

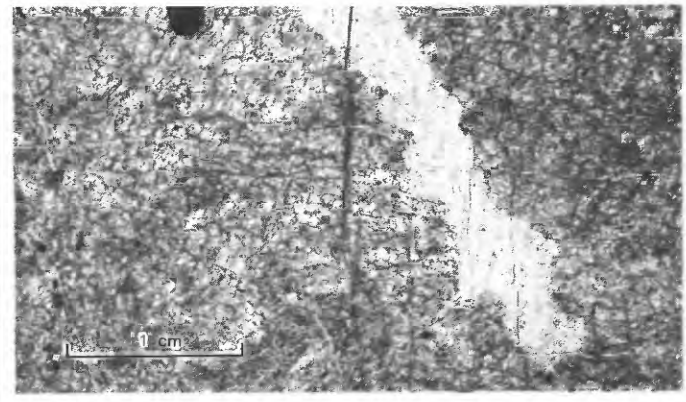


FIGURE 52.—Thin section of sample J7, a dunite. Olivine textures are obscured by serpentinization. Irregular light area is intensely serpentinized and bleached zone. Minute black grains are chromite.

dike; five maxima on or near the former girdle: one 4σ, one 6σ, and three 8σ. The 6σ maximum is perpendicular to the dike.

*Y fabric (fig. 53B).*—Girdles crossed at a large angle; three maxima, two 6σ and one 8σ.

*Z fabric (fig. 53C).*—Two maxima, one 8σ and one 12σ.

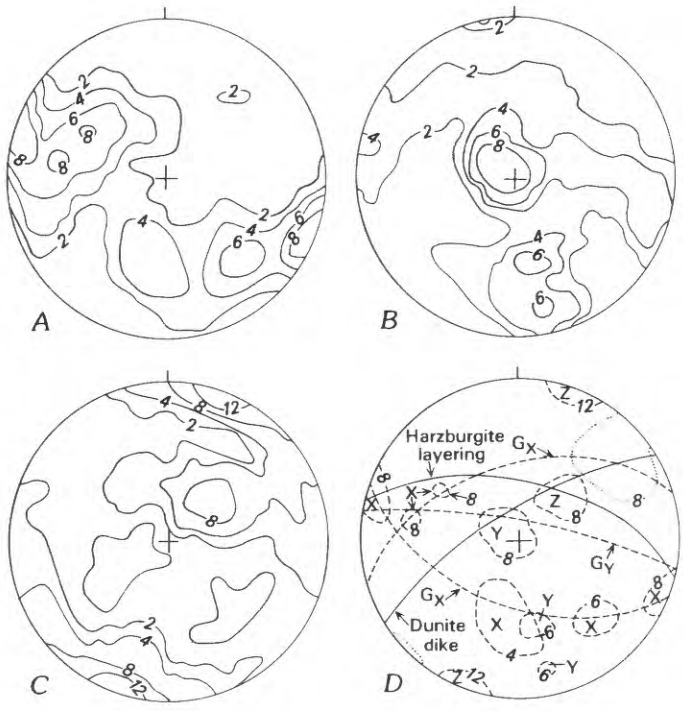


FIGURE 53.—Olivine-fabric diagrams for sample J7, a dunite. 151 points. Contours: 2σ, 4σ, 6σ, 8σ, 12σ, and pole-free area (unlabeled contours). *A*, X-axes. *B*, Y-axes. *C*, Z-axes. *D*, Synopsis of fabric features. Dashed lines, concentrations of X-, Y-, and Z-axes and girdle distributions (*G*) of X and Y; dotted line, concentration of northeast-trending fold axes measured in area I (fig. 1).

The fabric elements are summarized in figure 53*D*. The total fabric has triclinic symmetry. The Z maxima are close to the northeast-trending linear elements in area I.

## SAMPLE J8

Sample J8, a medium-grained wehrlite, is from an exposure along Wimer Road near the California-Oregon State line. The rock is layered, with alternating diopside- and olivine-rich layers about 5 mm thick (fig. 54); this layering is interpreted to be of probable cumulate origin. No mineral lineations were found on the layering surfaces. Subhedral diopside, which is more abundant than anhedral olivine, occurs in grains 1 to 8 mm long. Elongation, as much as 2:1, is in the plane of layering, with no preferred direction visible. The diopside grains have straight as well as sutured boundaries, with interpenetrating grains. Many of the diopside grains have serpentine cores, and some have kink bands. Many diopside grains have euhedral grain boundaries with olivine; other grains have margins embayed by olivine. Olivine is almost completely altered to serpentine; however, relict grains and serpentine pseudomorphs of olivine suggest that the olivine was mostly anhedral and

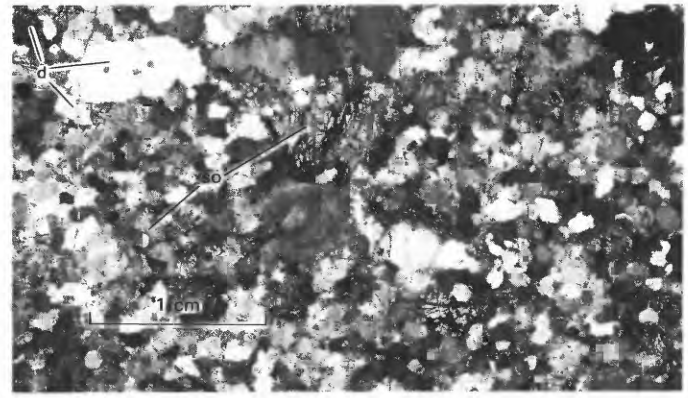


FIGURE 54.—Thin section of sample J8, a wehrlite. Subhedral grains showing no serpentinization are diopside (d). Anhedral grains with dark veinlets are nearly completely serpentinized olivine grains (so). Layering is oriented parallel to long dimension of section.

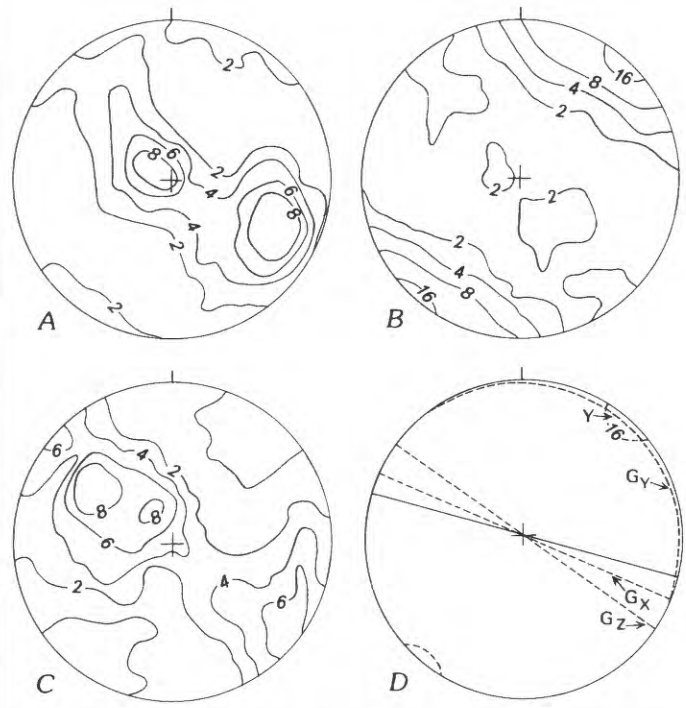


FIGURE 55.—Diopside-fabric diagrams for sample J8, a wehrlite. 146 points. Contours: 2σ, 4σ, 6σ, 8σ, 16σ, and pole-free area (unlabeled contours). *A*, X-axes. *B*, Y-axes. *C*, Z-axes. *D*, Synopsis of fabric features. Dashed lines, concentration of Y-axes and girdle distributions (*G*) of X, Y, and Z; solid line, layering.

interstitial to diopside. Some rounded diopside grains in serpentine suggest that the olivine grains contained diopside inclusions.

The optical fabric of diopside is moderately homogeneous in 50-grain samples:

*X fabric (fig. 55A).*—A girdle close to layering; two maxima of 8σ, both in the girdle.

*Y fabric (fig. 55B).*—One maximum of 16σ at a high angle to layering and to the X-girdle.

*Z fabric (fig. 55C).*—A girdle close to layering and to the X-girdle; three maxima, one 6σ and two 8σ, in the girdle.

The fabric elements are summarized in figure 55*D*. The total fabric has nearly orthorhombic symmetry. The optical fabric elements are clearly related to the layering and could, therefore, reflect a primary fabric if the layering is primary. If the {010} had been well developed during crystallization, Y would be perpendicular to layering, but the double X and Z maxima in the plane of layering cannot be explained solely by crystal settling. The X and Z maxima, however, could also be a result of alignment of the c-axes of diopside grains due to a current in the magma. Poorly developed {010} in the diopside in thin section and interpenetration of the grains indicate some recrystallization. This recrystallization could have altered the primary settling fabric such that the Y maximum is not exactly perpendicular to layering and the X- and Z-girdles do not coincide with layering.

## DISCUSSION OF OLIVINE FABRICS

The olivine fabric of sample J1, a harzburgite, is of particular interest as an example of the dominant rock type in the peridotite. The orthorhombic microfabric, with the greater X maximum nearly perpendicular to the axial plane of an isoclinal fold (fig. 41), resembles the $S_2$-related olivine fabric of the harzburgite studied by Loney and Himmelberg (1976, p. 270) in the Vulcan Peak area. Their sample, however, was not so closely associated with mesoscopic fold axes as is sample J1. The relation of X normal to the axial plane of isoclinal folds in the early layering and foliation (deformation 1, table 1) suggests that X tends to align with the maximum principal compressive stress, $\sigma_1$. Experimental compressive deformation of peridotite supports this conclusion; under certain physical conditions X aligns with $\sigma_1$ by intragranular glide on the system $T=(010)$, $t=[100]$, and by syntectonic recrystallization (Avé Lallemant and Carter, 1970; Carter and Avé Lallemant, 1970; Nicolas and others, 1973). Sample J1, in contrast to the Vulcan Peak peridotite, has rare kink bands, and so significant intragranular gliding appears to have been unlikely in development of the fabric. Annealing could have eliminated most of the kink bands, but, in the process, the olivine fabric would probably have been significantly weakened. Because of the absence of kink bands and the association of Z-axes and axes of folds with the strong fabric, syntectonic recrystallization is concluded to be the dominant orienting mechanism.

Orientation of X parallel to $\sigma_1$ and perpendicular to the axial plane of a nearly isoclinal fold is consistent with the conclusions based on analysis of mesoscopic structures that $\sigma_1$ is oriented at large angles to the axial planes of isoclinal folds and to the harzburgite foliation. In the doubly folded outcrop from which sample J1 was taken (figs. 22, 23), the later episode of open folding did not greatly affect the olivine fabric in the harzburgite. Olivine fabrics analogous to that of sample J1 occur in the peridotite on Cypress Island, Wash. (Raleigh, 1965, p. 735), in the French Pyrenees (Avé Lallemant, 1967, p. 25–43), and in New Zealand (Battey, 1960). An olivine fabric like like that of sample J1 but with no clear relation to mesoscopic fabric elements—more like the Vulcan Peak rock—was found at Burro Mountain, Calif. (Loney and others, 1971, p. 264–267).

The olivine fabric of sample J2, a dunite, is nearly identical to the fabric of sample J1, except that, in sample J2, the two X maxima are equally developed, and there is no significant subordinate Z maximum (fig. 43). However, the mesoscopic planar and linear structures with which the olivine fabric is associated are correlated with the group of east-west-trending folds (deformation 4, table 1) that formed later than the early, northwest-trending isoclinal folds (deformation 1). In this rock, any olivine fabric related to the episode of early folding was obliterated. Kink bands are uncommon, and, using the same arguments as for sample J1, syntectonic recrystallization is the preferred orienting mechanism.

The suborthorhombic fabric of sample J3 may be related to a late phase of deformation 3 or to local deformation in the vicinity of the dunite dike from which the sample was taken (fig. 45). The Z fabric resembles the olivine Z fabric of harzburgite in the Vulcan Peak area, in which the Z maximum is parallel to northeast-trending folds (Loney and Himmelberg, 1976, p. 267, fig. 22*C*). Formation of the olivine fabric of sample J3 was probably by syntectonic recrystallization because the olivine has no kink bands.

The olivine fabrics of samples J4 through J7 are triclinic. Subfabrics that are suborthorhombic can be inferred that appear to be related to mesoscopic planar and linear elements, and suggest that the triclinic fabrics are a result of superposed suborthorhombic subfabrics. Although a degree of uncertainty exists in attempting to differentiate superposed subfabrics, constraints are inherent in the subfabrics, such as the orthogonality of axes of the olivine indicatrix and the apparent relations of X, Y, and Z to mesoscopic structures.

In sample J4, inferred subfabrics are: (1) a Z maximum near chromite folds and lineations, an X maximum nearly perpendicular to the axial-plane foliation,

and a Y maximum trending northwest; and (2) a northeast-plunging Z maximum unrelated to mesoscopic structures, three X maxima at large angles to Z, a Y maximum close to Z, and a Y maximum in the X-girdle (fig. 47). Subfabric 1 may be related to early, northwest-trending folds (deformation 1, table 1). Subfabric 2 is not closely related to northwest-trending folds of the area but could have developed during the episode of formation of northeast-trending folds (deformation 3). The chromite schlieren, early mesoscopic structures, do not appear to be related to the olivine fabric. Any early olivine fabric that may have been formed with the schlieren appears to have been obliterated; however, such an early fabric may have influenced olivine orientations during subsequent episodes of deformation.

In sample J5, the inferred olivine subfabrics are: (1) a principal Z maximum and Z-girdle at a low angle to chromite schlieren, with Y contributing to the principal and subordinate maxima and the principal maximum subparallel to chromite folds and rods plunging northeast at low angles, a Y-girdle nearly coincident with the Z-girdle, and an X maximum at large angles to chromite schlieren; (2) a subordinate Z maximum close to a steeply northeast plunging fold axis, with Y contributing to the principal Y maximum and a subordinate X maximum nearly perpendicular to the axial plane of the steep northeast-trending fold (fig. 49). Lappin (1971, p. 733) attempted to define approximately a relatively high pressure (0.8–2.0 GPa) and low-temperature (400°–700° C) field in which olivine fabrics form with X perpendicular to a dominant $S$-surface and Y tending to parallel lineations and fold axes, as well as other kinds of linear fabric elements, as in subfabric 1 above. Such fabrics occur in rocks of Japan (Yoshino, 1961), Norway (Lappin, 1967), and the Alps (Ladurner, 1954). These rocks, however, have cataclastic textures that are absent in sample J5. In contrast, sample J5 has textures that may be relict cumulate. Turner (1942, p. 296) gave an example of a peridotite from Rhum, Scotland, with X perpendicular to igneous layering and Y parallel to a weak lineation, possibly owing to dimensional orientation of magmatic olivine elongate parallel to Y. Jackson (1961, fig. 43) found a dimensionally oriented Y linear fabric in undeformed peridotite of the Stillwater Complex; his rock contained two Y maxima as suggested for subfabric 1 of sample J5. Therefore, subfabric 1 could be a primary cumulate fabric. The chromite rods and fold axis parallel to the Y maximum would have formed during movement of the crystal mush; the northeast trend of these linear elements could be fortuitous and does not necessarily point to a correlation with deformation 3 (table 1). Subfabric 2 appears to be related to the steep north-northeast-trending fold, which, if subfabric 1 is cumulate, probably postdates subfabric 1. Subfabric 2, however, is not easily correlated with any of the deformations recognized from mesoscopic data.

The numerous maxima in the olivine fabric of dunite samples J6 and J7 suggest superposed fabrics, but the various subfabrics are difficult to infer in detail. In sample J6, four of the five Z maxima are close to mesoscopic fold axes (fig. 51*D*). These relations suggest that these Z maxima are related to the respective groups of folds (northeast-and east-west-trending folds; deformations 3 and 4, table 1). The northwest-trending Z maximum seems to be unrelated to the other Z maxima and the folds, but could be related to another episode of deformation, possibly deformation 1 or 2.

If the dunite dike from which sample J7 was taken intruded parallel to the generally northeast striking axial planes of the northeast-trending folds (deformation 3, table 1) in area I, then the microfabric must postdate those folds. The two Z maxima, 50° apart, however, are close to the maximum of large northeast-trending folds for the area (see fig. 53). Moreover, the steeply plunging, subordinate Z maximum (subfabric 1) lies at the intersection of the dunite dike with adjacent harzburgite layering, a coincidence strongly suggestive of a relation between the optical fabric and some northeast- trending minor structures. These structures, however, may have formed as a result of localized strain associated with the dike, or during later stages of deformation 3. The principal Z maximum (subfabric 2) may also be related to a stage of formation of northeast-trending folds but may belong to a distinct stage following dike emplacement because it appears to be unrelated to the dike.

A synopsis of Z maxima is presented in figure 56. On the basis of correlations with folds of the northwest-, northeast-, and east-west-trending groups, these Z maxima are labeled I, II, and III, respectively. Most of the Z maxima can be associated with these three main groups of folds.

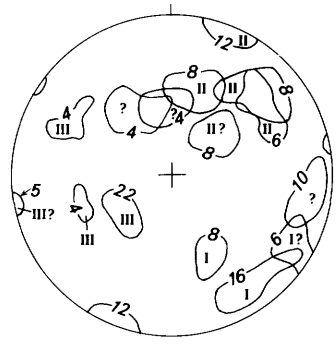


FIGURE 56.—Synoptic diagram of Z maxima for samples J1 through J7. Contours: 4σ, 5σ, 6σ, 8σ, 10σ, 12σ, 16σ, and 22σ. Maxima labeled "I" are associated with early northwest-trending folds, maxima labeled "II" with northeast-trending folds, and maxima labeled "III" with east-west-trending folds; queried maxima are not clearly associated with any group of mesoscopic linear elements.

The scarcity of kink bands in the olivine in samples J1 through J7, and the parallelism of Z maxima and fold axes, point to syntectonic recrystallization as the dominant orienting mechanism during at least deformations 1 or 2, and deformations 3 and 4 (table 1). Recrystallization of olivine occurred nonuniformly, and so primary cumulate fabrics and early tectonic fabrics appear to be preserved locally; in some rocks, olivine fabrics appear to be superposed.

## SUMMARY

### ORIGIN

Little evidence of the early history of the harzburgite remains. Poikilitic enstatite suggests a magmatic stage, probably early in its development, but textures do not clearly distinguish between igneous or pyrometamorphic origins. Enstatite layering, possibly in part a product of cumulus processes, may have formed at that time. Dunite masses of unknown form were probably present in the early harzburgite.

### DEFORMATION 1

Plastic deformation, including recrystallization of olivine and possible metamorphic differentiation to form layering, affected most of the harzburgite. Folds of layering were mostly isoclinal and plunged at low angles, chiefly northwest. Detached isoclinal fold hinges suggest large extension parallel to axial planes; some extension occurred parallel to early-fold hinges and rods. Many hinge zones may have been obliterated by slip on the axial planes. Preexisting structures were altered in form and orientation, and so a clear record of primary structures or earlier deformations was obliterated. Enstatite foliation parallel to the axial planes of isoclinal folds developed in harzburgite. Enstatite layers and dunite bodies were rotated into parallelism with the foliation and axial planes. Olivine fabric, with X perpendicular to layering and foliation, developed and was preserved in some harzburgite (sample J1). Maximum principal compressive stress during this deformation most likely coincided with the maximum principal strain and was oriented at a large angle to the axial planes of isoclinal folds and the enstatite foliation.

Harzburgite sample J1 has a total fabric like the peridotite from the French Pyrenees described by Avé Lallemant (1967, p. 26-35). According to Avé Lallemant and Carter (1970, p. 2212), the total fabric of this peridotite suggests that $\sigma_1$ parallels the olivine X maximum and that $\sigma_3$ parallels the lineation, fold axis, and olivine Z maximum. According to this scheme, linear elements, including folds, probably become aligned parallel or close to the direction of maximum yield or the slip direction in this rock. For the Josephine Peridotite, these relations imply that the concentration of early linear elements trending north-northwest lay parallel or close to the slip direction in the rock during the early ductile deformation. Because slip folds cannot form with axes parallel to the direction of slip (Turner and Weiss, 1963, p. 483–484; Ramsay, 1967, p. 424–426), the early structural development of the Josephine Peridotite must have included one or both of the following components: (1) slip in a plane oriented at small angles to preexisting layering, or (2) passive rotation of fold axes and lineations, formed at low to high angles to the slip direction, toward the slip direction. After large strain, the linear elements would be oriented almost in the slip direction (Turner and Weiss, 1963, p. 392–395; Ramsay, 1967, p. 471–472). A model implying large early ductile deformation of this type in the Josephine Peridotite is consistent with the field observations.

### DEFORMATION 2

After the stage of intense plastic deformation, the early isoclinal folds were refolded in an open style about northwest-trending axes. The refolding, observed in outcrop and also evident on a broad scale (see fig. 39*A*), may have been dominantly by flexural slip, indicating that the layering behaved as an active structural element. No evidence was found to suggest that the subparallelism of these open folds with the early isoclinal folds reflects a close relation between these two kinds of folds. On the contrary, the differences in fold styles in this case suggests large differences in physical conditions between the deformations, as well as large differences in the orientations of slip directions and the axes of stress and strain ellipsoids. These differences lead to the conclusion that the two types of folds developed in distinct episodes and that the more open folds are younger. Syntectonic recrystallization of olivine could have occurred during deformation 2 but would be difficult to differentiate from an earlier recrystallization event on the basis of orientation of Z-axes.

### DEFORMATION 3

The next episode of deformation resulted in abundant minor open folds, plunging northeast. Axial planes are generally steep. In some areas, apparent rotation of these axial planes about a northeast-trending axis suggests either heterogeneity of the axial planes or refolding of northeast-trending folds. In places, steep folds formed perpendicular to the dominant, northeast-trending folds. Chromite foliations in dunite developed parallel to the axial planes of these folds. Flattening of

olivine grains parallel to the chromite foliation suggests that the maximum principal strain and, possibly, the maximum principal stress for the deformation were at a large angle to these foliations. Subparallelism of the isoclinal folds of chromite layers in dunite to the open northeast-trending folds of dunite layers in harzburgite suggests a more nearly plastic behavior for chromitiferous dunite during this deformation. Olivine fabrics related to northeast-trending folds were probably developed by syntectonic recrystallization. Mesoscopic fabric and petrofabric studies suggest that this deformation may have included more than one stage, interrupted by at least one period of strain relaxation or rebound during which dunite dikes were emplaced.

### DEFORMATION 4

Folds plunging both east and west developed after the episode of formation of northeast-trending folds. Early isoclinal folds, rotated in small circles about east-west-trending axes, point to a flexural-slip mechanism for the folding. As in the preceding deformation, the subparallelism of nearly isoclinal folds of chromite layers in dunite to open east-west-trending folds of dunite in harzburgite suggests a more nearly plastic mode of deformation within chromitiferous dunite. Olivine fabrics related to east-west-trending folds probably developed by syntectonic recrystallization. In some areas, east-west-trending folds are approximately perpendicular to northeast-trending folds, but this angular relation is not consistent throughout the peridotite. Scanty mesoscopic-fabric data bearing on the relative ages of these two sets of folds suggest that the east-west-trending folds are younger.

### DEFORMATION 5

Steep open folds are abundant in a few outcrops and in a few areas. The relation of these folds to other fold groups is not known. In some places, the few steep folds appear to be conjugate folds perpendicular to the more dominant, northeast-trending folds; in other areas, abundant steep folds may represent a distinct episode of folding that was well developed locally. The relative age of this episode is not known.

### DEFORMATION 6

Broad warping and faulting of late-stage orthopyroxenite dikes points to late, low-intensity deformation.

### DEFORMATION 7

The Josephine Peridotite, the overlying parts of the ophiolite, and the metasedimentary rocks above the ophiolite were folded into a broad syncline plunging at a low angle south-southeast. Minor structures related to this deformation were not found in the peridotite.

### DEFORMATIONS 8 AND 9

The Josephine Peridotite underwent postcrystalline deformation during which peridotite was altered to serpentinite and the ultramafic mass was intensely fractured. Fracturing was most intense along the highly serpentinized margins, as the peridotite was emplaced during the post-Late Jurassic along the Madstone Cabin thrust and, later, during the Coast Range orogeny in the Late Cretaceous, along the South Fork Mountain and other faults.

## AGE OF CRYSTALLINE DEFORMATIONS

The 300-m-thick chromite-bearing zone in the Josephine Peridotite is near the top of the peridotite and is approximately concentrically folded with the ophiolitic rocks overlying the peridotite (Evans, 1984). This relation suggests that the chromitiferous dunite was emplaced at about the time of formation of the Late Jurassic ophiolitic rocks. According to this model, the episodes of deformation datable relative to the chromitiferous dunite can be assigned an approximate age: deformations 1, and 2, and, possibly, part of 3 would be pre-Late Jurassic; part of deformation 3 and deformations 4 through 6 would be approximately Late Jurassic; and deformation 7 would be post-Late Jurassic.

## LIMITATIONS OF THIS STUDY

The areas studied constitute a small percentage of the outcrop area of the peridotite. Ten of the smaller areas on the index map (fig. 1) are in the chromite-bearing zone, which may have had a somewhat different history from the peridotite above and below the zone. Generalizations made here concerning the deformation of the peridotite apply principally to the chromite-bearing zone. Area XII, for example, is in peridotite below the chromite-bearing zone. In this area, the relative abundance of steep folds suggests that the lower parts of the peridotite were deformed somewhat differently from the upper parts. Also, differences in the style and complexity of deformation of the peridotite and the upper parts of the ophiolite imply a tectonic uncoupling of the peridotite from the overlying rocks (Evans, 1984).

The sequence of deformations undergone by the peridotite reflects changes in strain regimes either as the peridotite approached converging plate boundaries and (or) as the peridotite was obducted. Possibly simultaneous deformation of parts of the peridotite under

different conditions of confining pressure, temperature, stress, ductility, and strain rate accounts for the vertical changes in deformation suggested by the steep folds in area XII (fig. 1).

The geographic orientations of slip directions and of the principal axes of stress and strain ellipsoids suggested by this study may actually be of little value to our understanding of regional tectonics because of the translations and rotations of the peridotite during its postcrystalline emplacement. Moreover, the Josephine Peridotite makes up part of a terrane that is one of several such terranes recently interpreted to have been displaced many kilometers northward from their sites of origin during Mesozoic and Cenozoic time (Beck, 1980; Beck and others, 1980; Coney and others, 1980). During their northward translation, the Josephine Peridotite and adjacent rocks may have undergone large clockwise rotation. Therefore, the primary value of this study is in illuminating the complex deformational history of this alpine-type peridotite.

Harding and Bird (1983) inferred an east-west paleoridge direction from flow fabrics in the Josephine Peridotite. Harper (1984) also reported a similar ridge orientation inferred from sheeted dikes in the Josephine ophiolite and from the strike of a fossil fracture zone. These agreements may point to an absence of large-scale rotation within the Josephine ophiolite but do not bear on how much rotation the paleoridge indicators may have undergone.

## REFERENCES CITED


Anderson, E.M., 1951, The dynamics of faulting and dyke formation with applications to Britain (2d ed.): Edinburgh, Oliver and Boyd, 206 p.

Avé Lallemant, H.G., 1969, Structural and petrofabric analysis of an "alpine-type" peridotite: The lherzolite of the French Pyrenees: Leidse Geologische Mededelingen, v. 42, p. 1–57.

——— 1976, Structure of the Canyon Mountain (Oregon) Ophiolite Complex and its implication for sea-floor spreading: Geological Society of America Special Paper 173, 49 p.

Ave Lallemant, H.G., and Carter, N.L., 1970, Syntectonic recrystallization of olivine and modes of flow in the upper mantle: Geological Society of America Bulletin, v. 81, no. 8, p. 2203–2220.

Bailey, E.H., Blake, M.C., Jr., and Jones, D.L., 1970, On-land Mesozoic oceanic crust in California Coast Ranges, *in* Geological Survey research, 1970: U.S. Geological Survey Professional Paper 700–C, p. C70–C81.

Battey, M.H., 1960, The relationship between preferred orientation of olivine in dunite and the tectonic environment: American Journal of Science, v. 258, no. 10, p. 716–727.

Beck, M.E., Jr., 1980, Paleomagnetic record of plate-margin tectonic processes along the western edge of North America: Journal of Geophysical Research, v. 85, no. B12, p. 7115–7131.

Beck, M.E., Jr., Cox, Allen, and Jones, D.L., 1980, Mesozoic and Cenozoic microplate tectonics of western North America: Geology, v. 8, no. 9, p. 454–456.

Boudier, Françoise, and Nicolas, Adolphe, 1977, Structural controls on partial melting in the Lanzo peridotites, *in* Dick, H.J.B., ed., Magma genesis: Oregon Department of Geology and Mineral Industries Bulletin 96, p. 63–78.

Bowen, N.L., and Tuttle, O.F., 1949, The system $MgO$-$SiO_2$-$H_2O$: Geological Society of America Bulletin, v. 60, no. 3, p. 439–460.

Carter, N.L., and Avé Lallemant, H.G., 1970, High-temperature flow of dunite and peridotite: Geological Society of America Bulletin, v. 81, no. 8, p. 2181–2202.

Coney, P.J., Jones, D.L., and Monger, J.W.H., 1980, Cordilleran suspect terranes: Nature, v. 288, no. 5789, p. 329–333.

Dick, H.J.B., 1973, K-Ar dating of intrusive rocks in the Josephine peridotite and Rogue Formation west of Cave Junction, southwestern Oregon [abs.]: Geological Society of America Abstracts with Programs, v. 5, no. 1, p. 33–34.

——— 1976, The origin and emplacement of the Josephine Peridotite of southwestern Oregon: New Haven, Conn., Yale University, Ph.D. thesis, 409 p.

——— 1977a, Evidence of partial melting in the Josephine Peridotite, *in* Dick, H.J.B., ed., Magma genesis: Oregon Department of Geology and Mineral Industries Bulletin 96, p. 59–62.

——— 1977b, Partial melting in the Josephine Peridotite I, The effect on mineral composition and its consequence for geobarometry and geothermometry: American Journal of Science, v. 277, no. 7, p. 801–832.

Diller, J.S., 1902, Topographic development of the Klamath Mountains: U.S. Geological Survey Bulletin 196, 69 p.

Dungan, M.A., and Avé Lallemant, H.G., 1977, Formation of small dunite bodies by metasomatic transformation of harzburgite in the Canyon Mountain ophiolite, Oregon, *in* Dick, H.J.B., ed., Magma genesis: Oregon Department of Geology and Mineral Industries Bulletin 96, p. 109–128.

Evans, J.G., 1984, Structure of part of the Josephine Peridotite, northwestern California and southwestern Oregon: U.S. Geological Survey Bulletin 1546–A, p. 7–37.

Fyfe, W.S., Price, N.J., and Thompson, A.B., 1978, Fluids in the Earth's crust: N.Y., Elsevier, 383 p.

George, R.P., Jr., 1978, Structural petrology of the Olympus ultramafic complex in the Troodos ophiolite, Cyprus: Geological Society of America Bulletin, v. 89, no. 6, p. 845–865.

Griscom, Andrew, 1984, A magnetic interpretation of the Josephine Peridotite, Del Norte County, California: U.S. Geological Survey Bulletin 1546–C, p. 53–63.

Harding, D.J., and Bird, J.M., 1983, Accreting plate margin structures in the Josephine ophiolite tectonite and cumulate sequences [abs.]: Eos (American Geophysical Union Transactions), v. 64, no. 45, p. 846.

Harper, G.C., and Saleeby, J.B., 1980, Zircon ages of the Josephine ophiolite and the Lower Coon Mountain pluton, Western Jurassic Belt, NW California [abs.]: Geological Society of America Abstracts with Programs, v. 12, no. 3, p. 109–110.

Harper, G.D., 1980a, Structure and petrology of the Josephine ophiolite and overlying metasedimentary rocks, northwestern California: Berkeley, University of California, Ph.D. thesis, 259 p.

——— 1980b, The Josephine ophiolite—remains of a Late Jurassic marginal basin in northwestern California: Geology, v. 8, no. 7, p. 333–337.

——— 1983, A depositional contact between the Galice Formation and a Late Jurassic ophiolite in northwestern California and southwestern Oregon: Oregon Geology, v. 45, no. 1, p. 3–9.

——— 1984, The Josephine ophiolite, northwestern California: Geological Society of America Bulletin, v. 95, no. 9, p. 1009–1026.

Himmelberg, G.R., and Loney, R.A., 1973, Petrology of the Vulcan Peak alpine-type peridotite, southwestern Oregon: Geological Society of America Bulletin, v. 84, no. 5, p. 1585–1600.

Hotz, P.E., 1971, Plutonic rocks of the Klamath Mountains, California and Oregon: U.S. Geological Survey Professional Paper 684–B, p. B1–B20.

Imlay, R.W., 1980, Jurassic paleobiogeography of the conterminous United States in its continental setting: U.S. Geological Survey Professional Paper 1062, 134 p.

Irwin, W.P., 1964, Late Mesozoic orogenies in the ultramafic belts of northwestern California and southwestern Oregon, *in* Geological Survey research, 1964: U.S. Geological Survey Professional Paper 501–C, p. C1–C9.

Jackson, E.D., 1961, Primary textures and mineral associations in the ultramafic zone of the Stillwater Complex, Montana: U.S. Geological Survey Professional Paper 358, 106 p.

Kamb, W.B., 1959, Ice petrofabric observations from Blue Glacier, Washington, in relation to theory and experiment: Journal of Geophysical Research, v. 64, no. 11, p. 1891–1909.

Ladurner, Josef, 1954, Das Verhalten des Olivins als Gefügekorn in einigen Olivingesteinen: Tschermaks Mineralogische und Petrographische Mitteilungen, ser. 3, v. 5, no. 1–2, p. 21–36.

Lappin, M.A., 1967, Structural and petrofabric studies of the dunites of Almklovdalen, Nordfjord, Norway, *in* Wyllie, P.J., ed., Ultramafic and related rocks: New York, John Wiley and Sons, p. 183–190.

———1971, The petrofabric orientation of olivine and seismic anisotropy of the mantle: Journal of Geology, v. 79, no. 6, p. 730–740.

Loney, R.A., and Himmelberg, G.R., 1976, Structure of the Vulcan Peak alpine-type peridotite, southwestern Oregon: Geological Society of America Bulletin, v. 877, no. 2, p. 259–274.

Loney, R.A., Himmelberg, G.R., and Coleman, R.G., 1971, Structure and petrology of the alpine-type peridotite at Burro Mountain, California, U.S.A.: Journal of Petrology, v. 12, no. 2, p. 245–309.

Nicolas, Adolphe, Boudier, Françoise, and Boullier, A.M., 1973, Mechanisms of flow in naturally and experimentally deformed peridotites: American Journal of Science, v. 273, no. 10, p. 853–876.

Pike, J.E.N., and Schwarzman, E.C., 1977, Classification of textures in ultramafic xenoliths: Journal of Geology, v. 85, no. 1, p. 49–61.

Raleigh, C.B., 1965, Structure and petrology of an alpine peridotite on Cypress Island, Washington, U.S.A.: Beiträge zur Mineralogie und Petrographie, v. 11, no. 7, p. 719–741.

Ramp, Len, 1975, Geology and mineral resources of the Upper Chetco drainage area, Oregon, including the Kalmiopsis Wilderness and Big Craggies Botanical areas: Oregon Department of Geology and Mineral Industries Bulletin 88, 47 p.

Ramsay, J.G., 1967, Folding and fracturing of rocks: New York, McGraw-Hill, 568 p.

Saleeby, J.B., Harper, G.D., Snoke, A.W. and Sharp, W., 1982, Time relations and structural-stratigraphic patterns in ophiolite accretion, west-central Klamath Mountains, California: Journal of Geophysical Research, v. 87, p. 3831–3848.

Thayer, T.P., 1969, Gravity differentiation and magmatic re-emplacement of podiform chromite deposits, *in* Wilson, H.D.B., ed., Magmatic ore deposits: A symposium: New Haven, Conn., Economic Geology Publishing Co. (Economic Geology Monograph 4), p. 132–146.

Turner, F.J., 1942, Preferred orientation of olivine crystals in peridotites, with special reference to New Zealand examples: Royal Society of New Zealand Transactions and Proceedings, v. 72, no. 3, p. 280–300.

Turner, F.J., and Weiss, L.E., 1963, Structural analysis of metamorphic tectonites: New York, McGraw-Hill, 545 p.

Vail, S.G., 1977, Geology and geochemistry of the Oregon Mountain area, southwestern Oregon and northern California: Corvallis, Oregon State University, Ph.D. thesis, 159 p.

Wells, F.G., Hotz, P.E., and Cater, F.W., Jr., 1949, Preliminary description of the geology of the Kerby quadrangle, Oregon: Oregon Department of Geology and Mineral Industries Bulletin 40, 23 p.

Yoshino, Gensei, 1961, Structural-petrological studies of peridotite and associated rocks of the Higashi-akaishi-yama district, Shikoku, Japan: Hiroshima University Journal of Science, ser. C, v. 3, no. 3–4, p. 343–402.

GPO 785-048/48020